



Faculty of Electrical Technology and Engineering



**IMPLEMENTATION OF VECTOR CONTROL ON ELECTRIC
VEHICLE TRACTION SYSTEM BY PID GAIN SCHEDULING**

TANHA CHOWDHURY

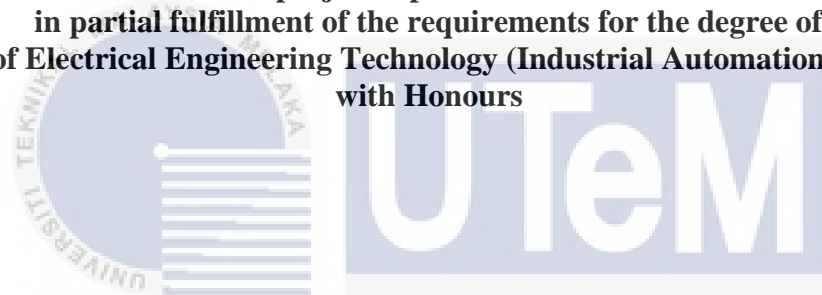
**Bachelor of Electrical Engineering Technology (Industrial Automation & Robotics)
with Honours**

2023

**IMPLEMENTATION OF VECTOR CONTROL ON ELECTRIC VEHICLE
TRACTION SYSTEM BY PID GAIN SCHEDULING**

TANHA CHOWDHURY

**A project report submitted
in partial fulfillment of the requirements for the degree of
Bachelor of Electrical Engineering Technology (Industrial Automation & Robotics)
with Honours**



اونيورسيتي تيكنيكل مليسيا ملاك

Faculty of Electrical Technology and Engineering
UNIVERSITI TEKNIKAL MALAYSIA MELAKA

UNIVERSITI TEKNIKAL MALAYSIA MELAKA

2023

BORANG PENGESAHAN STATUS LAPORAN
PROJEK SARJANA MUDA II

Tajuk Projek : **Implementation of Vector Control on Electric Vehicle Traction System by PID Gain Scheduling**

Sesi Pengajian : **1 2023/2024**

Saya **Tanha Chowdhury** mengaku membenarkan laporan Projek Sarjana Muda ini disimpan di Perpustakaan dengan syarat-syarat kegunaan seperti berikut:

1. Laporan adalah hakmilik Universiti Teknikal Malaysia Melaka.
2. Perpustakaan dibenarkan membuat salinan untuk tujuan pengajian sahaja.
3. Perpustakaan dibenarkan membuat salinan laporan ini sebagai bahan pertukaran antara institusi pengajian tinggi.
4. Sila tandakan (✓):

SULIT*

(Mengandungi maklumat yang berdarjah keselamatan atau kepentingan Malaysia seperti yang termaktub di dalam AKTA RAHSIA RASMI 1972)

TERHAD*

(Mengandungi maklumat terhad yang telah ditentukan oleh organisasi/badan di mana penyelidikan dijalankan)

TIDAK TERHAD

Disahkan oleh:

Tanha



(TANDATANGAN PENULIS)
Alamat Tetap: UTeM Campus, Hang Tuah
Jaya, 76100 Durian Tunggal, Melaka

(COP DAN TANDATANGAN PENYELIA)

TS. DR. MOHD HANIF BIN CHE HASAN
PENSYARAH
Fakulti Teknologi dan Kejuruteraan Elektrik
Universiti Teknikal Malaysia Melaka

Tarikh: 08/02/2024

Tarikh: 15 February 2024

DECLARATION

I declare that this project report entitled “IMPLEMENTATION OF VECTOR CONTROL ON ELECTRIC VEHICLE TRACTION SYSTEM BY PID GAIN SCHEDULING” is the result of my own research except as cited in the references. The project report has not been accepted for any degree and is not concurrently submitted in candidature of any other degree.

Signature

:

Tanha

Student Name

:

TANHA CHOWDHURY

Date

:

8 February 2024

اونيورسيتي تيكنيكل مليسيا ملاك

UNIVERSITI TEKNIKAL MALAYSIA MELAKA

APPROVAL

I hereby declare that I have checked this project report and in my opinion, this project report is adequate in terms of scope and quality for the award of the degree of Bachelor of Electrical Engineering Technology (Industrial Automation & Robotics) with Honours.

Signature



Supervisor Name

: TS. DR. HANIF BIN CHE HASAN

Date

: 15 February 2024



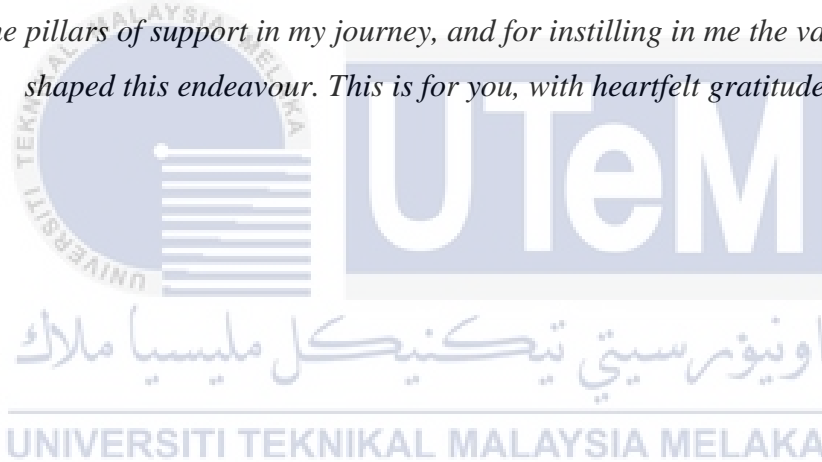
DEDICATION

To my beloved father, ENAYET HOSSAIN CHOWDHURY, who struggled and fought more than me to fulfil my dreams.

To my late Grandfather SHAHIDUL ISLAM CHOWDHURY and my late Grandmother AMINA KHATUN.

To my cherished family members, with warmest appreciation for your unwavering support and encouragement. Your guidance has been my compass, and your belief in my abilities has been the driving force behind this project. This endeavour stands as a tribute to the love, strength, and inspiration you have provided throughout.

To all my friends and well-wishers for your support and compassion toward me. Thank you for being the pillars of support in my journey, and for instilling in me the values that have shaped this endeavour. This is for you, with heartfelt gratitude.



ABSTRACT

Electric vehicles have become increasingly important nowadays due to their many advantages including lower greenhouse gas emissions, enhanced air quality, higher energy efficiency, and utilization of renewable energy sources. It is important to ensure proper power and torque distribution, controllability, and overall operation for safe driving. Torque distribution imbalances and instability can cause vehicle wheels to vibrate, become unsmooth, and jolt as a result, the vehicle may lose control which can cause risk to the driver and passengers' safety and accidents. To ensure the stability and controllability of the vehicle in any condition, it is crucial to have a balanced torque distribution in the vehicle control system. Additionally, unbalanced torque output from the wheel motors would result in extra power consumption, lowering the vehicle's overall efficiency and infecting its range negatively. The project proposed a system adding vector control with PID gains scheduling on the traction system of EVs to minimize these critical issues such as torque at low speeds, responsiveness on load changes, and speed holding capability. The design and implementation are conducted on a Go-Kart developed by the Autotronic research team FKM-UTeM. Two permanent magnet synchronous motors (PMSM) are used to drive the rear wheels while the front wheels are used for steering. Arduino UNO microcontroller is used as the electronic control unit (ECU) of this vehicle and by implementing the PID gain scheduling on the traction system, the torque distribution ability and stability of the vehicle at any driving condition have improved. The desired outcomes are analyzed and evaluated at the end of this project.

ABSTRAK

Kenderaan elektrik telah menjadi semakin penting pada masa kini kerana banyak kelebihannya termasuk pelepasan gas rumah hijau yang lebih rendah, meningkatkan kualiti udara, kecekapan tenaga yang lebih tinggi, dan penggunaan sumber tenaga boleh diperbaharui. Adalah penting untuk memastikan pengagihan kuasa dan tork yang betul, kebolehkawalan, dan operasi keseluruhan untuk pemanduan yang selamat. Ketidakseimbangan agihan tork dan ketidakstabilan boleh menyebabkan roda kenderaan bergetar, menjadi tidak lancar, dan tersentak akibatnya, kenderaan mungkin hilang kawalan yang boleh menyebabkan risiko kepada keselamatan dan kemalangan pemandu dan penumpang. Untuk memastikan kestabilan dan kebolehkawalan kenderaan dalam apa jua keadaan, adalah penting untuk mempunyai pengagihan tork yang seimbang dalam sistem kawalan kenderaan. Selain itu, output tork yang tidak seimbang daripada motor roda akan mengakibatkan penggunaan kuasa tambahan, mengurangkan kecekapan keseluruhan kenderaan dan menjangkiti julatnya secara negatif. Projek ini mencadangkan sistem menambah kawalan vektor dengan penjadualan keuntungan PID pada sistem daya tarikan EV untuk meminimumkan isu kritikal ini seperti tork pada kelajuan rendah, responsif pada perubahan beban dan keupayaan memegang kelajuan. Reka bentuk dan pelaksanaan dijalankan pada Go-Kart yang dibangunkan oleh pasukan penyelidikan Autotronic FKM-UTeM. Dua motor segerak magnet kekal (PMSM) digunakan untuk memacu roda belakang manakala roda hadapan digunakan untuk stereng. Pengawal mikro UNO Arduino digunakan sebagai unit kawalan elektronik (ECU) kenderaan ini dan dengan melaksanakan penjadualan keuntungan PID pada sistem daya tarikan, keupayaan pengagihan tork dan kestabilan kenderaan pada sebarang keadaan pemanduan telah bertambah baik. Hasil yang dikehendaki dianalisis dan dinilai pada akhir projek ini.

ACKNOWLEDGEMENTS

First and foremost, I would like to express my gratitude to my supervisor, TS. DR MOHD HANIF CHE HASAN for his precious guidance, words of wisdom and patience throughout this project.

I am also indebted to Universiti Teknikal Malaysia Melaka (UTeM) and Faculty of Electrical Technology and Engineering (FTKE) for the financial support through BDP2 session which enabled me to accomplish the project. Not forgetting my senior from Autotronic Lab, MUHAMMAD SHUKRI AZIZI BIN RAZAK for the willingness of sharing his thoughts and ideas regarding the project.

My highest appreciation goes to my father ENAYET HOSSAIN CHOWDHURY, and family members for their love and prayer during the period of my study. An honourable mention also goes to my close friends DINESVARI A/P THANASAKRAN and RATUL ISLAM RUHIN for all the motivation and understanding. Thanks for all the love, kindness, and support.

Finally, I would like to thank all the staffs at the Autotronic Lab, fellow classmates, the Faculty members, as well as other individuals who are not listed here for being co-operative and helpful.

TABLE OF CONTENTS

	PAGE
APPROVAL	
ABSTRACT	i
ABSTRAK	ii
ACKNOWLEDGEMENTS	iii
TABLE OF CONTENTS	iv
LIST OF TABLES	vii
LIST OF FIGURES	viii
LIST OF SYMBOLS	xi
LIST OF ABBREVIATIONS	xii
LIST OF APPENDICES	xiii
CHAPTER 1 INTRODUCTION	1
1.1 Background	1
1.2 Addressing Environmental Impacts through Electric Vehicle Project	2
1.3 Problem Statement	2
1.4 Project Objective	3
1.5 Scope of Project	4
CHAPTER 2 LITERATURE REVIEW	5
2.1 Introduction	5
2.2 Understanding Control Theory Algorithms in the Literature	5
2.3 Vehicle Control System	8
2.3.1 Steering control	9
2.3.2 Braking system	10
2.3.3 Throttle control	10
2.4 Vehicle dynamics	11
2.4.1 Dynamic modelling	12
2.4.1.1 Bicycle modelling or two-degree-of-freedom (2DOF) modelling	12
2.4.1.2 "6DOF" and "7DOF" model	13
2.5 Steering Kinematics Modeling	14
2.6 Traction Control System	15
2.6.1 Slip control of vehicle wheels	16
2.6.2 Brake System	17
2.6.3 Acceleration pedal	18
2.7 Go-kart Vehicle	18
2.8 Vector Control	20

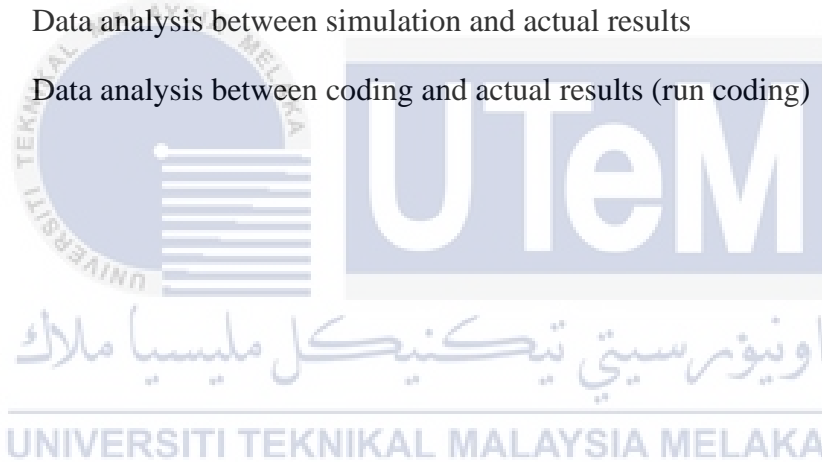
2.8.1	Indirect vector control	21
2.9	Space Vector	22
2.10	Gain Scheduling	22
2.10.1	PID Controller related to Gain scheduling	23
2.11	Comparison table of previous papers	25
2.12	Summary	27
CHAPTER 3 METHODOLOGY		28
3.1	Introduction	28
3.2	Sustainable Consideration and Development	28
3.3	Methodology representation (Flowchart)	29
3.4	System Flowchart	31
3.5	System Operation Analysis	32
3.6	Software	33
3.6.1	MATLAB/ Simulink	33
3.6.2	Arduino IDE	34
3.7	Hardware	35
3.7.1	Microcontroller board	35
3.7.2	Brushless Permanent Magnet Synchronous Motors or PMSM motors	37
3.7.3	LM393 Hall sensor module	37
3.7.4	Pulse width modulation	38
3.7.5	LM2596 DC-DC Adjustable Step-Down Voltage Regulator Power Supply	39
3.7.6	E-bike brushless sine wave controller	40
3.7.7	Potentiometer	41
3.8	Additional Components (if required)	42
3.8.1	Voltage Regulators	42
3.8.2	The Filtering Components	42
3.9	Steering Kinematic and geometrical modelling (Ackermann-Jeantnat)	43
3.9.1	Mathematical approach	44
3.10	Overview of the mechanism	46
3.11	Steady-State Handling Characteristics	47
3.12	Force, velocity and load difference based on cornering angle	48
3.13	Simulation Diagram	49
3.14	PID without Gain Scheduling	50
3.15	Sub-system – Reference Model (Vector Control)	51
3.16	Gain Scheduler – RRW	52
3.17	Gain Scheduler – RLW	53
3.18	Experiment Diagram for Hardware	54
3.19	Circuit connection	55
3.20	Conclusion	56
CHAPTER 4 RESULTS AND DISCUSSIONS		57
4.1	Introduction	57
4.2	Simulation Results and Analysis	58
4.2.1	Analysis of simulation result on different inputs	61
4.2.2	Analysis of Gain Scheduler effectiveness	62
4.3	Hardware Implementation, Results and Analysis	63
	64	

4.3.1	Actual results from EV	65
4.3.2	Performance analysis	69
4.4	Coding implementation, Results and Analysis	70
4.5	Conclusion	72
CHAPTER 5	CONCLUSION AND RECOMMENDATIONS	73
5.1	Conclusion	73
5.2	Future works	73
REFERENCES		75
APPENDICES		78



LIST OF TABLES

TABLE	TITLE	PAGE
Table 2.1	Correlation of previous works	25
Table 3.1	Arduino UNO hardware specifications	36
Table 3.2	An LM393 Hall sensor module features	38
Table 3.3	The specification of e-bike brushless sine wave controller	40
Table 4.1	Obtained Data from Simulation	61
Table 4.2	Difference between PID and GSPID	62
Table 4.3	Data analysis between simulation and actual results	69
Table 4.4	Data analysis between coding and actual results (run coding)	71



LIST OF FIGURES

FIGURE	TITLE	PAGE
Figure 2.1	Dynamic Control System Structure of Pure Electric Vehicle	6
Figure 2.2	Electric Vehicle Control System based on a CAN bus	8
Figure 2.3	Dynamic Model of DSV	9
Figure 2.4	2DOF modelling	13
Figure 2.5	6DOF modelling	13
Figure 2.6	7DOF modelling	14
Figure 2.7	Ackermann-Jeantat steering geometry model	15
Figure 2.8	Block diagram of the optimal slip ratio controller	17
Figure 2.9	Electric go-kart	19
Figure 2.10	Ackerman geometry on Go-kart	20
Figure 2.11	Transfer function (TC) for vector control algorithm based on improved variable gain PID controller	24
Figure 3.1	Project Flow chart	30
Figure 3.2	System Flow chart	31
Figure 3.3	Diagram of the system	32
Figure 3.4	MATLAB-Simulink interface	34
Figure 3.5	A sample of coding in Arduino IDE.	35
Figure 3.6	Arduino UNO R3 pinout diagram	36
Figure 3.7	Vehicle wheel with PMSM motor	37
Figure 3.8	A 5V DC LM393 Hall-effect sensor module	38
Figure 3.9	A Pulse Width Modular Converter	39
Figure 3.10	An LM2596 Voltage Regulator	39
Figure 3.11	The used E-bike brushless sine wave controller	40

Figure 3.12	(a) Steering connection with potentiometer and (b) Rotary precision potentiometer	41
Figure 3.13	The working area of driving and the steering wheels control system	43
Figure 3.14	Block Diagram of the Mechanism	46
Figure 3.15	Steering Condition	47
Figure 3.16	(a) Top view and (b) Front view of EV in right direction.	48
Figure 3.17	Simulation Diagram with PID Gain Scheduling	49
Figure 3.18	PID without Gain Scheduling (including PID gain values)	50
Figure 3.19	Sub-system – Reference Model or Vector Control	51
Figure 3.20	Gain Scheduler of Rear Right Wheel (RRW)	52
Figure 3.21	Gain Scheduler of Rear Left Wheel (RLW)	53
Figure 3.22	Experiment diagram for hardware simulation	54
Figure 3.23	Circuit connection of the system	55
Figure 4.1	Throttle = 5 and Steering angle, $\delta = 0^\circ$ (Straight path)	58
Figure 4.2	Throttle = 10 and Steering angle, $\delta = 5^\circ$ (cornering left)	58
Figure 4.3	Throttle = 10 and Steering angle, $\delta = -5^\circ$ (cornering right)	59
Figure 4.4	Throttle = 20 and Steering angle, $\delta = 10^\circ$ (cornering left)	59
Figure 4.5	Throttle = 20 and Steering angle, $\delta = -10^\circ$ (cornering right)	60
Figure 4.6	Throttle = 30 and Steering angle, $\delta = 15^\circ$ (cornering left)	60
Figure 4.7	Throttle = 50 and Steering angle, $\delta = -15^\circ$ (cornering right)	61
Figure 4.8	(a) Wiring Connection and (b) Wiring connection with EV	63
Figure 4.9	(a) Hardware setup and (b) Hardware implementation	64
Figure 4.10	V_{RRW} and V_{RLW} when $\delta = 0^\circ$ and throttle = 5	64
Figure 4.11	V_{RRW} and V_{RLW} when $\delta = -5^\circ$ and throttle = 10 (right turn)	65
Figure 4.12	V_{RRW} and V_{RLW} when $\delta = 5^\circ$ and throttle = 10 (left turn)	65
Figure 4.13	V_{RRW} and V_{RLW} when $\delta = -10^\circ$ and throttle = 20 (right turn)	66

Figure 4.14	V_{RRW} and V_{RLW} when $\delta = 10^\circ$ and throttle = 20 (left turn)	66
Figure 4.15	V_{RRW} and V_{RLW} when $\delta = -15^\circ$ and throttle = 30 (right turn)	67
Figure 4.16	V_{RRW} and V_{RLW} when $\delta = 15^\circ$ and throttle = 30 (left turn)	67
Figure 4.17	Final value from the actual results	68
Figure 4.18	Coding output from serial monitor	70
Figure 4.19	Wheel run from coding implementation	70



LIST OF SYMBOLS

δ	-	Steering angle
ω_r^*	-	Slip speed
ω_r	-	Rotor mechanical speed
θ_r	-	Rotor angle
ω	-	Vehicular velocity



LIST OF ABBREVIATIONS

<i>EV</i>	-	Electric Vehicle
<i>FOC</i>	-	Field Oriented Control
<i>PID</i>	-	Proportional – Integral – Derivative
<i>ECU</i>	-	Electric Control Unit
<i>PMSM</i>	-	Permanent Magnet Synchronous Motor
<i>HOSM</i>	-	Higher-Order Sliding Mode Observer
<i>NMPC</i>	-	Nonlinear Model Predictive Control
<i>Eco – ACC</i>	-	Ecological Adaptive Cruise Controller
<i>PHEV</i>	-	Plug-in hybrid Electric Vehicles
<i>TCH</i>	-	Traction Control System
<i>ESC</i>	-	Electric Stability Control
<i>4WID</i>	-	Four-Wheel Independent-Drive
<i>SBW</i>	-	Steer-by-Wire System
<i>SSV</i>	-	Skid Steering Vehicle
<i>DSV</i>	-	Differential Steering Vehicle
<i>LQR</i>	-	Linear Quadratic Regulator
<i>SMC</i>	-	System Management Controller
<i>HEV</i>	-	Hybrid Electric Vehicles
<i>ETCS</i>	-	Electric Throttle Control System
H_{∞}	-	Robust Controller
<i>2 – DOF</i>	-	Two-degree-of-freedom
<i>6 – DOF</i>	-	Six-degree-of-freedom
<i>7 – DOF</i>	-	Seven-degree-of-freedom
<i>ARTE</i>	-	Acoustic Road Type Estimation
<i>MTTE</i>	-	Maximum Transmissible Torque Estimation
<i>SOSM</i>	-	Sub-Optimal Sliding Mode
<i>MFC</i>	-	Ecological Adaptive Cruise Controller
<i>ABS</i>	-	Anti-lock Braking Systems
<i>IFOC</i>	-	Indirect Field Oriented Control
<i>TV</i>	-	Torque-vectoring Controllers
<i>GS</i>	-	Gain Schedulling
<i>IM</i>	-	Induction Motor
<i>FGPID</i>	-	Fuzzy Gain Scheduling Proportional, Integral, and Derivative
<i>FLS</i>	-	Full Load Setting
<i>RRW</i>	-	Rear Right Wheel
<i>RLW</i>	-	Rear Left Wheel
<i>DTC</i>	-	Direct Torque Control
<i>SVM</i>	-	Space Vector Modulation

LIST OF APPENDICES

APPENDIX	TITLE	PAGE
Appendix A	Coding	78
Appendix B	Gantt Chart for Final Year Project 2	82
Appendix C	Gantt Chart for Final Year Project 2	83



CHAPTER 1

INTRODUCTION

1.1 Background

The twenty-first century is being recognized as the period of environmental concerns, the creation of an alternative, clean, efficient, intelligent, and environmentally friendly transportation system is one of the most pressing demands of that. By combining artificial intelligence, intelligent navigation, advanced control, and communication systems, electric vehicles (EVs) provide a solution to improve traffic safety, reduce dependency on fossil fuels, increase energy efficiency, and improve air quality. Due to energy-related problems, interest in EVs has increased over the past 50 years, and great progress has been achieved in proving their feasibility in contemporary society.

There are many research and studies have been conducted to improve the field of electric vehicle technology Based on patterns of subsystem participation, the researchers divided the control system into different categories for example, acceleration slip revolution (ASR) approach appropriate for four wheels independently actuated EV. Vector control mechanism is one of the essential control methods to apply on electric vehicles.

Vector control system or field-oriented control (FOC) is a variable-frequency drive (VFD) control method used in electric vehicle systems to ensure accurate control of wheel motor torque and speed, which involves controlling the motor currents and voltages by controlled along two orthogonal axes. Due to rapid advancement in industrial automation

and robotics industries, precise and efficient vehicle control is crucial. Apart from electric vehicles (EVs), vector control methods are extensively used in Renewable Energy Systems, HVAC Systems as well as Mechatronics applications.

1.2 Addressing Environmental Impacts through Electric Vehicle Project

Environmental issues are becoming more concerning and having significant impacts on our planet. There are several key factors of environmental damage involving greenhouse gas emissions, air pollution, fossil fuel dependency which damage the atmosphere and eventually cause climate change. Considering these issues, electric vehicle usage can bring significant environmental benefits since battery, hydrogen fuel cell and renewable energy sources are used in EVs. They can contribute to changes in weather patterns through inducing zero tailpipe emissions and minimizing air pollution and greenhouse gas including reliance on fossil fuel. Efficiency of EVs can be a critical intervention, cause EVs are often considered as sustainable transportation because of multimodal mobility. Additionally, the quiet engine feature of EVs is correlated to lessen noise pollution and help the environment to be more peaceful. Overall, implementing vector control on EVs project can be immensely helpful to balance the energy and resources demand and supply resulting environmental improvement and mitigate the impacts of climate change.

1.3 Problem Statement

Traditional configurations of single motor may involve complicated mechanical system that includes brushes resulting potential drivetrain efficiency losses. In-wheel motor implementation in rear wheel is a way to overcome these obstacles and provide a more effective and comprehensive method to electric propulsion in vehicles [1]. In-wheel motors (IWMs) are crucial to the development of effective, secure, and pleasant EVs. The

advantages of IWMs' compactness and controllability enable improved vehicle maneuverability and space utilization as well as divides sources into internal and external variables [2]. Single motor for each rear has issues while managing torque distribution due to absence of a differential system. Thus, performance might be negatively impacted by uneven traction and stability problems while moving on uneven roads. While cornering, vehicle's agility might also be impacted by limited capacity to independently optimize torque. In order to maximize performance, stability, and efficiency, sophisticated and complex control algorithms are crucial which is possible by using independent motor control for each wheel. Implementing vector control on EVs proficiently requires a very deep knowledge and understanding of vehicle control theory. These factors give rise to the challenges to achieve an effective vector control method using PID gain scheduling.

1.4 Project Objective

The main aim of this project is to propose a systematic and effective methodology of advanced vector control method to ensure safety, controllability, and more stability of EVs with reasonable accuracy. Specifically, the objectives are as follows:

- a) To design and simulate a vector control technique by using Arduino UNO as the ECU with PID gain scheduling.
- b) To implement a control mechanism on EVs to maintain speed and react quickly to rapid changes in load as well as to improve the torque performance at low speeds.
- c) To evaluate the EVs control precision, dynamic response, and overall EV traction control system's controllability with hardware implementation and data analysis.

1.5 Scope of Project

The scope of this project are as follows:

- a) Design an electronic differential dynamic controller (EDDC) mechanism using Arduino UNO based on in-wheel PMSM motors.
- b) The traction system computes throttle input from acceleration pedal and cornering angle from steering. After implementation, the desired outputs deliver to the in-wheel motors (right and left rear wheels).
- c) MATLAB/Simulink is to build and simulate the system and implement into real-time simulation. Arduino IDE platform is to run C++ coding and implement into the hardware.
- d) The analysis conducts to optimize the better performance of EV traction system during low speeds driving conditions.



CHAPTER 2

LITERATURE REVIEW

2.1 Introduction

In the vast advancement of technologies, electric vehicles (EVs) have attained remarkable attention due to their potential to lower greenhouse gas emissions and reliance on natural resources like fossil fuels in recent years. To achieve high-performance operation and expand energy efficiency in EVs, the traction system must be effectively controlled. The vector control or FOC method is broadly used in EVs due to various distinct benefits of improving the overall effectiveness, range, and reliability. A proportional-integral-derivative or PID controller is frequently used to produce efficient vector control. Based on the discrepancy between the desired and actual values, the PID controller modifies the control variables of the motor. However, gain scheduling adjusts the gains of a PID controller depending on operating states. By dynamically adjusting the gains, the controller can adapt to changes in system parameters and ensure stable and optimal performance across different operating points. In this chapter, the effectiveness of each method related to the project will be discussed and analyzed. The recent studies and previous experiments that are mainly cited from journals, conference papers and articles will be justified and evaluated.

2.2 Understanding Control Theory Algorithms in the Literature

According to a study [3], the dynamic control system of pure electric vehicles can consist of three parts, the power supply system, the motor drive system, and the vehicle control system, respectively. In a vehicle control system, the core control mechanism

involves control strategy, design of control software, and energy management. Simultaneously, when the vehicle controller serves as an objective reflection of the actual development of a single-chip micro control system, the ECU measures the performance and function level of the main part of the vehicle control system. One of the key factors for determining the vehicle controller operations is the “function realization degree”, which influences directly on the control effect of EVs’ system. Figure 2.1 shows a dynamic control system structure of pure electric vehicle.

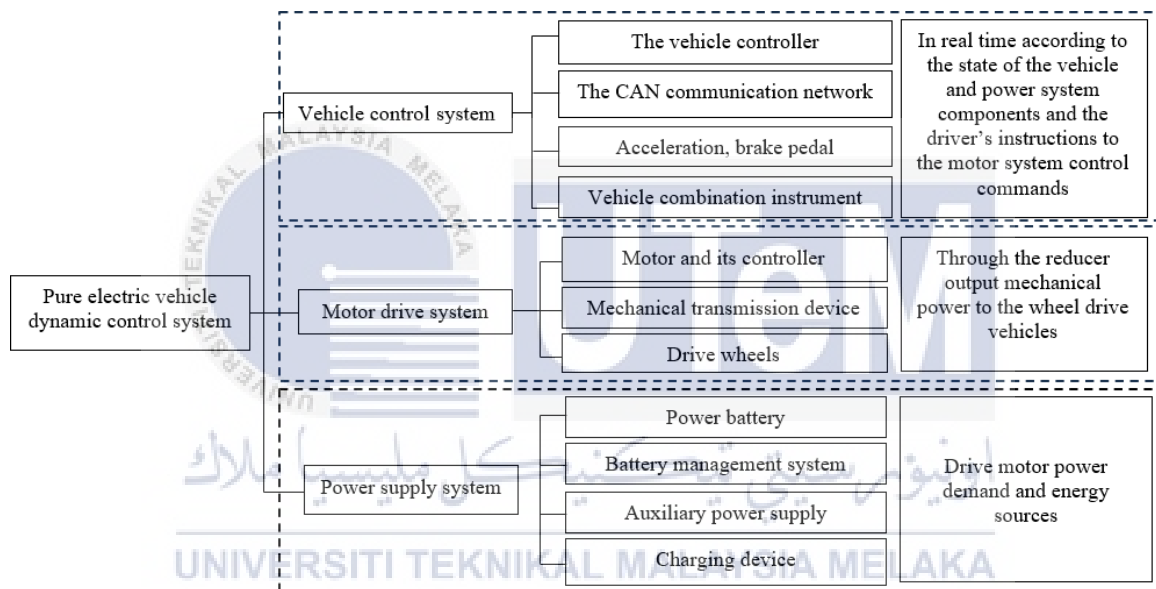


Figure 2.1 Dynamic Control System Structure of Pure Electric Vehicle [3].

The authors investigated [4] an automatic speed-tracking control for EVs with a permanent magnet synchronous motor (PMSM). Even if there are any sensor malfunctions or failures, a reconfiguration scheme has been used for maintaining precise control of speed, where a higher-order sliding mode observer (HOSM) got utilized. Also, the sensor FTC is applied as a selection mechanism to detect the sensor fault and determine between measured and estimated speeds. Another control strategy resolved by [5], is to increase the efficiency of the vehicle system by regulating an ideal velocity profile for EVs. As an optimal multi-

stage control problem, the research constructed ideal speed regulation on signalized arterials. The proposed model inspects the effect of intersection queues whether it is a temporal or spatial dimension, also by introducing an approximation model it enables a real-time operation and increases computation efficiency as well.

A paper focused [6] on modelling along with control features of parallel hybrid EVs, also discussed a comprehensive review of existing articles and analysis. The application of optimal and suboptimal control algorithms is specifically focused in terms of the development of parallel HEVs that allow the internal combustion engine to perform only in high-efficiency regions. This has helped to reduce the deficiency of ICE speed controllability because of its mechanical linkage to the wheels. Besides, another paper [7] specifically based on a Toyota Prius Plug-in Hybrid vehicle demonstrated the development and assessment of the Eco-ACC, an ecological adaptive cruise controller. Although safety and fuel efficiency are the main concerns, an onboard sensor has collected trip data in order to optimize vehicle speed. To accomplish optimal speed control, the nonlinear model predictive control technique is applied. A fast and effective control-oriented model is created and validated using a high-fidelity PHEV model to enable real-time use of the NMPC controller. A comparison of PID and linear MPC controllers and other control techniques can be used to assess the effectiveness of the controller. Resultantly, NMPC controller performance exceeds the other control mechanisms, the controller's design optimizes vehicle speed and enhances up to 19% safety and reduces overall energy consumption. To amplify vehicle stability in any critical situation. The authors proposed [8] a control strategy which is an application of direct yaw-moment in in-wheel EVs. To obtain the goal of yaw-moment control, it is possible to design an ideal yaw-moment by increasing and reducing the torque at individual wheels and then applying it to the entire vehicle model. By using linear two-degrees-of-freedom modelling, the optimum angle of slide side-slip, and the yaw rate at the

center of gravity have been calculated. A state observer gets constructed to determine and estimate the accurate side slip angle. Here, a conventional discontinuous sliding mode direct yaw-moment controller is formulated to help reduce the differentiation of actual and ideal side-slip angles and yaw rate. Consequently, the depicted second order sliding mode successfully maintained the vehicle stability as well as minimized the extreme chattering present in traditional sliding mode control.

2.3 Vehicle Control System

Vehicle control comprises the implementation and operation of different methods and Systems to regulate and control a vehicle's behaviour and performance. For a safe transition between human and automated vehicle control when the control commands are sent to the actuators that control the steering, throttle, and brakes. There are two control systems in a vehicle, namely active control systems to intervene in real-time to make optimal vehicle behaviour and passive control system in order to enhance safety and stability. Anti-lock braking systems, TCS, ESC, as well as adaptive cruise control (ACC) systems, are involved in the active control method. While, on the other hand, chassis design, steering systems, braking, and suspension systems are considered passive control techniques [7].

Figure 2.2 presents an electric vehicle control system based on a CAN bus.

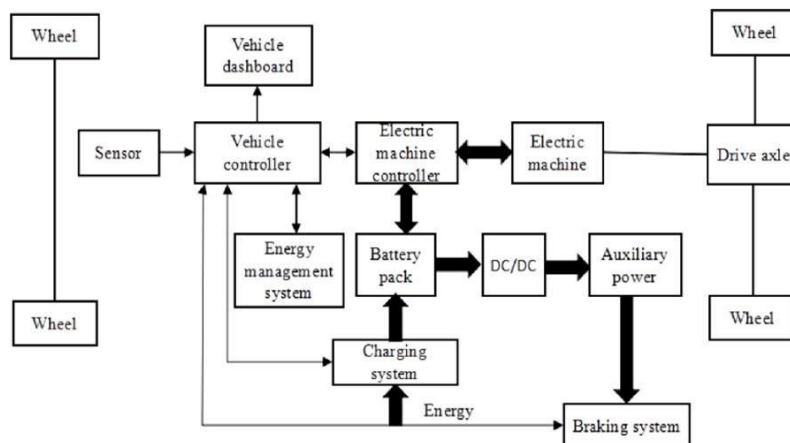


Figure 2.2 Electric Vehicle Control System based on a CAN bus.

2.3.1 Steering control

To solve the steering failure problem [9], focused on the steering and differential steering of four-wheel independent-drive (4WID) electric vehicles, as well as examining the implementation of a backup steer-by-wire system (SBW). Two controls are intended to track the yaw rate and angle of the side slip in a reference model. Compared to the SSV controller, the designed controller for DSV effectively regulates an accurate yaw rate and angle for the side slip. After investigating the overall control strategies and dynamics for differential steering and skid steering, research concluded DSV to be more effective, and robust in terms of solving the steering failure problem. A dynamic model of DSV has shown in Figure 2.3.

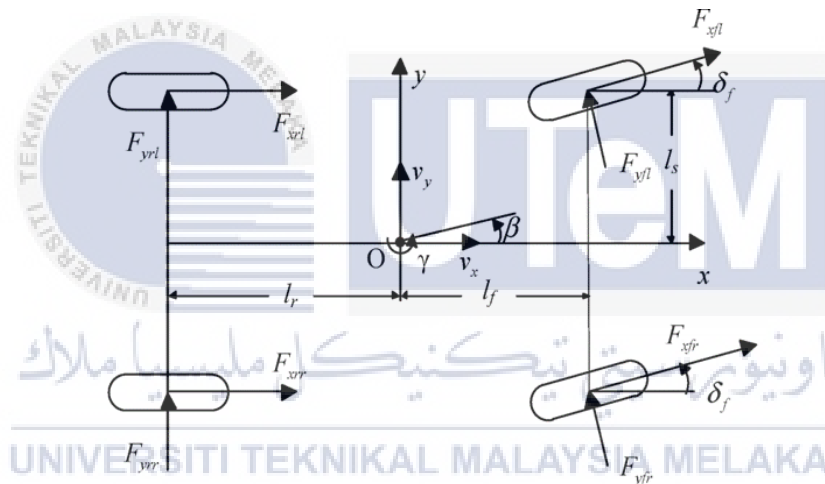


Figure 2.3 Dynamic Model of DSV [9] .

Another research [10] focuses on the improvement of stability handling capacity and robustness under different driving conditions and proposed a method by merging a 4WID control method with a (4WIS) control method. A torque distributor along with LQR, fuzzy logic, PID, and SMC controllers have been used to achieve the project objective. The 4WIS mechanism used an LQR controller to regulate the steering angles of four-wheelers meanwhile, to modify the control parameters of LQR based on the steering states, fuzzy logic parameter adjustor is applied dynamically. A PID controller is implemented in order

to track the intended speed and then the SMC controller has been implemented to respond when certain requirements are fulfilled.

2.3.2 Braking system

Regenerative braking systems are quite different from the structure of traditional friction braking systems. Usually, hybrid braking strategies can be divided into two categories, and the system is critical to acquire more recovery energy. A work illustrated [11] a procedure for delivering the braking torque for EVs with regenerative braking and four in-wheel motors. The braking torque optimization controller increases regeneration effectiveness in the case of brake safety. The MPC method solved optimization issues with various constraints and objectives effectively. The distribution of braking torque between the front and rear wheels is combined with hydraulic and in-wheel motor braking that increases the space for potential energy recovery and the stability of the vehicle. To handle safety-critical driving situations, [12] focused on the control procedure of the regenerative braking mechanism in EVs. Phase plane theory can determine the ideal brake torque for anti-lock braking system regulation. The control allocation technique splits the necessary optimal brake torque between friction brakes and regenerative brakes. The novel control strategy, namely as “Serial control strategy” successfully evaluated and validated the results through tests in different road conditions for tire adhesion.

2.3.3 Throttle control

The control strategy for hybrid electric vehicles (HEVs) that aims to achieve robust longitudinal speed control is discussed in the study [13]. The location of the electric throttle control system (ETCS) is precisely tracked in order to increase fuel efficiency and a longitudinal speed operation of EVs. Many factors like nonlinearities interrupt robust control

achievement. Basically, friction, uncertain system parameters (resulting from production errors), return springs (of ETCS), gearbox, air flow fluctuation (occurs on throttle plate), uncertain vehicle acceleration etc. are the factors that cause nonlinearities. A particularly designed speed cascade control technique is suggested that can operate the longitudinal velocity kinematics, ETCS, and intrinsic nonlinearity. Another documentation [14] specifically focuses on nonlinear HEV speed control utilizing a variety of control strategies to improve the effectiveness through throttle position control. The settling time, rise time, and no steady-state error are the important factors for examining performance analysis. Researchers have suggested many technologies for EVs; basically, the techniques are divided into two: conventional controllers like PID and artificial controllers such as fuzzy controllers, neural, and GA controllers. Traditional feedback control mechanisms or PID modify the control variable that processes all the potential error values and finally reduces them. A fuzzy controller is better suited for those structures where the mathematical formulation is hard, and operations are complex with nonlinearity and uncertainty. Robust Controller (H_∞) is used when it is challenging to apply to nonlinear systems due to the presence of noise, uncertain parameters, or disturbance.

2.4 Vehicle dynamics

In vehicle dynamics [15], the motions accomplished by accelerating, braking, turning, and riding are actions used in reaction to external influences. The empirical level and the analytical level are two ways to comprehend vehicle dynamics. In its broadest definition, the term "vehicle dynamics" refers to all modes of transportation, including aeroplanes, ships, truck-laying vehicles, and any rubber-tired vehicles. The empirical knowledge can be obtained by trial and error, the understanding of how different factors influence vehicle operation, and under what circumstances. Nevertheless, this approach can

often lead to failure. Hence, to establish an analytical model, the analytical method helps to characterize the mechanics' interest based on physics laws. Analytical methods are not full proof either; historically, many of these faults were a result of the mathematical restrictions on problem-solving. Supported by the book [16], in a dynamic system, kinematic, geographic restrictions, and physical principles are responsible for regulating the analytical formulation behaviour.

2.4.1 Dynamic modelling

While approaching dynamic modelling, along with modelling longitudinal vehicle dynamics [6], it also models the behaviour of internal combustion engines during transients. A dynamic modelling approach represents the consumption and exhaust systems of an internal combustion engine as a network of ducts linked by junctions that might characterize physical joints between the ducts like changes in area or volume, or any subsystems like an engine cylinder. Since dynamic modelling is extremely time and resource-intensive to implement, its use is frequently restricted to research fields. By concerned with the advancement of internal combustion engines, researchers suggested a number of methods to deal with these issues.

2.4.1.1 Bicycle modelling or two-degree-of-freedom (2DOF) modelling

One of the most widely used types of vehicle representation is the 2-DOF linear bicycle model due to its simplicity and low processing features. This simplified model has many great applications for control design demands that do not require hypercritical dynamics analysis. To maintain vehicle stability [8], 2DOF is used to get the optimal sideslip angle and yaw rate in this calculation as well as used to determine and gauge the real sideslip angle. While designing this dynamic model [17] certain freedoms like roll bounce and beach

get ignored, and steering angles and lateral sliding of the front and rear tires are also disregarded. When it is presumed that the velocity (longitudinal) stays constant; the tire forces (lateral) and the sliding angle have a linear relationship. A 2DOF modelling is presented in Figure 2.4.

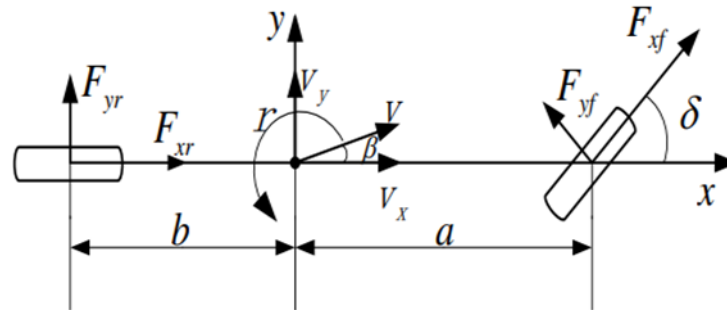


Figure 2.4 2DOF modelling [8] .

2.4.1.2 "6DOF" and "7DOF" model

6 DOF model consists of six degrees of freedom. In a controlled mobile vehicle, this model is illustrated as four DOF of rotational motion of 4 wheels, while the rest of the two DOF are conveyed as lateral and longitudinal motion. The study [18] demonstrated a model constructed by the angle of the front wheel (right) being equal to the angle of the front wheel (left) when the vehicle is moving slowly. Figure 2.5 has shown a 6DOF modelling.

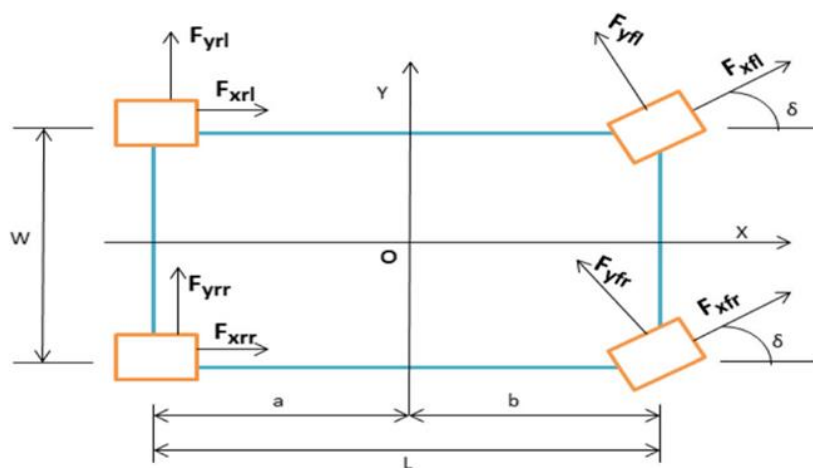


Figure 2.5 6DOF modelling [18].

The 7DOF model is equivalent to the 6DOF model though it contains extra degrees of freedom for the suspension dynamics of vehicles.

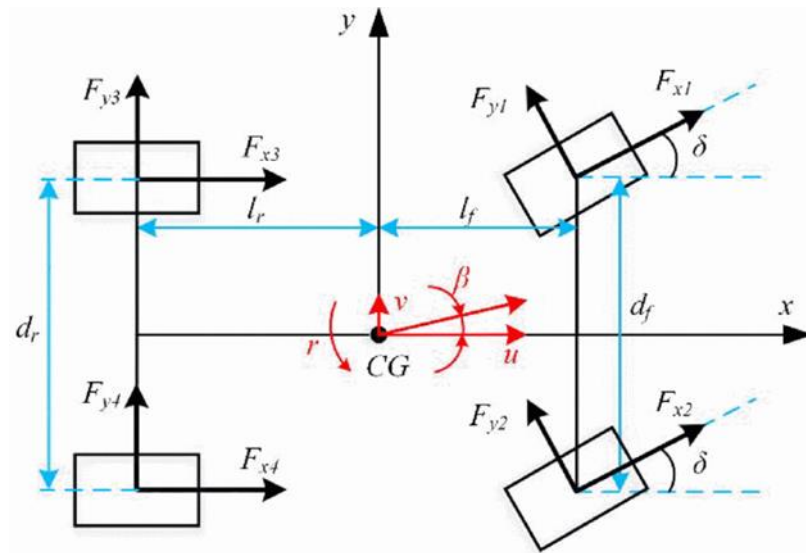


Figure 2.6 7DOF modelling [8].

2.5 Steering Kinematics Modeling

The Ackermann-Jeantnat steering geometry model is a mechanism where the steering linkages are arranged geometrically when an automobile or other vehicle is moving at a low speed. The goal of this geometry model is to accomplish a static study for vehicle steering by neglecting the effects of centrifugal force and tire side slips. According to [19], the robot's both front wheels are operated to guide the angle, and both rear wheels are utilized to move the robot. Calculating the speed of two rear wheels throughout rotation and steering is the primary aim of this mechanism. Supported by [18], the Ackermann-Jeantnat model is used for the steering operation for low-speed mode and also used to combine the vector control method with power steering. The front wheels are in control of steering the vehicle at an angle, while the rear wheels are in charge of driving with two independent hub motors. When the mechanism demonstrates the kinematic relationship between the internal and the external wheels, steering in various directions, the outer speed of the motor is greater rather

than the internal one. The Ackermann-Jeantnat steering geometry model has shown in Figure 2.7.

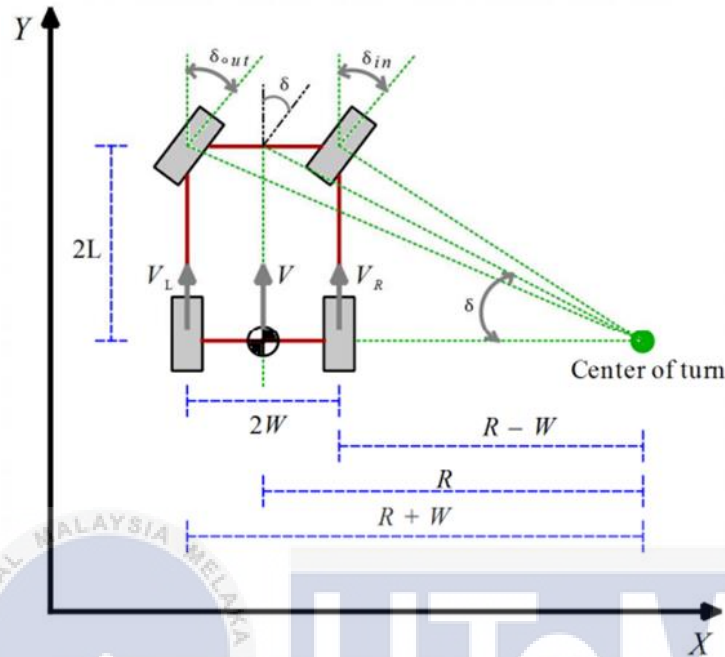


Figure 2.7 Ackermann-Jeantnat steering geometry model [19].

2.6 Traction Control System

Traction control is a system that prevents tire slides when a vehicle accelerates on an icy or slippery road, for instance. When the traction force is controlled, the driving and the operation of driving and cornering get enhanced. Two forces are exerted on the body: (longitudinal) driving and side (lateral); the slip ratio can greatly influence these force properties [20]. While designing TC systems for electric cars with onboard drivetrains, the model should consider the relaxation dynamics for tires and, more significantly, torsional dynamics for drivetrains. Moreover, the utilization of electric drivetrains can enhance the operation of traction controllers, for example, traction can be controlled through certain continuous feedback controllers that can track a reference slip ratio [21]. The research [22] applied a smart TC system by using acoustic road type estimation (ARTE) and presented the

straightforward implementation after control with direct-drive motors making the application of TCS for EVs quite promising. However, the slip ratio and road tire friction numbers are typically needed for the control system and must be estimated. The road type detection capability of the ARTE unit is utilized to retrieve the appropriate lookup table between the friction coefficient and slip ratio.

2.6.1 Slip control of vehicle wheels

The paper [23] suggested a wheel slip controller structure where the total brake torque for the vehicle is based on the driver's demand; the dynamics of the actuated brake pedal such as displacement speed can determine this. The direct slip control technique is used in the proposed WSC architecture for vehicles with IWMs, which also creates the necessary electric motor torque requirement. When the wheel slip is greater than the reference value, the WSC is independently triggered for each wheel. The study [21] discussed and implemented five slip ratio control strategies: the maximum transmissible torque estimation (MTTE) management, a first-order sliding mode control, a second-order control (using sub-optimal sliding mode or SOSM), gain scheduling (with proportional-integral (PI) control which is parameterized by vehicle speed), and/or gain scheduling (based on vehicle speed), and loop shaping-based control. The paper [20] proposed an optimum control technique of slip ratio based on a model-following approach (MFC). MFC is considered a hard approach because a more exact strategy is required if we try to adjust the slip ratio more precisely within the specified range. The slip ratio controller gets instructions and attempts to execute it when the estimator analyses road conditions and determines the ideal ratio. Figure 2.8 shows a block diagram of the optimal slip ratio controller.

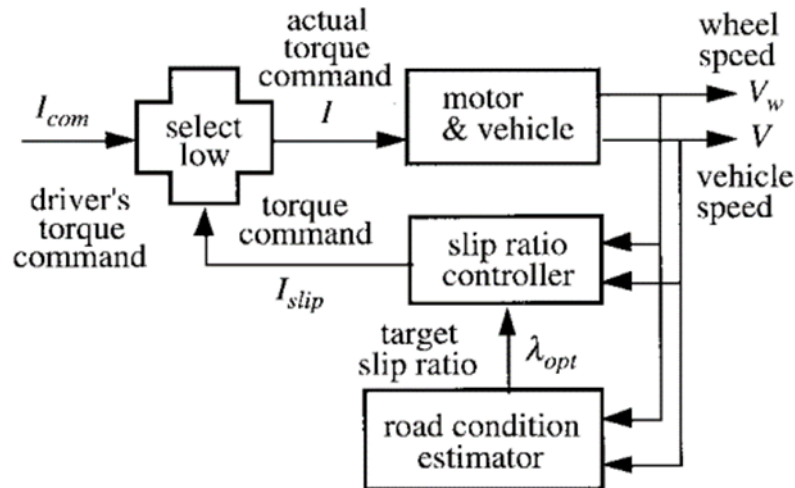


Figure 2.8 Block diagram of the optimal slip ratio controller [20].

2.6.2 Brake System

Various braking techniques are examined in this research [24]. Fully electric regenerative braking systems are very effective and have a huge future potential, therefore conventional mechanical braking systems are not used once. However, the “Hybrid Braking System” is significantly more advanced and assures comfort and safety. Regenerative braking expands a vehicle's travelling range, lessens risk, and also maximizes battery life. In advanced braking control algorithms, techniques like sophisticated electronics techniques, energy storage systems, and hybrid energy storage systems ensure high efficiency and maximum energy recovery. The authors researched [22] anti-lock braking systems (ABS), which are referred to as vehicle safety. Anti-lock braking is a usual and significant emergency condition among a number of safety-critical driving situations that include vehicle lateral and longitudinal dynamics. Only when the friction brake assumes control of the ABS does the regenerative brake force quickly disappear when the commercial EV enters an emergency braking condition.

2.6.3 Acceleration pedal

The study analyzed [18] an accelerator pedal fusion along with the brake and also a power steering pedal with Field-oriented control. The elemental component in charge of acceleration and deceleration in EVs is an accelerator pedal. If 0 is the angle value in steering, then the pedal is directly linked to vector control. Every position on the pedal signifies a particularly needed speed signal by adjusting the FOC method to the specified speed; these positions can be detected by sensors like potentiometers. If the modified speed signal is greater than the default one, FOC delivers greater positive torque to the motors for acceleration, resultantly reaching the new speed and accelerating the vehicle. On the other hand, if the produced signal is lower, the FOC delivers lower negative torque to decelerate the vehicle. The research [25] examined the control algorithm and analysis for the single-pedal function where PID control method is used to implement the launch, acceleration, braking, and parking of EVs. Resultantly, the new energy cars like pure electric vehicles are compatible with the single-pedal feature. The feature can only be utilized by regulating motor power while driving. Since the research only uses motor torque to implement the parking function, the parking deceleration at lower speeds is small; thus, it does not assure precise parking distance. Hence, researchers suggest coordination between braking systems and single-pedal.

2.7 Go-kart Vehicle

Go-kart is a compact and small, four-wheeler used especially for racing in sports. Road racing in motorsports often involves a go-kart with an open wheel or four wheels [26]. Go-kart is a single-seater driven by a two-stroke or four-stroke internal combustion machine or an electric motor [27].

The research implemented [27] some simulation design, fabrication, and chassis design as well as specific two innovative features: the usage of ultrasonic sensors for non-spatial region perception and an ignition interlock for excessive temperature. Basically, the purpose of this study is to enhance the go-kart's navigational capacities and increase the driver's comfort, potentially improving performance and safety. This reference highlighted a simple mathematical model to simulate the path travelled by the go-kart based on a specific steer angle. While another project [26] introduced a hybrid system with an additional electric motor alongside the petrol engine, to develop robustness, effectiveness, and safety features. Even though the paper focused on go-kart design, simulation, and fabrication, it specified the components used including a petrol engine (Rotax FR 125 Max) that supplies 28Hp or 21kW and a 4Hp or 3kW brushless motor. The formula K KF-2 model with FK01 Chassis gets applied to the hybrid technology. An electric go-kart is shown in Figure 2.9.



Figure 2.9 Electric go-kart.

Documentation [28] provided a thorough explanation of the design procedures involved in developing steering mechanisms for a go-kart, distinctively focusing on Ackermann Geometry. A four-bar Ackermann mechanism helps in attaining the fastest cornering speed without a tire slide. Providing the minimum turning radius, it assists to take

sharp turns when the driver is required to take sharp corners. Since the technique contains 4 links but no gears, the procedures and energy requirements for steering are easier compared to other mechanisms.

Supported by another research, [29] Ackerman geometry is perfect to prevent the front tires from sliding when both tires are turning by different angles, compared to the rack and pinion which is a simpler mechanism. The linkage arrangement allows the driver to solve the trouble of wheels on the front axle on the inside and outside while taking turns on the road. Figure 2.10 shows a Ackerman geometry on Go-kart.

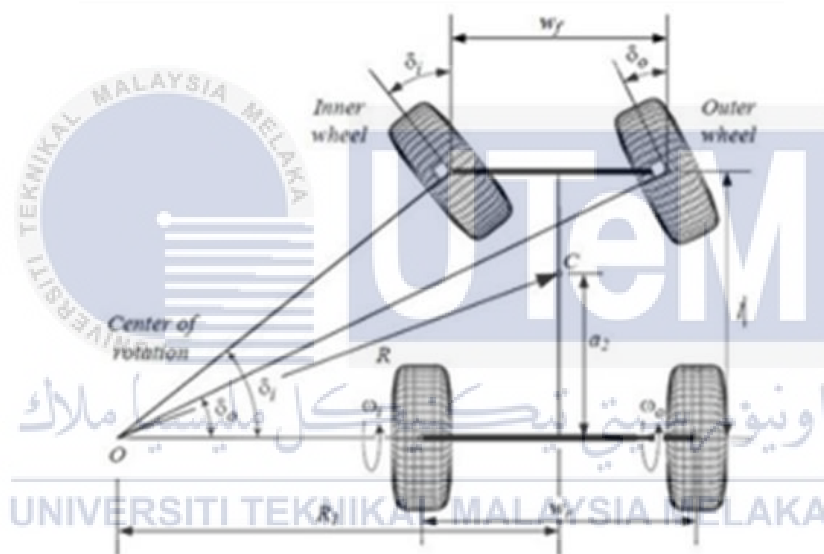


Figure 2.10 Ackerman geometry on Go-kart [29].

2.8 Vector Control

According to research [18], FOC (direct vector control) and IFOC (indirect vector control) are the two fundamental methods of vector control. For brushless DC motors and AC machines, vector control provides improved dynamic performance, allowing FOC to drive motors smoothly and precisely over their whole speed ranges with less troubleshooting; also, with optimum stable torque.

The literature [30] extensively discussed torque-vectoring control in EVs, its advantages with multiple drivetrains and the methodology to enhance stability, handling, and overall safety. A traditional TV controller consists of a reference generator, a low-level controller or a control allocator and a high-level controller. By applying torque to each wheel or drivetrain, the method can improve traction, reduce understeer, or oversteer situations as well as maximize the energy efficiency of the torque-vectoring control system with proper adjustment and modification of the reference understeer features. Additionally, the developed methods can also analyze and handle the resultant power loss of the tire slide and the drivetrain. The efficient rule-based algorithms allow the TV controller to be configured with a feedforward yaw moment, precise wheel torque distribution, and an energy-efficient reference yaw rate.

2.8.1 Indirect vector control

The primary variance [18] between indirect and direct vector control is the computing method that calculates the used number of sensors and electrical rotor angle. To determine the rotor angle, indirect vector control uses some rotor position estimation and machine parameter assessment, where the integrating summation of the calculated slip speed ω_r^* and rotor mechanical speed (ω_r) computes the rotor angle θ_r , enables precise control of the controlled motor's speed, torque, and rotor position. The high-performance technique [31] of IFOC is used to regulate the stator currents to control the induction motor (I.M.) of EVs. It operates by transforming the stator's three-phase currents into two orthogonal components.

2.9 Space Vector

An integration of Space Vector Modulation (SVM) [32] into the Direct Torque Control (DTC) approach for a Four-Wheel-Drive EV had been researched and demonstrated the emphasis of drivetrain performance, implicit switching states of inverters and properties of traction chain's dynamic. Specifically on uneven and rough roads, wheel speeds control and motor control reach great precision. Focusing on the DTC performance on the traction motor control system of a battery-based EV, another research [33] explored the effectiveness of DTC with and without SVM. Resultantly, DTC with SVM signified well-controlled and fast response torque as well as sensor less control accuracy exceeding 98% covering whole speed range. Apart from DTC, the effective use of SVM algorithms and desired motor control outcomes establish the efficiency of space vector technique in power delivery system of EV [34]. In this motor operation, intermediate and big vectors are used in SVM allowing it to control the inverter's switching states precisely. Another study [35] particularly in the context of semiconductor switch failures and their impact on degraded operating modes synthesize PWM with space vector control methods for an H-bridge inverter that is capable to power up a 3-phase PMSM. Distinctively one method integrates a number of advantageous as switching losses minimization, maximize drive performance, resist to duty-cycle changes, small current ripple in zero-sequence validates the proficiency of space vector.

2.10 Gain Scheduling

The documentation [36] addressed the basic characteristics of gain scheduling for non-linear control design. The paper discussed two procedures for designing these models: a manifold of constant equilibria linearization and quasi-LPV process, also demonstrated using a pitch-axis missile model and a first-order PID control problem. As concluded, the

gain-scheduling controller is designed to provide expectant stability and performance characteristics. Evidently, gain scheduling also functions effectively under different operating situations and during changes in operating conditions as well. Supported by the following study, [37] articulated that one of the most widely used techniques for nonlinear control design is gain scheduling (GS) and GS controllers are recognized for their better performance than robust ones. To ensure closed-loop durability and guaranteed expense for all set parameter modifications, the paper suggested a method based on the Lyapunov theory and BMI. According to the results, in a closed-loop system, gain schedule controllers perform better than traditional robust controllers. Furthermore, they are also able for weighting matrices R , Q , and S to impact quality and cost.

2.10.1 PID Controller related to Gain scheduling

When the common PID control algorithm is used in driving control, it usually restricts the acceleration capacity and dynamic operation of the driving system. Thus, [38] proposed a developed variable gain PID control method to enhance the acceleration operation of EVs, more specifically increase motor velocity rapidly without any overshooting. Based on certain operating circumstances and acceleration requirements, the modified gains along with proportional, integral, and derivative terms of PID can acquire the EV's response and improve acceleration performance. Besides the strategy meets the objective of optimal acceleration capability and performance when EV operates at high, moderate, low, or irregular velocity. A Transfer function (TC) for vector control algorithm based on improved variable gain PID controller has shown in Figure 2.11.

2.11 Comparison table of previous papers

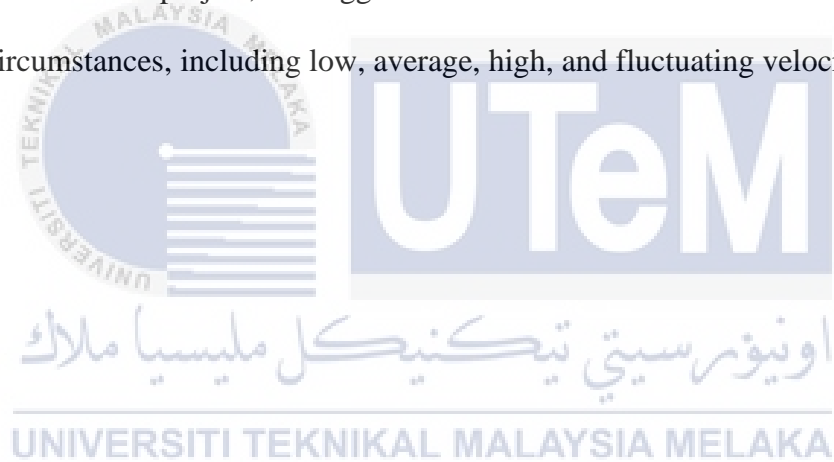
Table 2.1 Correlation of previous works

No.	Reference	Author(s)	Component/ Mechanism	Advantage	Disadvantage
1	[3]	Haiying Wang, Tianjun Sun	ECU, Motor Controller.	Improved energy efficiency, reduced emissions, enhanced performance, regenerative braking.	Complex system integration, limited driving range, higher initial cost, charging infrastructure.
2	[4]	Michael Defoort, Hamid R. Karimi	HOSM Observer, Sensor Fault Detection Threshold, Motor Torque Control.	Improved driver comfort, robustness to sensor faults, real-time performance.	Sensitivity to threshold selection, limitations of threshold-based approach.
3	[7]	Mahyar Vajedi, Nasser L. Azad	Onboard Sensor, Nonlinear Model Predictive Control, Control-oriented Model.	Enhanced driving safety, trip-specific optimization, fuel economy improvement.	Parameter sensitivity, computational requirements.
4	[8]	Lu Liu, and Wei Xing Zheng	State Observer, Sliding Mode Controllers, Nonlinear Disturbance Observer.	Enhanced vehicle stability, improved control performance, disturbance rejection.	Controller tuning, sensitivity to model accuracy, complexity of implementation.
5	[9]	Jie Tian, Jun Tong, Shi Luo.	Steer-by-Wire (SBW) System, Yaw Rate and Sideslip Angle Control	Skid steering limitations addressed, backup steering system, enhanced control flexibility.	Torque limitations, potential system complexity.
6	[12]	Lisheng Jin, Linlin Gao	4WID, 4WIS, Coordination System.	Handling stability, robustness on different road conditions, comprehensive control effect	Validation requirement.

7	[13]	Jiaqi Xue, Xiaohong Jiao	Primary Speed Adaptive Controller, ETCS.	Enhanced longitudinal speed performance, improved fuel economy	Complexity of control design
8	[18]	Nady Ibrahim , Mohamed Abdelaziz, Maged Ghoneima	Induction Motors, Power Steering System, Vector Control System, Ackermann-Jeantnat Model.	Efficiency, safety, controllability, troubleshooting.	Manual switching, dependency on battery.
9	[23]	Dzmitry Savitski, Valentin Ivanov	Wheel Slip Control (WSC) Architecture, Integral Sliding Mode Controller.	Improved traction and stability, enhanced driving safety, control quality.	Sensitivity to model parameters, complexity, validation requirements.
10	[25]	Zhao Yongqiang, Zhang Xin	Pure Electric Vehicle, Single-Pedal Function, PID Control Algorithm.	Enhanced efficiency, optimization support, simplified experience.	Parking control limitations.
11	[26]	Mohamed Haseb	Rotax FR 125 Max Petrol Engine, Electric Brushless Motor, Formula-K FK 01 Chassis	Increased reliability, improved Efficiency and reduced emissions, enhanced safety	Manual switching, limited electric-Only operation, complexity.
12	[34]	Gang Qin, Mushuang Liu	Variable Gain PID Control Algorithm, Asynchronous Motor Model.	Improved acceleration performance, dynamic performance, simplicity and compatibility.	Switching impact.

2.12 Summary

Studying different papers and reviewing literature offers a thorough understanding and analysis of previous research and academic paper on a specific topic. In this chapter comprehensive reviews and findings from previous works have been documented. Although there are relatives' methods and mechanisms have been found in the previous works, they are not entirely similar to the project of implementing vehicle vector control with PID gain scheduling. Though, the review critically analyzes the correlations and necessary methods to apply. The authors have suggested different techniques and mechanisms to apply on electric vehicles. In this project, the suggested method was created to accommodate a range of driving circumstances, including low, average, high, and fluctuating velocities.



CHAPTER 3

METHODOLOGY

3.1 Introduction

The methodology is an essential step when we are performing any research or project. The systematic procedures and framework help us structure, execute and optimize the performance and achieve the project's goal. In this chapter, the step-by-step methods used in this project will be explained, involving the mechanisms, works, components, resources, and so on.

In my project, the methodology is conducted to reach the aim of how to implement vector control on an electric vehicle traction system where an Arduino-based ECU is used for better speed holding and better response to sudden load changes; secondly, PID gain scheduling is utilized for higher accuracy, safety, durability, controllability in any unstable surface. The methodology will assist to evaluate the whole system according to different phases such as analysis, planning, designing, implementing, and assessing. Research papers, articles, journals, books, and various other sources are used to complete the system.

3.2 Sustainable Consideration and Development

While designing and implementing an EV-based project, sustainability is an important aspect. Selecting appropriate components and techniques is one of the key factors to reduce a negative environmental impact and maintain sustainability. In that case, it may include choosing materials that are biodegradable, and recyclable and techniques that consume less energy which can improve energy efficiency throughout the project.

Since EVs are known for low carbon emissions features, by enhancing their performance, it is possible to reduce extra power oscillations and emissions. Meanwhile, control algorithms will also help to manage and maintain longer battery life. Thus, the battery will rarely need any replacement subsequently, contributing to sustainable resources and also cost-efficient. A regenerative braking system is another factor that can help sustainability by increasing energy recovery and minimizing energy wastage in the vehicle. Moreover, a lifecycle analysis can be conducted to support and ensure the sustainable development of this project, including environmental impacts related to the usage, and disposal of the components as well as areas where sustainability improvement is possible.

3.3 Methodology representation (Flowchart)

To perform a successful and effective project, it is necessary to organize the procedures in the form of visual representation or diagram. A flow chart uses different symbols to categorize the type of activity and helps to illustrate the flow of the whole system. Flow charts also help to break down any complex problem in a simpler form, find any errors or limitations and solve them in a constructive way. The process flow or flow chart of the project has been demonstrated in Figure 3.1.

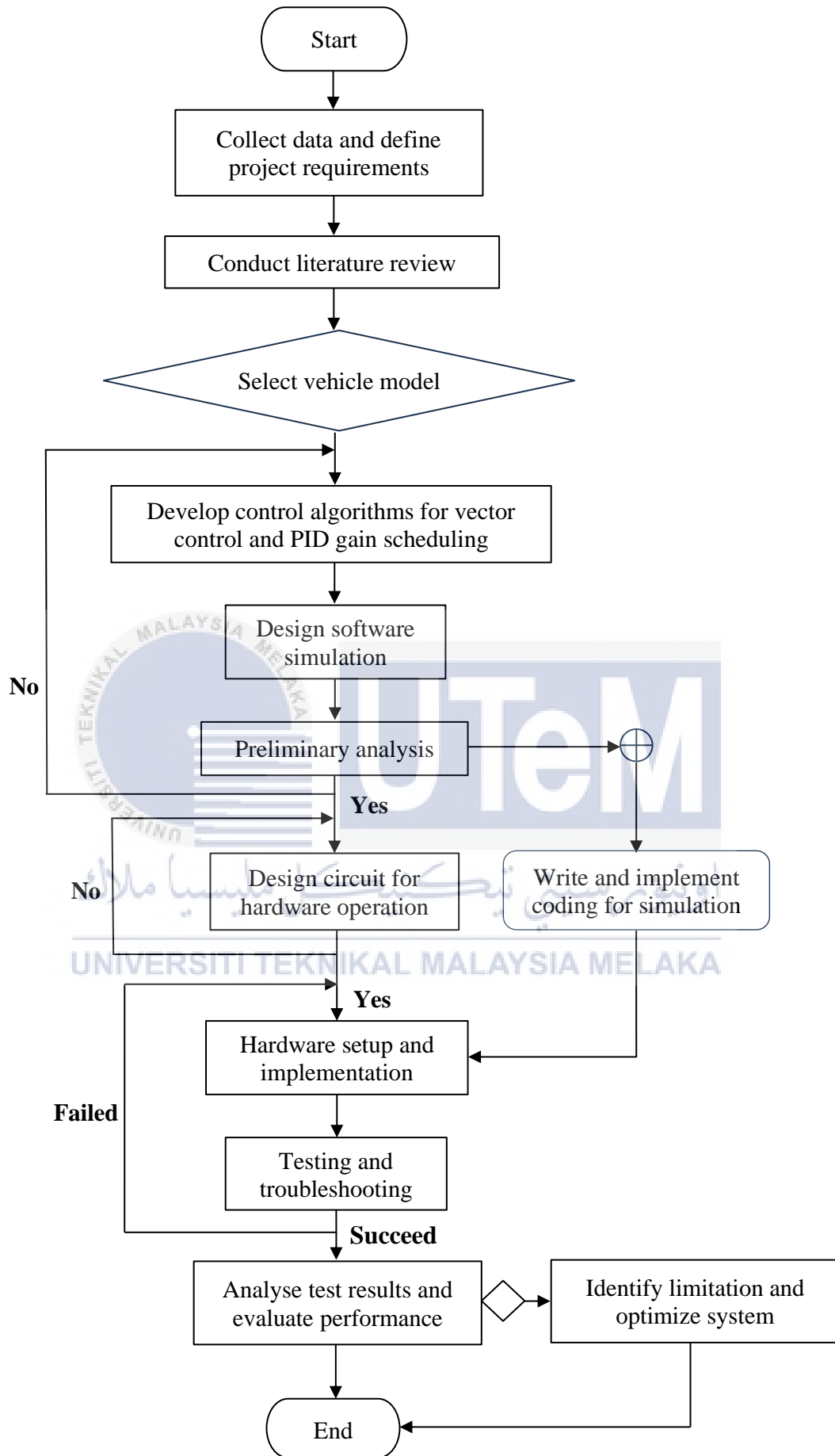


Figure 3.1 Project Flow chart

3.4 System Flowchart

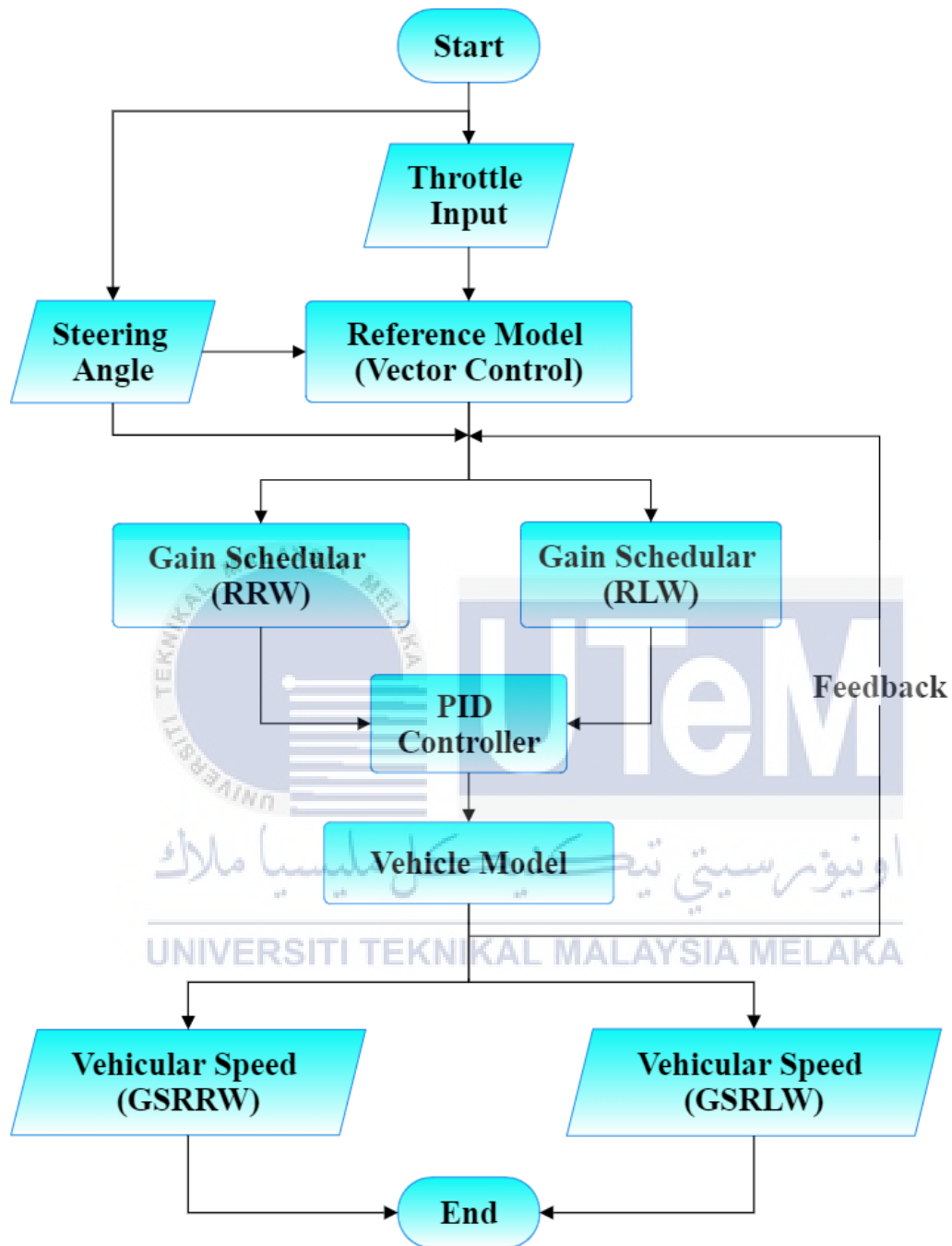


Figure 3.2 System Flow chart

Figure 3.2 illustrates the workflow of the system including feedback, where the two inputs are throttle and steering angle, and the two outputs are vehicular speed come from right rear wheel and left rear wheel.

3.5 System Operation Analysis

The traction control system for the EVs' rear wheels is the main focus of my project where the execution of the vector control method is applied to the PMSM motors installed on the rear wheels. The use of vector control is to establish an optimum torque and better stability during the load change when the vehicle is at low-speed conditions. For operating the system, the input comes from the steering and acceleration pedal. The control algorithm (Vector control with PID gain scheduling) will accept the obtained data to accomplish the desired motor performance. The controller tools are used to produce proper signals such as adjusting the voltage and current level. Safety precautions and monitoring of the system operation are also important to ensure safe and effective performance.

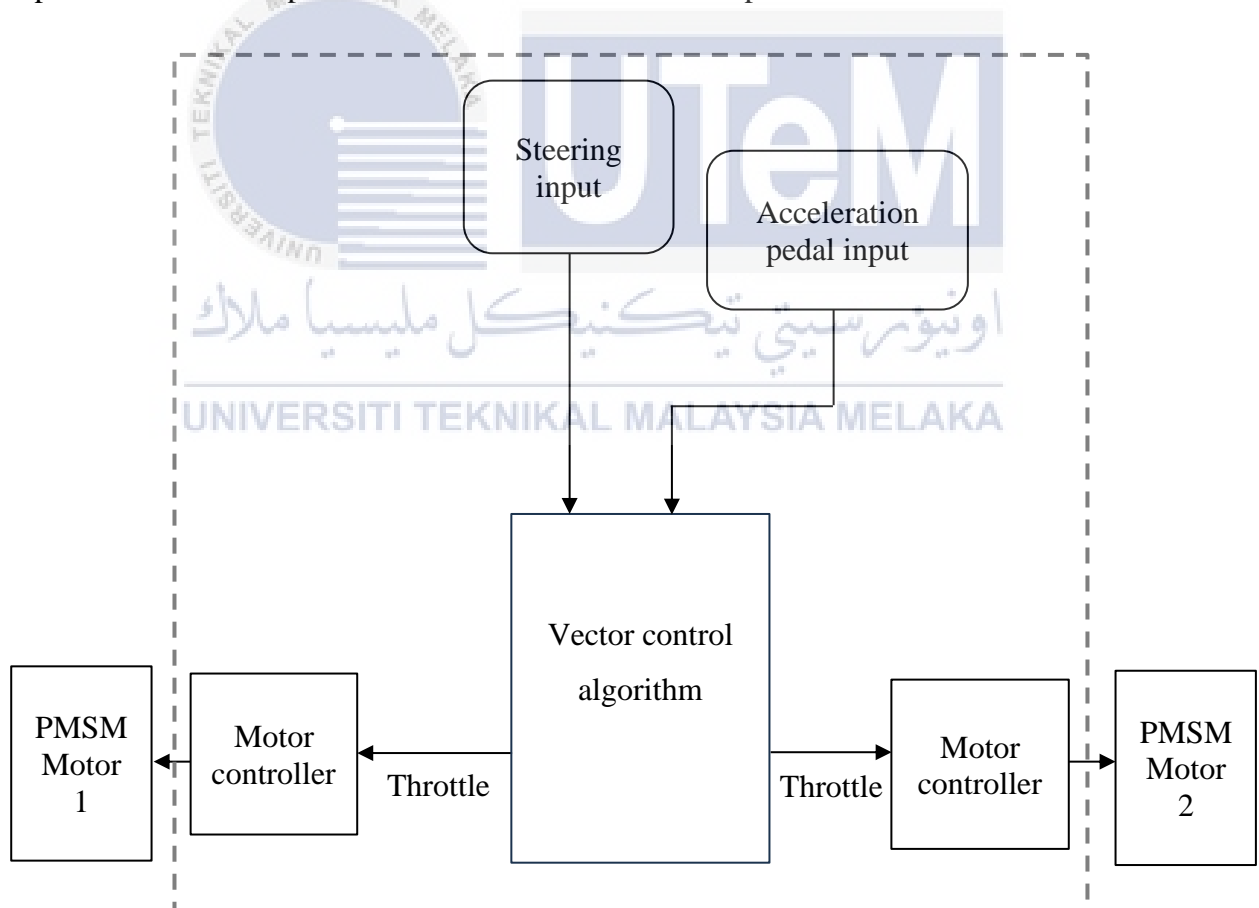


Figure 3.3 Diagram of the system

A diagram of the system has shown in Figure 3.3.

3.6 Software

Software implementation is a crucial part of this project. Designing and simulating in a software platform allows us to simplify and understand complex algorithms before real-time adjustment. Particularly in this project, the gain PID scheduling needs continuous monitoring of all the parameters and variables. It also helps to visualize inside operations, determine errors, and problems also solve them before operating in the real system.

3.6.1 MATLAB/ Simulink

Apart from the development and analysis of algorithms, it is also possible to perform complex mathematical equations and simulations in MATLAB software. For my project, MATLAB/Simulink is crucial software since no other software is appropriate to construct and implement gain PID scheduling. Specifically, Simulink will be used for gain scheduling of the PID controller due to its built-in blocks and library features. Model-In-The-Loop (MIL) and Hardware-in-the-Loop (HIL) testing is also possible to conduct. The MIL simulation model is based on the Simulink platform and allows for a detailed analysis of the electric vehicle traction system, including the torque control and dynamic performance of the electric motors. It includes a detailed vehicle model, an electric machine model, and power electronics model as well. HIL testing allows to combine of control algorithms with actual hardware parts, besides evaluating the behaviour of the system in real-time by connecting the Simulink model to real-time hardware interfaces (motor controllers or sensors). Figure 3.5 shows a MATLAB-Simulink interface example.

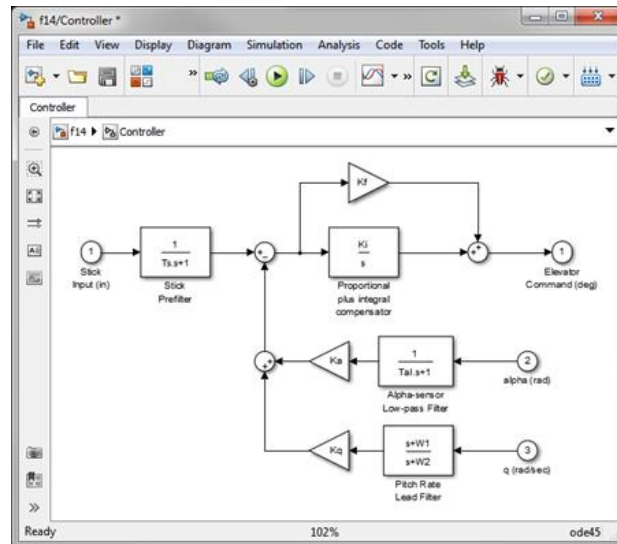
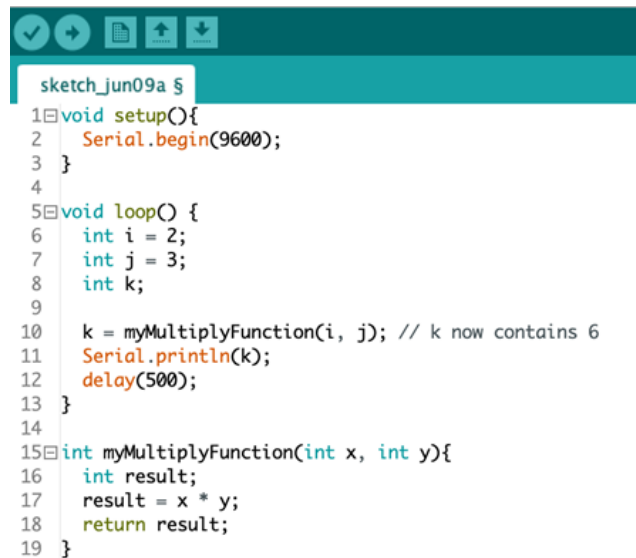


Figure 3.4 MATLAB-Simulink interface.

3.6.2 Arduino IDE

The software was created particularly for programming Arduino microcontrollers. The Integrated Development Environment enables users to create and upload code to boards using Arduino microcontrollers, the widely used Arduino Uno, Raspberry PI, and Arduino Nano for instance. It is best suited to create firmware for electric car traction systems using the programming language, which is mainly C/C++. It allows the code to communicate with the hardware elements linked to the Arduino board without any trouble. Additionally, the serial monitor adds debugging tools to work to analyze the ports and monitor the system behaviors and also, solve if there is any issue occurs. For the control mechanism, it is easier to write, build and upload in Arduino IDE. Then transfer and simulate it to the Proteus circuit design and observe the operational behaviors. Figure 3.4 has shown a sample coding in Arduino IDE software.



```
sketch_jun09a $
1 void setup(){
2   Serial.begin(9600);
3 }
4
5 void loop() {
6   int i = 2;
7   int j = 3;
8   int k;
9
10  k = myMultiplyFunction(i, j); // k now contains 6
11  Serial.println(k);
12  delay(500);
13 }
14
15 int myMultiplyFunction(int x, int y){
16   int result;
17   result = x * y;
18   return result;
19 }
```

Figure 3.5 A sample of coding in Arduino IDE.

3.7 Hardware

First, selecting appropriate components is essential to design a hardware electric circuit. Second, for implementation, it is necessary to assemble the PMSM motors, Arduino board, sensors and other required parts or components of the hardware together physically and ensure they are compatible with one another and have compatible electrical connections.

3.7.1 Microcontroller board

The Arduino Uno microcontroller board consists of a ceramic resonator (CSTCE16M0V53-R0) with 16 MHz, a total of 22 pins, 6 PWM outputs (included in the digital pins, a USB port, also a power connector. It also contains a reset button, an internal LED attached to pin 13, and an ICSP connector for externally programming the microcontroller. To get started, it must link to a USB cable for computer connection, or a suitable battery or an AC-to-DC converter for power supply. An external DC power source (7-12V) or USB port can be used to power the Arduino Uno though it runs on a 5V DC voltage. The microcontroller board will handle the processing and control functions of the

PMSM motors by taking input from sensors. Figure 3.6 demonstrates a pinout diagram of Arduino UNO R3.

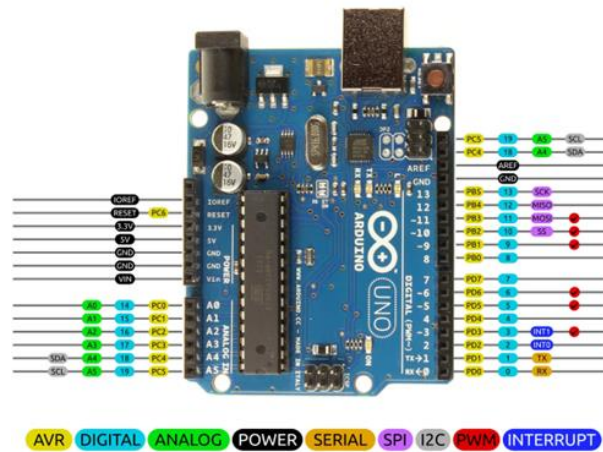


Figure 3.6 Arduino UNO R3 pinout diagram

Table 3.1 Arduino UNO hardware specifications

Microcontroller:	ATmega328P
Operating Voltage:	5V
Input Voltage (recommended):	7-12V
Input Voltage (limit):	6-20V
Digital I/O Pins:	14 (0 – 13) (of which 6 provide PWM output)
PWM Digital I/O Pins:	6 (3, 5, 6, 9, 11)
Analog Input Pins:	6 (A0 – A5)
DC Current per I/O Pin:	20 mA
DC current for 3.3V Pin:	50 mA
Flash Memory:	32 KB of which 0.5 KB used for Bootloader)
SRAM:	2 KB (ATmega328P)
EEPROM:	1 KB
Clock Speed:	16 MHz
LED_BUILTIN:	13
Length and Width	68.6 mm × 53.4 mm
Weight	25g

3.7.2 Brushless Permanent Magnet Synchronous Motors or PMSM motors

PMSM motors are highly effective and safe. They contain more torque than AC Induction Motors (AICMs) while having 0 rotor current and smaller frame size due to their rotor (a permanent magnet). The high power-to-size ratio helps to minimize the system design without any torque loss. Commutation is a must for PMSMs because the winding design and waveforms must be sinusoidal for optimum operation. PMSM motors are applied in electric go-karts' rear wheels because their power density, precise torque control, and speed control help to obtain great performance and good controllability. Figure 3.7 shows the vehicle wheel with PMSM motor.



Figure 3.7 Vehicle wheel with PMSM motor

3.7.3 LM393 Hall sensor module

A hall-effect sensor module is utilized to identify if there is any magnetic field. If there is any existence of a magnetic field, the module increases the output, whereas if there is no magnetic field it decreases. In this project, a hall-effect sensor module is an ideal choice to determine the position and speed of the PMSM motor because based on the variations in magnetic fields it can detect the location and speed information. As the rotors' magnetic poles or magnets pass the sensor it can measure the angular position of the rotor allowing accurate control. An LM393 Hall-effect sensor module with a 5V DC is compatible with the

system since the operating voltage of the microcontroller is also 5VDC. A 5V DC LM393 Hall-effect sensor module is shown in Figure 3.8.

Table 3.2 An LM393 Hall sensor module features

Component:	LM393 Hall sensor module
Input Power:	5VDC
Main chip:	LM393, Allegro 3144 Hall Effect Sensor
LED indicators:	2, 1 for power and 1 for digital output
Simple interface:	AO, DO, VCC, GND
Dimension:	2.7cm x 1.4cm

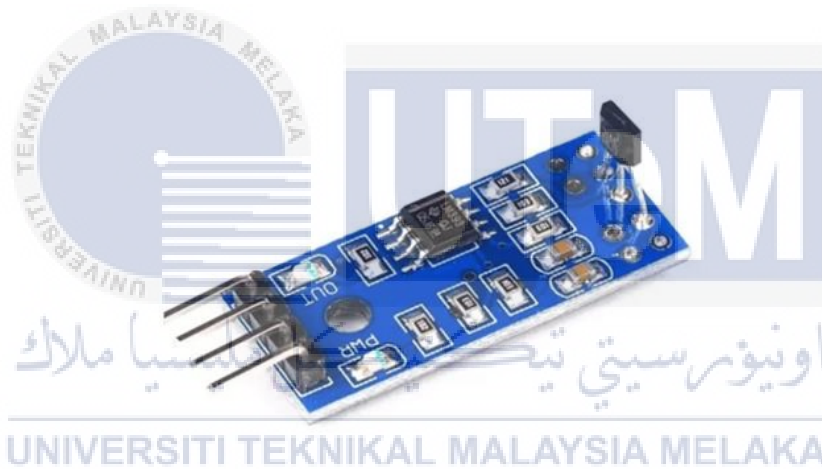


Figure 3.8 A 5V DC LM393 Hall-effect sensor module

3.7.4 Pulse width modulation

PWM is a process which generates width-varying pulses to simulate the amplitude of an analogue input signal. High-amplitude signals turn on the output switching more often compared to the time low-amplitude signals turn it off. This technique will help to control the voltage and current level delivered to the PMSM motors; if the power supply escalates, it changes the duty cycle and minimizes the level of power distribution. PWM is also useful in terms of regulating the motor output of torque and speed control. The PWM signals duty

cycle change if the average current changes thus, it alters the torque and helps to acquire precise torque control. Figure 3.9 shows a pulse width modular converter.

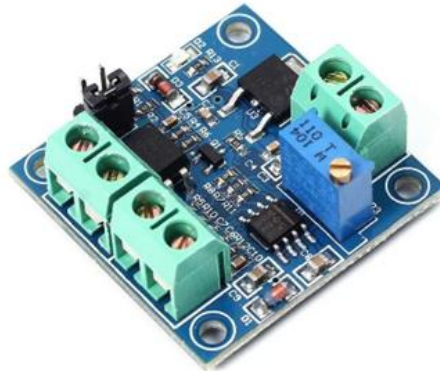


Figure 3.9 A Pulse Width Modular Converter

3.7.5 LM2596 DC-DC Adjustable Step-Down Voltage Regulator Power Supply

This regulator is a power supply that regulates consistent power and prevents voltage fluctuations when there are various components with different specifications. The microcontroller operates at a specified voltage level and this voltage regulator assures that the delivered voltage is at the minimum range when the input or battery voltage is high. By regulating a proper voltage, it also reduces the power loss during the conversion and improves the system's overall efficiency. An LM2596 Voltage Regulator is shown in Figure 3.10.



Figure 3.10 An LM2596 Voltage Regulator

3.7.6 E-bike brushless sine wave controller

Electric bike brushless sine wave controllers are electrical devices that can control brushless DC motors (BLDCs). It particularly creates a sine wave signal to regulate the motor speed and torque leading to smoother and more effective functioning, reducing motor noise and vibration. These controllers minimize energy losses and heat production in the system and improve motor performance. Apart from regulating better torque and acceleration, it also supports regenerative braking. This characteristic enables the motor to function as a generator and recharge the battery when the brakes are engaged. Figure 3.11 shows the E-bike brushless sine wave controller used in the system.

Table 3.3 The specification of e-bike brushless sine wave controller

Type:	ZL 48V 72V-15GMS-120°-1500W
Related Current:	Current 42A
Lot No:	ZL20L031
Function:	Cruise/Three speed



Figure 3.11 The used E-bike brushless sine wave controller

3.7.7 Potentiometer

A potentiometer is three terminal manually adjustable variable resistor. By rotating a potentiometer, it is possible to set and regulate desired inputs, outputs. “Rotary precision potentiometer” or “multi-turn POT” is ideal selection to sense the steering angle because of its inherent memory characteristic. Elaborately, if a magnetic encoder is used for input angle, once the power is removed or the system is restarted the encoder typically starts with initial states. But modern rotary precision potentiometer has non-volatile memory that can retain its settings position or other relevant data even when power is removed. It is also useful to deliver a reference signal for any adjustable speed or torque.



(a) Steering connection with potentiometer

(b) Rotary precision potentiometer

Figure 3.12 (a) Steering connection with potentiometer and (b) Rotary precision potentiometer

Figure 3.12 shows the Rotary precision potentiometer connected to the steering system of the EV.

3.8 Additional Components (if required)

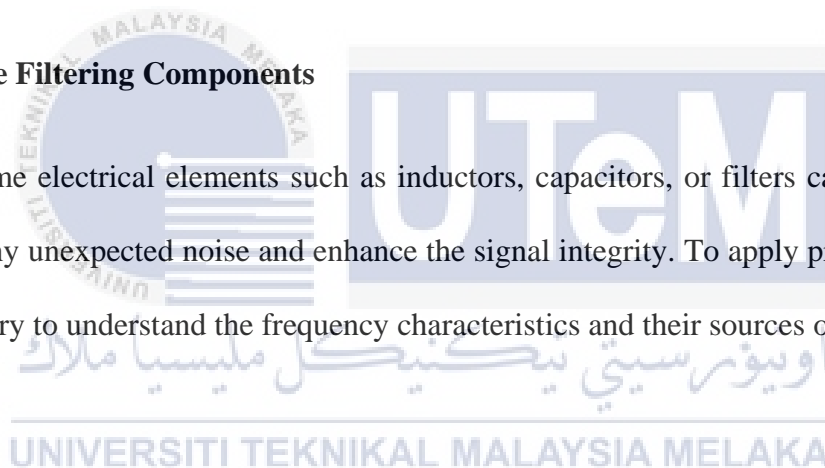
There are some additional components that might need to be used in certain circumstances or for any extra application.

3.8.1 Voltage Regulators

Since the system uses a hall sensor module, there is no need to use additional voltage regulators. However, it might be necessary for certain conditions if the power supply voltage varies and become uncontrollable. The voltage regulator also helps to complete the electrical components with different voltage ranges and assures are consistent voltage supply.

3.8.2 The Filtering Components

Some electrical elements such as inductors, capacitors, or filters can be useful to eliminate any unexpected noise and enhance the signal integrity. To apply precise filtering, it is necessary to understand the frequency characteristics and their sources of noise.



3.9 Steering Kinematic and geometrical modelling (Ackermann-Jeantnat)

While working on the in-wheel mechanism, Ackermann-Jeantnat is best as the steering geometry model as it analyzes the statics of the vehicle and eliminates the effects of centrifugal force and tire slip. Figure 3.12 demonstrates the working area of driving and the steering wheels control system.

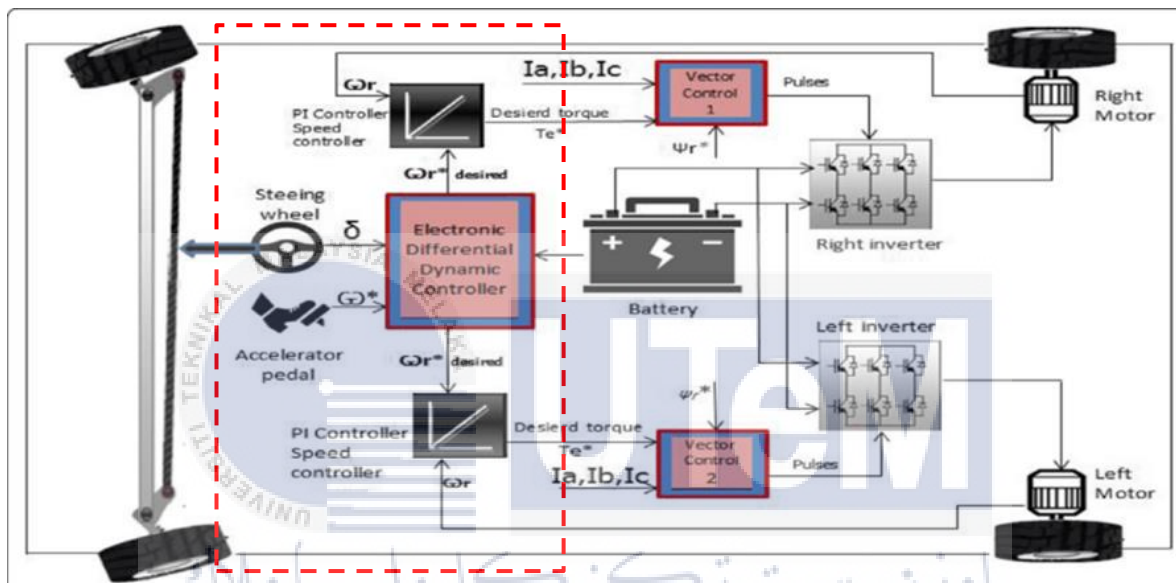


Figure 3.13 The working area of driving and the steering wheels control system

When there is no steering angle implemented, no cornering angle of the wheels and the vehicle moves in a straight line and there is no specific need for vector control. But, when there is a steering angle implemented there will be different loads and speeds in two rear wheels, to optimize the differentiation this project designs a vector control algorithm on the vehicle and build-in an electronic differential dynamic controller mechanism. The throttle wheel angle and steering angle work as inputs and the desired speed and voltage for both rear wheels work as output during rotation in steering.

3.9.1 Mathematical approach

The velocity of the rear right wheel motor, V_{rr} -

$$V_{rr} = \omega \left(1 + W \times \tan \left(\frac{\delta}{2 \times L} \right) \right) \quad (3.1)$$

The velocity of the rear left wheel motor, V_{rl} -

$$V_{rl} = \omega \left(1 - W \times \tan \left(\frac{\delta}{2 \times L} \right) \right) \quad (3.2)$$

where V_{rr} and V_{rl} are the vehicular velocity or vehicle speed calculated depending on the accelerator pedal position, δ is the vehicle steering angle, ω is used for throttle input, W is the distance between two rear wheels, L is the distance between front and rear wheels. The value is $L=1.35$ m and $W = 1.25$ m in the Go-kart.

As the steering angle δ specifies the trajectory direction, it can be defined, $\delta = 0$ when the EV is going in a straight line.

When $\delta = 0$,

$$\begin{aligned} V_{rr} &= \omega \left(1 + W \times \tan \left(\frac{0}{2 \times L} \right) \right) \\ &= \omega (1 + W \times \tan 0) \\ &= \omega (1 + W \times 0) \\ &= \omega (1 + 0) \end{aligned}$$

$\therefore V_{rr} = \omega$, or, $V_{rl} = \omega$, no difference.

When $\delta > 0$ turn left (assume $\delta = 5^\circ$)

$$\begin{aligned} V_{rr} &= \omega \left(1 + 1.25 \times \tan \left(\frac{5^\circ}{2 \times 1.35} \right) \right) \\ &= \omega (1 + 0.0404) \\ \therefore V_{rr} &= \omega (1.0404). \end{aligned}$$

$$V_{rl} = \omega \left(1 - 1.25 \times \tan \left(\frac{5^\circ}{2 \times 1.35} \right) \right)$$

$$= \omega (1 - 0.0404)$$

$$\therefore V_{rl} = \omega (0.9596),$$

Here, $V_{rr} = \omega (1.0404) > V_{rl} = \omega (0.9596)$. Thus, if $\delta > 0$ turning left, the right rear wheel velocity is more compared to the left one, and this difference will increase, if the steering angle increases.

Subsequently, $\delta < 0$ turns right (assume $\delta = -5^\circ$), $L=1.35$ m, $W = 1.25$ m

$$V_{rr} = \omega \left(1 + 1.25 \times \tan \left(\frac{-5^\circ}{2 \times 1.35} \right) \right)$$

$$= \omega (1 - 0.0404)$$

$$\therefore V_{rr} = \omega (0.9596),$$

$$V_{rl} = \omega \left(1 - 1.25 \times \tan \left(\frac{-5^\circ}{2 \times 1.35} \right) \right)$$

$$= \omega (1 - (-0.0404))$$

$$\therefore V_{rl} = \omega (1.0404),$$

Here, $V_{rl} = \omega (1.0404) > V_{rr} = \omega (0.9596)$. Thus, if $\delta < 0$ turns right, the left rear wheel speed is more compared to the right one, and this difference will increase if the steering angle increases.

The mathematical equations 3.1 and 3.2 are the reference for the system and the obtained results clearly indicated that there is always speed and velocity difference in two wheels depending on the steering angle value and direction. Hence, to minimize the differential condition by obtaining the desired outputs and achieve higher stability and controllability, the vector control algorithm using PID gain scheduling is conducted.

3.10 Overview of the mechanism

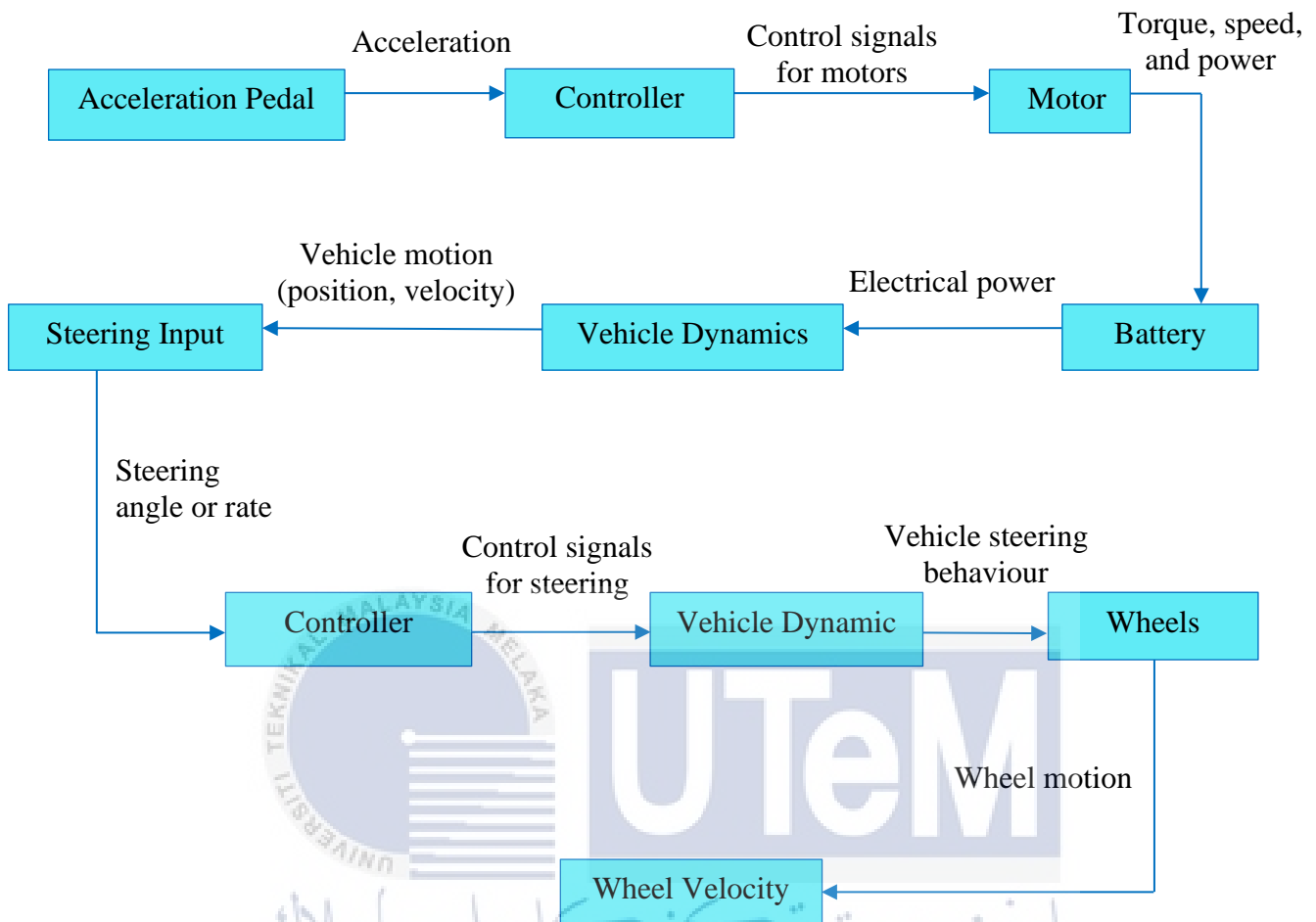


Figure 3.14 Block Diagram of the Mechanism

When the driver sets the input through accelerator pedal, it provides appropriate acceleration level. The required steering angle or rate comes from the steering wheel. The battery provides electricity to the motors. The controller processes steering, and accelerator pedal and generates signals for the vehicle system. Then, the motor transforms the mechanical energy into electrical energy. The vehicle dynamic interacts with the steering input and motor output and produces desired motion and steering behavior. Finally, the wheels convert the motion into real movement and direction. Figure 3.13 above demonstrates a block diagram of the mechanism.

3.11 Steady-State Handling Characteristics

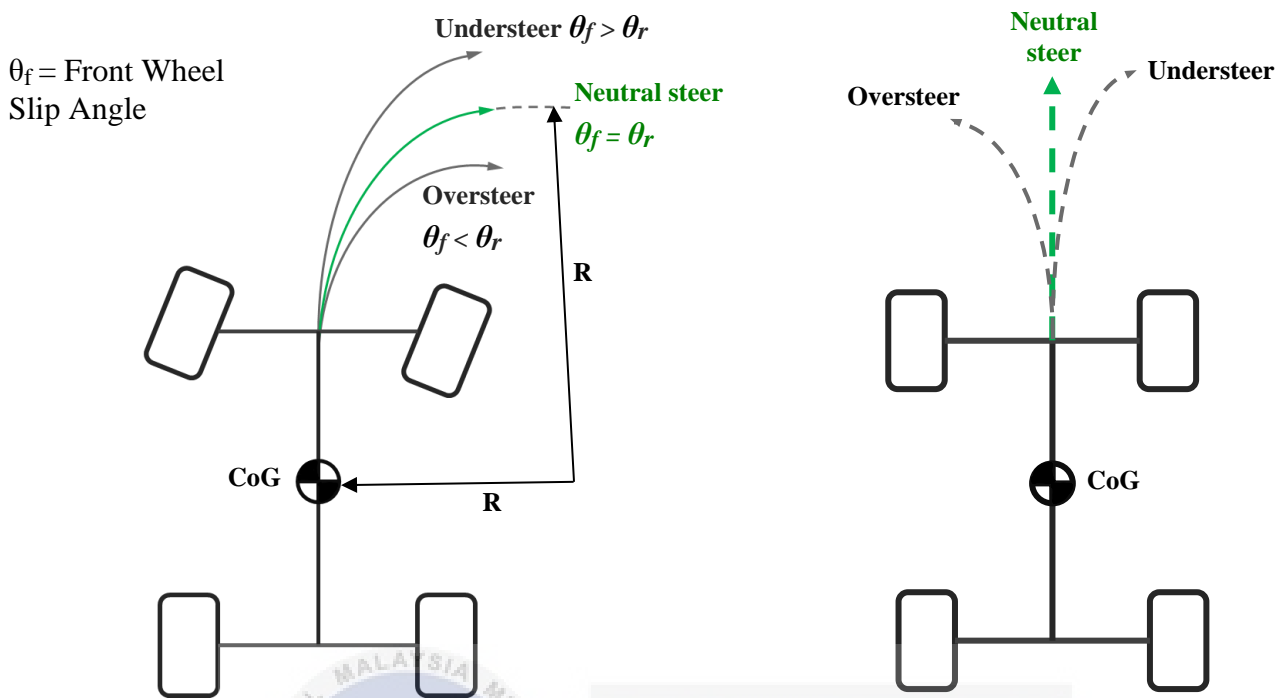


Figure 3.15 Steering Condition

The handling characteristics are divided into 3 categories depending on the tires slip angle. Neutral steering condition occurs when vehicle is in a constant radius turn and the driver can maintain the same steering wheel position.

In understeer condition, driver must increase the steer angle during a constant radius turn. Turning radius of an understeer is larger than that in a neutral steer vehicle, meaning when vehicle originally moving along in a straight line, a side force acts at the center of gravity (CoG) and the front tires develop slip angle greater than that of rear tires.

In oversteer condition, driver must decrease the steer angle during a constant radius turn. When vehicle is accelerated with the steering wheel fixed, turning radius decreases at the same steering wheel position and vehicle forward speed. Front tires develop slip angle less than that of rear wheels while moving along in a straight line. Figure 3.14 demonstrates the different steering conditions when the vehicle is accelerated in a constant radius turn.

3.12 Force, velocity and load difference based on cornering angle

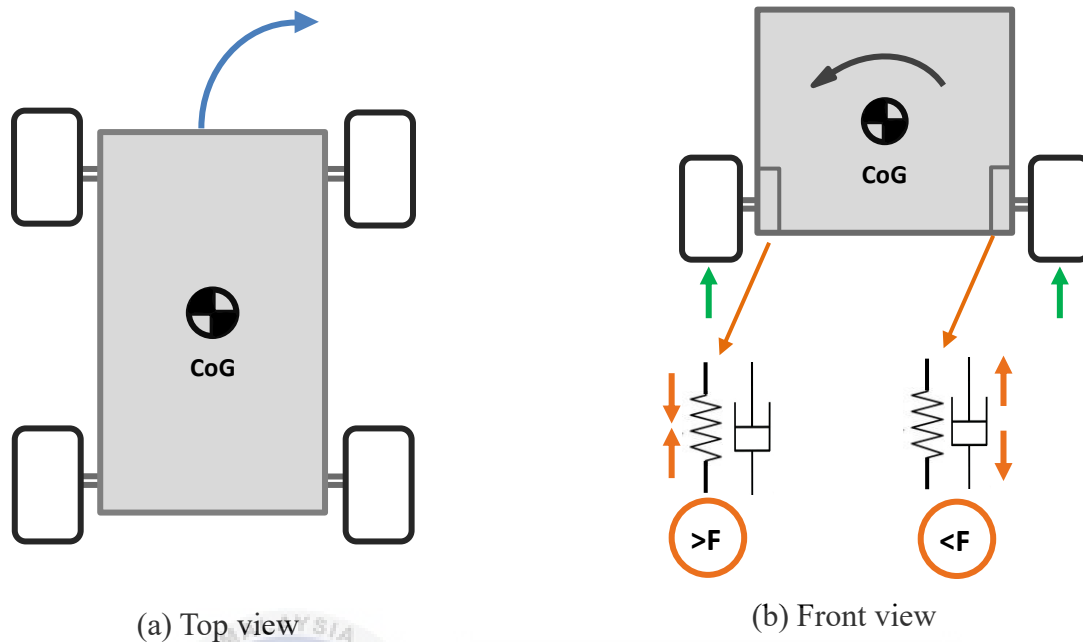


Figure 3.16 (a) Top view and (b) Front view of EV in right direction.

Vehicle turning motion encompasses movement coordination and application of various forces when the vehicle turns in any direction. The turning radius, vehicular velocity, speed, and force distribution in each wheel are influenced by the turning motion mechanism.

If the vehicle turns to the right corner, RLW (Rear Left Wheel) must cover a larger distance than RRW (Rear Right Wheel) resulting higher speed and higher vehicular velocity in the RLW rather than RRW. Meanwhile, RRR must cover larger radius and the wheel experiences higher centrifugal force, longitudinal force, and lateral force compared to RLW. Since, the vehicle leans toward right side, the suspension on the right rear side compress resulting increasing the load. Conversely, the suspension on the left rear side extends due to the decreased load on the left side. Figure 3.15 illustrates the top view and front view of EV during turning in right direction

3.13 Simulation Diagram

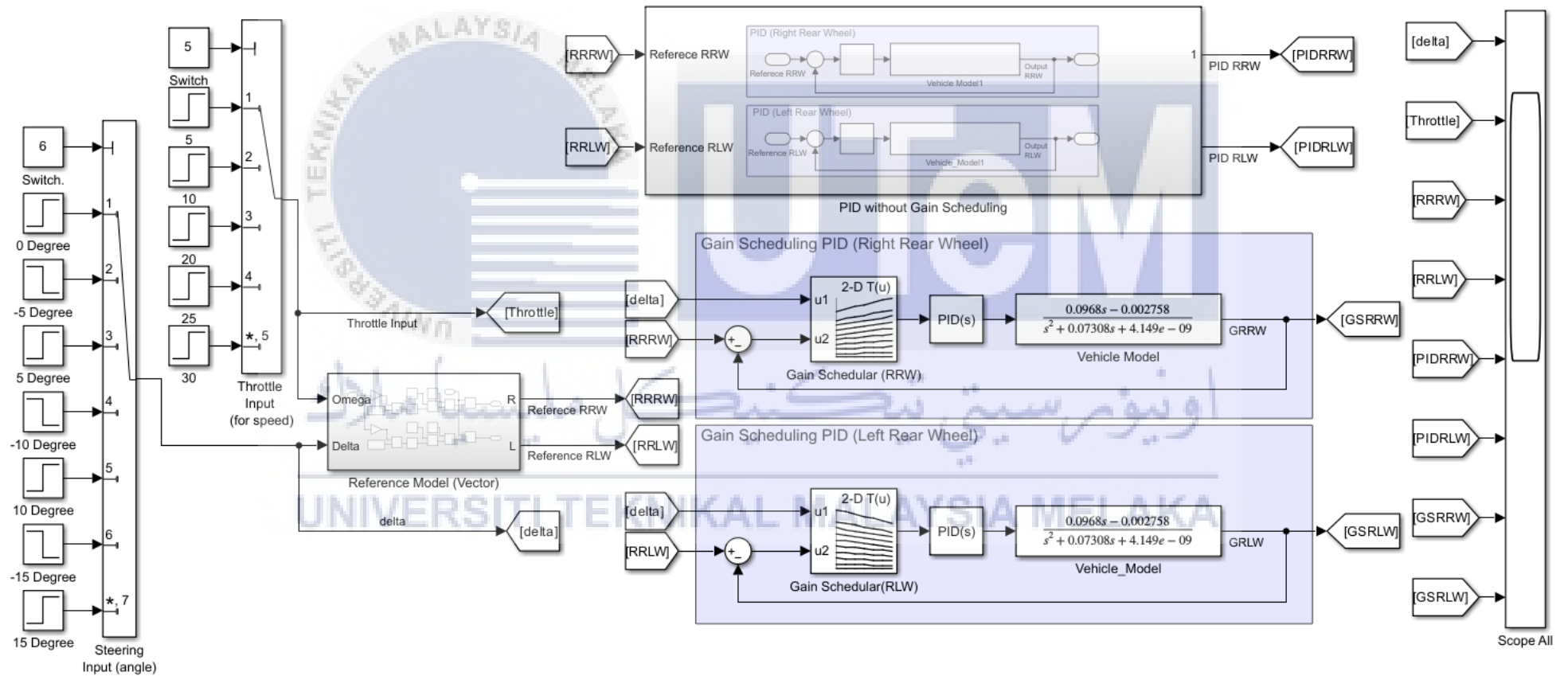


Figure 3.17 Simulation Diagram with PID Gain Scheduling

3.14 PID without Gain Scheduling

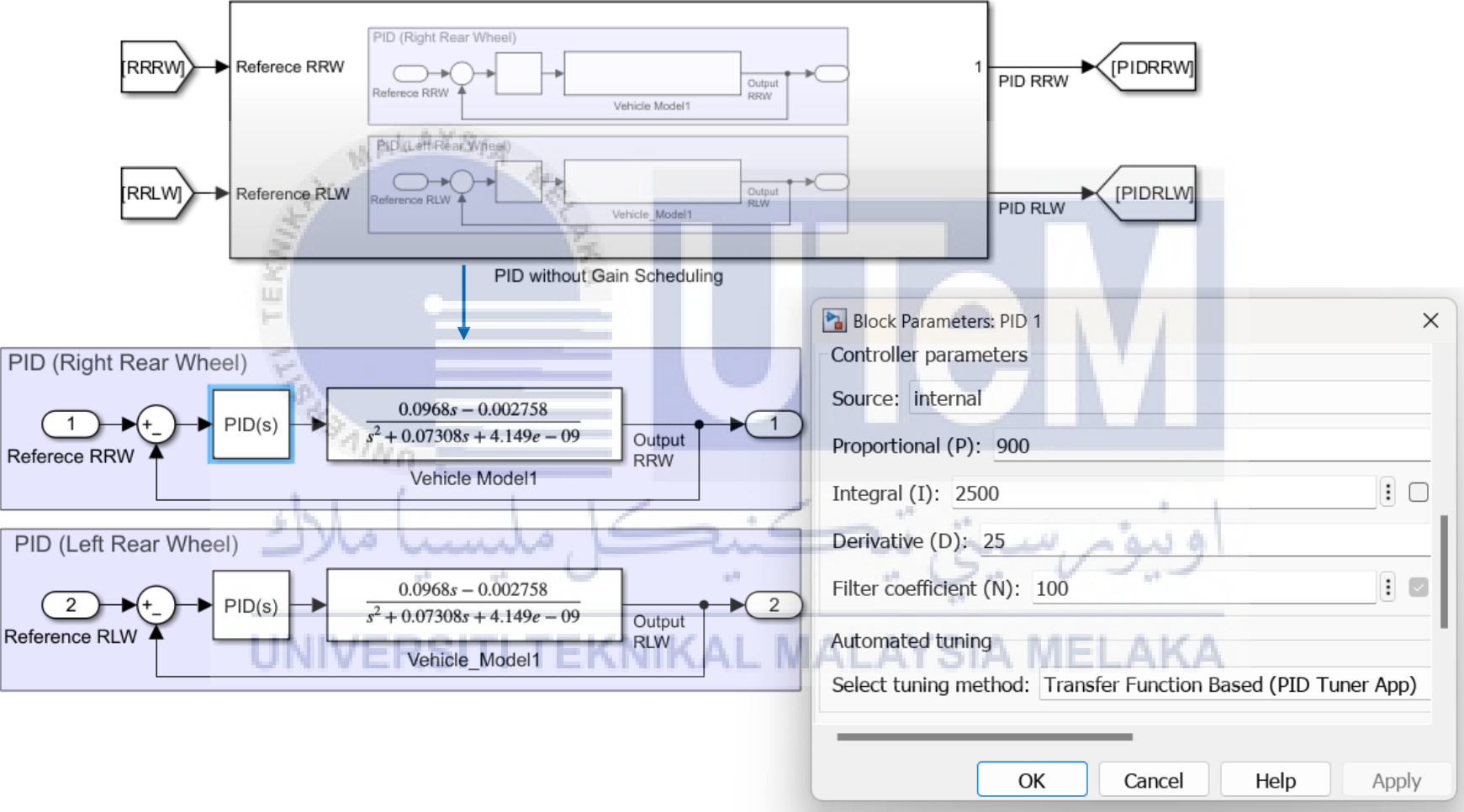


Figure 3.18 PID without Gain Scheduling (including PID gain values)

3.15 Sub-system – Reference Model (Vector Control)

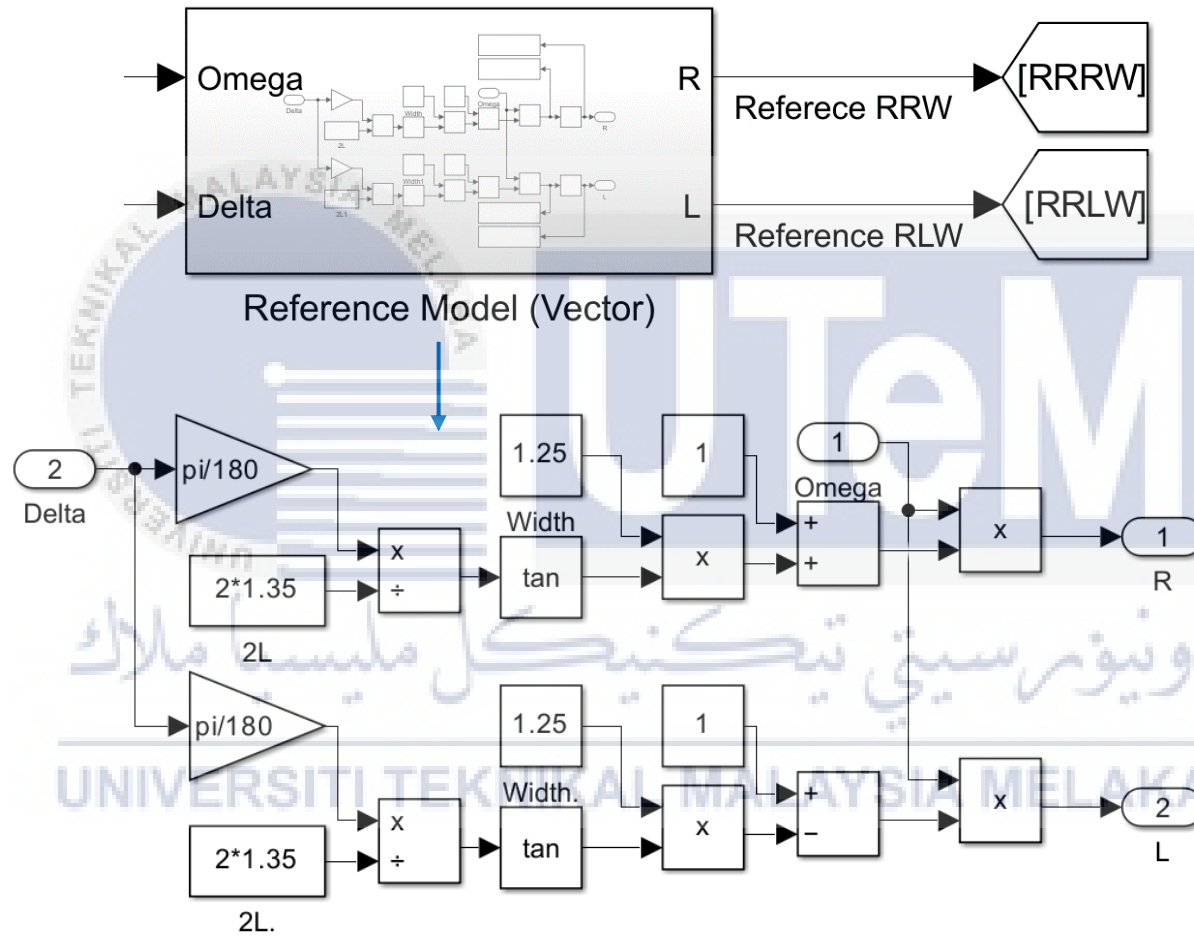


Figure 3.19 Sub-system – Reference Model or Vector Control

3.16 Gain Scheduler – RRW

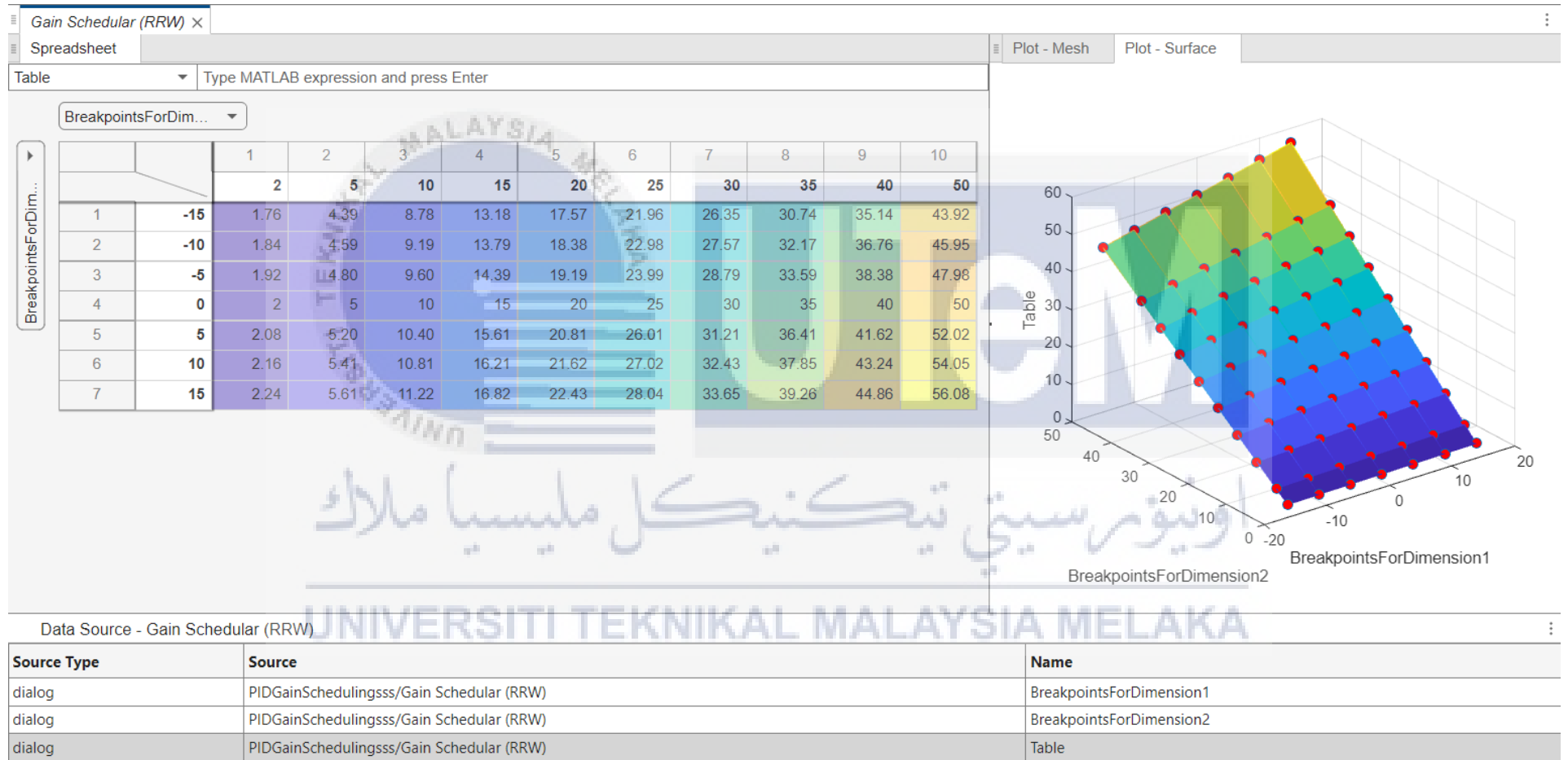


Figure 3.20 Gain Scheduler of Rear Right Wheel (RRW)

3.17 Gain Scheduler – RLW

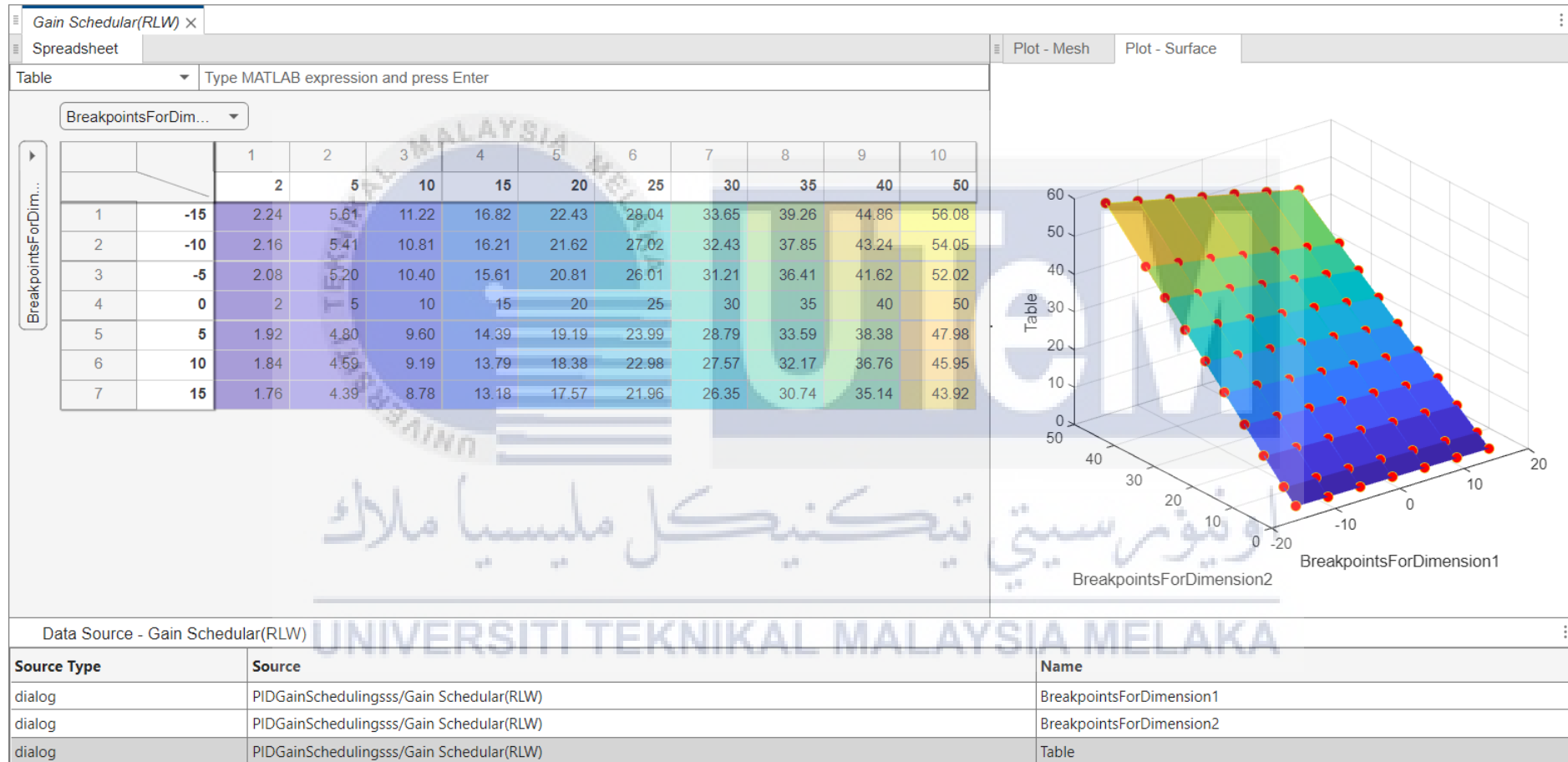


Figure 3.21 Gain Scheduler of Rear Left Wheel (RLW)

3.18 Experiment Diagram for Hardware

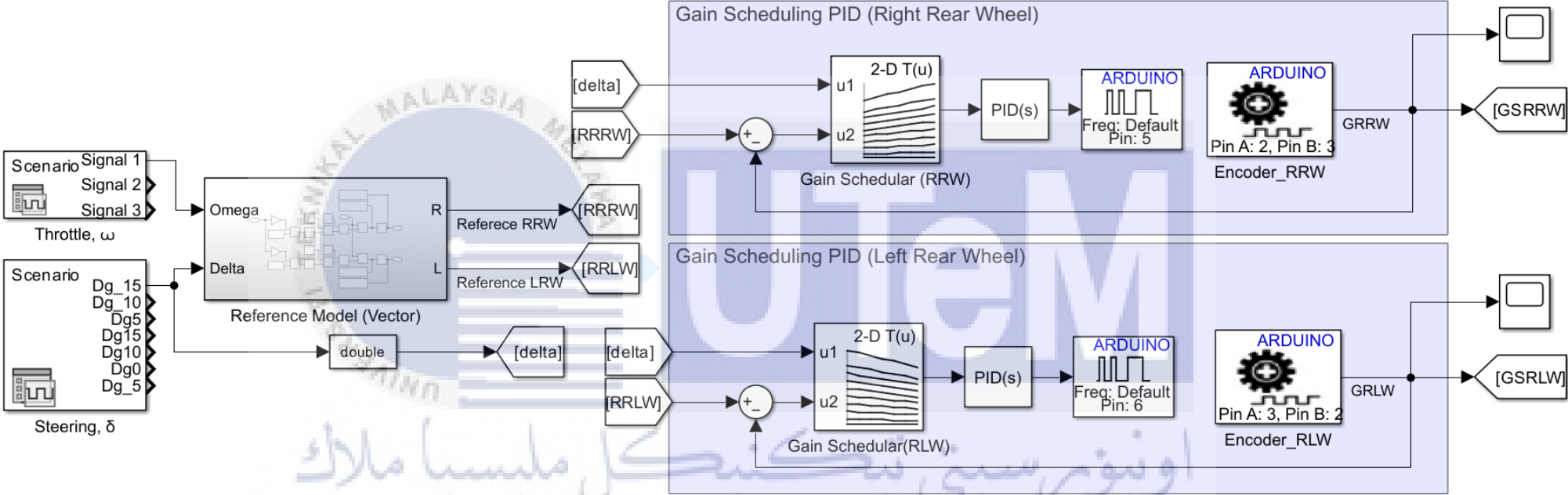


Figure 3.22 Experiment diagram for hardware simulation

3.19 Circuit connection

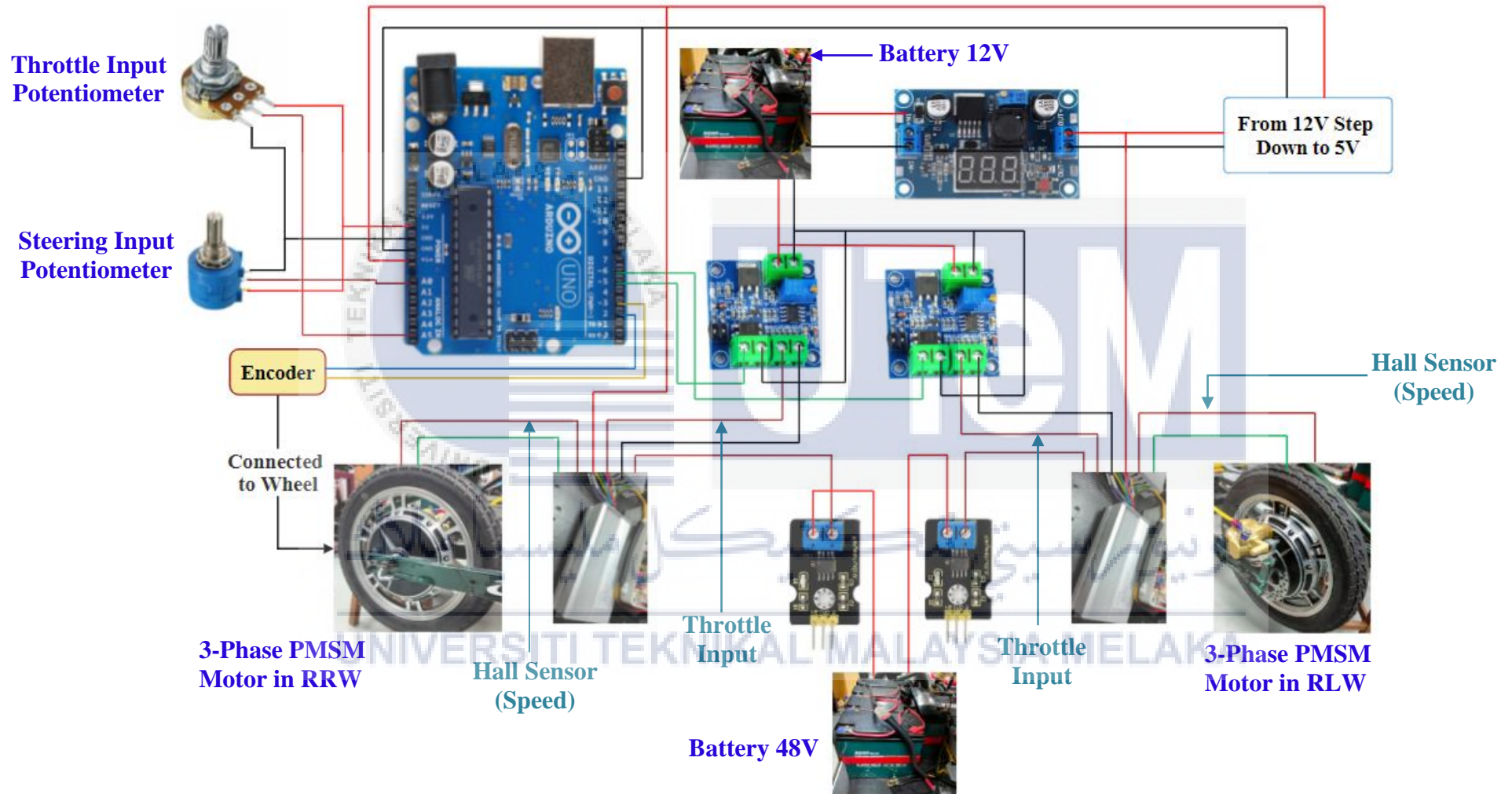


Figure 3.23 Circuit connection of the system

Figure 3.16 depicts the preliminary test circuit diagram for differential behaviour of rear wheels where the input angle is 30° left.

Figure 3.17 demonstrates the Simulation Diagram of PID Gain Scheduling as well as PID without Gain Scheduling in MATLAB/SIMULINK software. Figure 3.18 shows the diagram of PID without Gain Scheduling and the set PID gain values: K_p , K_i and K_d . Also, Figure 3.19 illustrates the Reference Model sub-system of Vector Control.

For Gain Scheduler set up, Figure 3.20 shows the Rear Right Wheel (RRW) GS setup using 2D lookup table where two breakpoints are throttle and steering input and Figure 3.21 shows the GS set up for Rear Left Wheel (RLW) using 2D lookup table where two breakpoints are throttle and steering input.

Figure 3.22 shows experimental diagram used to run the hardware.

3.20 Conclusion

The proposed methodology presented in this chapter is to develop and implement an effective vector control in the traction system of the vehicle for greater performance. “Zigler Nichol” method used to tune the PID controller. The final PID gains are $K_p = 900$, $K_i = 2500$ and $K_d = 25$.

CHAPTER 4

RESULTS AND DISCUSSIONS

4.1 Introduction

This chapter presents the results and analysis of the three different parts executed throughout the project. The simulation part is done using MATLAB/Simulink software. Hardware implementation has been set up using two methods. First implementation used Simulink hardware simulation method and second one is done by implementing coding through Arduino IDE software. The obtained outputs briefly demonstrate the nonlinear behaviors of both rear wheels when there is cornering angle in one direction. The signal parameters have been shown by transfer function and the lane change direction has been presented through sine wave signal. The circuit demonstrates estimated velocity for different steering angles in both directions when the voltage range starts with minimum 0.6V and the vehicle speed is 56km/h at 560 rpm.

4.2 Simulation Results and Analysis

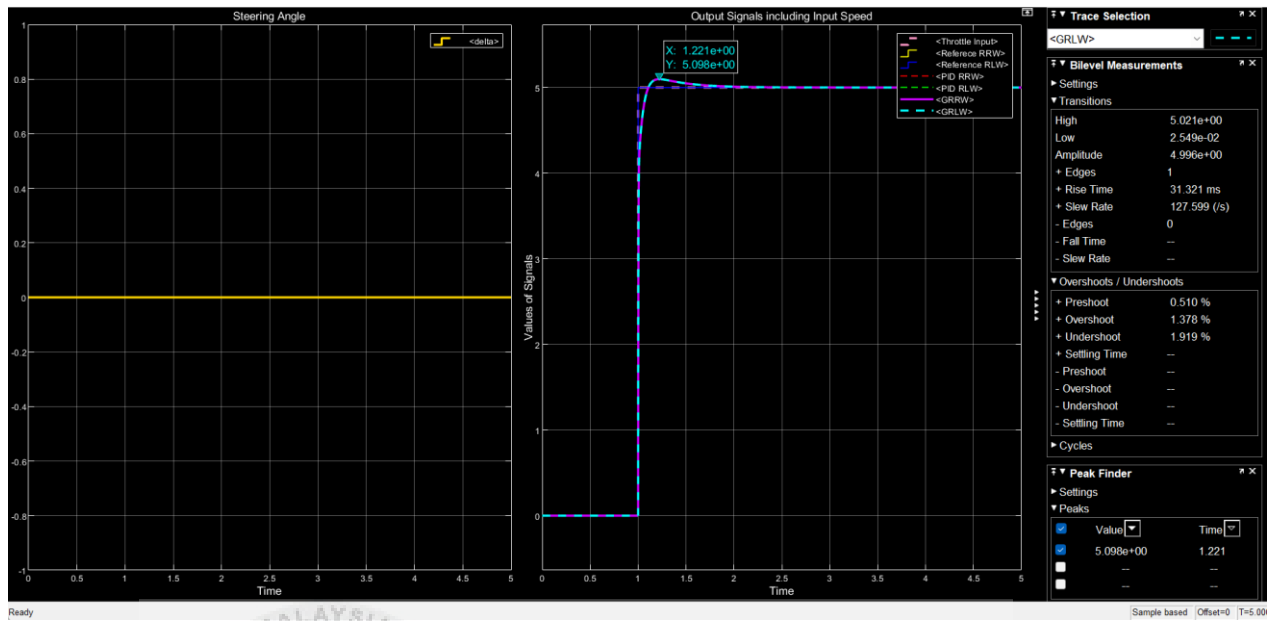


Figure 4.1 Throttle = 5 and Steering angle, $\delta = 0^\circ$ (Straight path)

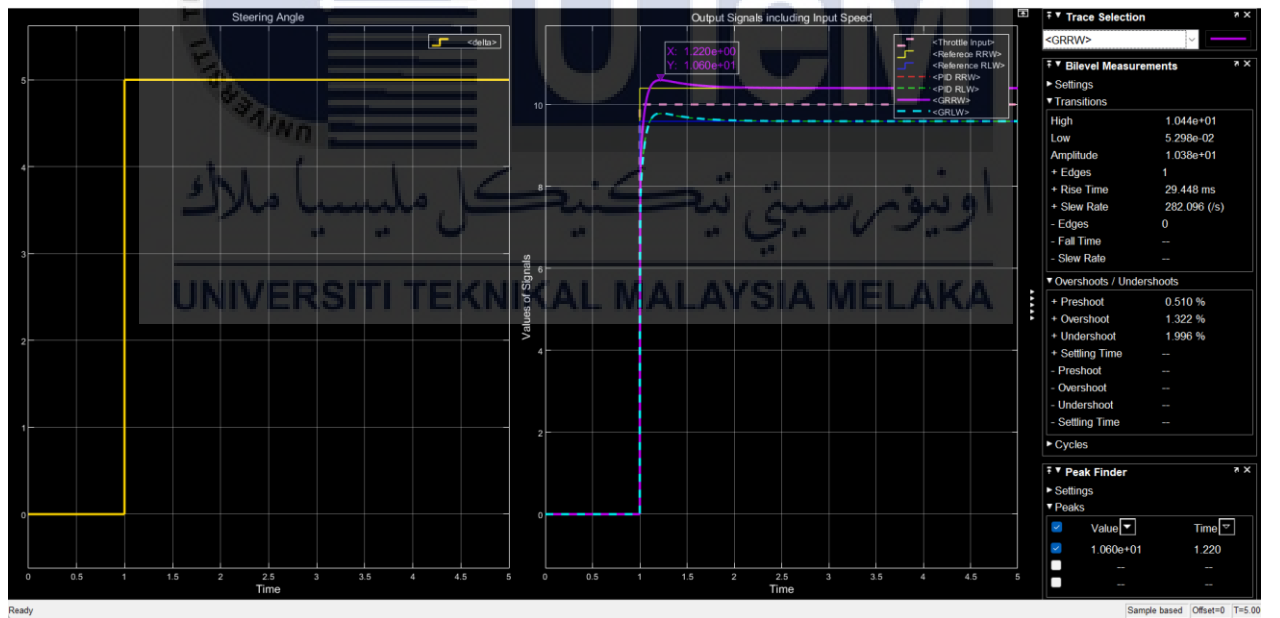


Figure 4.2 Throttle = 10 and Steering angle, $\delta = 5^\circ$ (cornering left)

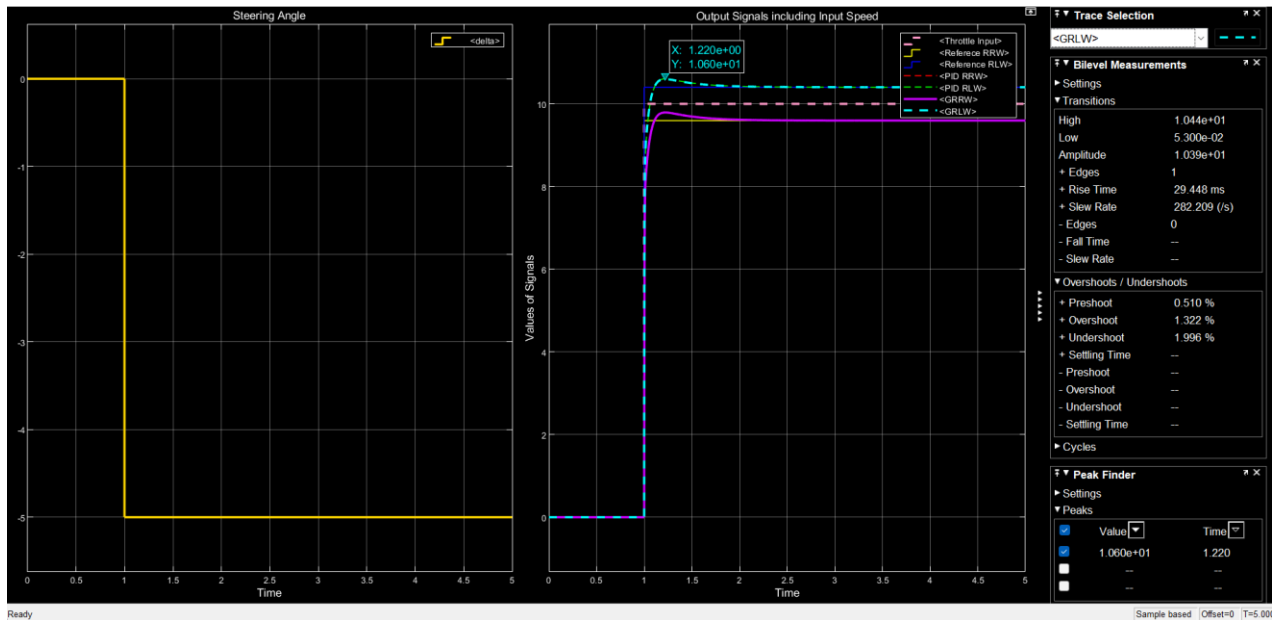


Figure 4.3 Throttle = 10 and Steering angle, $\delta = -5^\circ$ (cornering right)

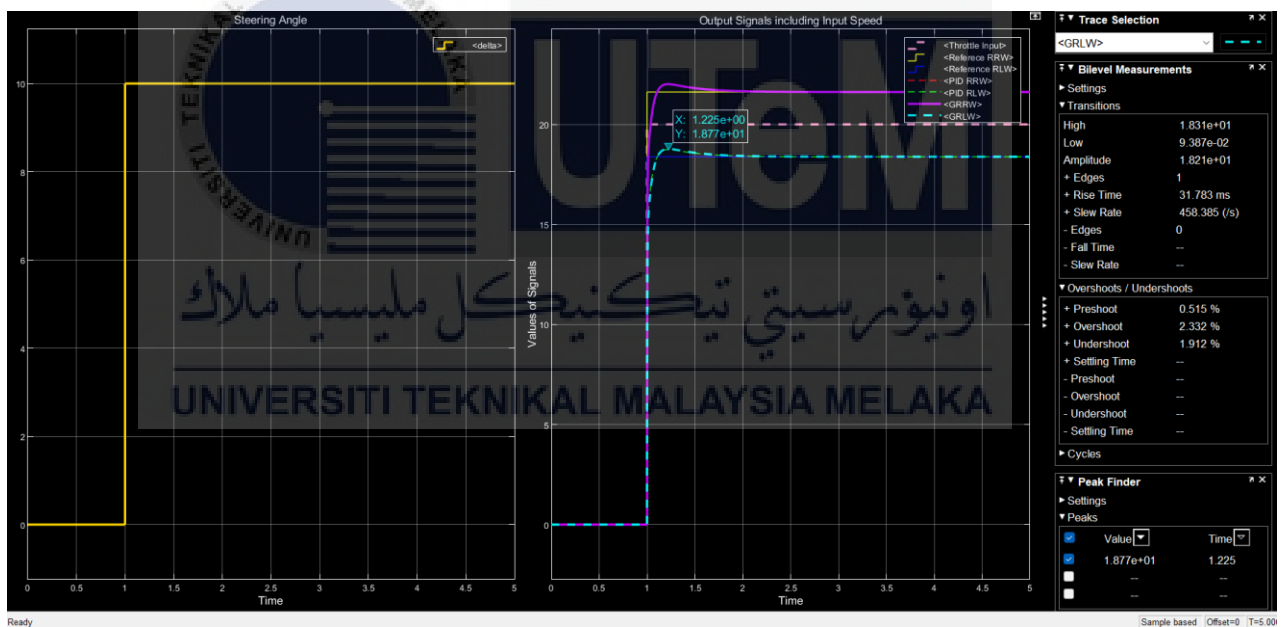


Figure 4.4 Throttle = 20 and Steering angle, $\delta = 10^\circ$ (cornering left)

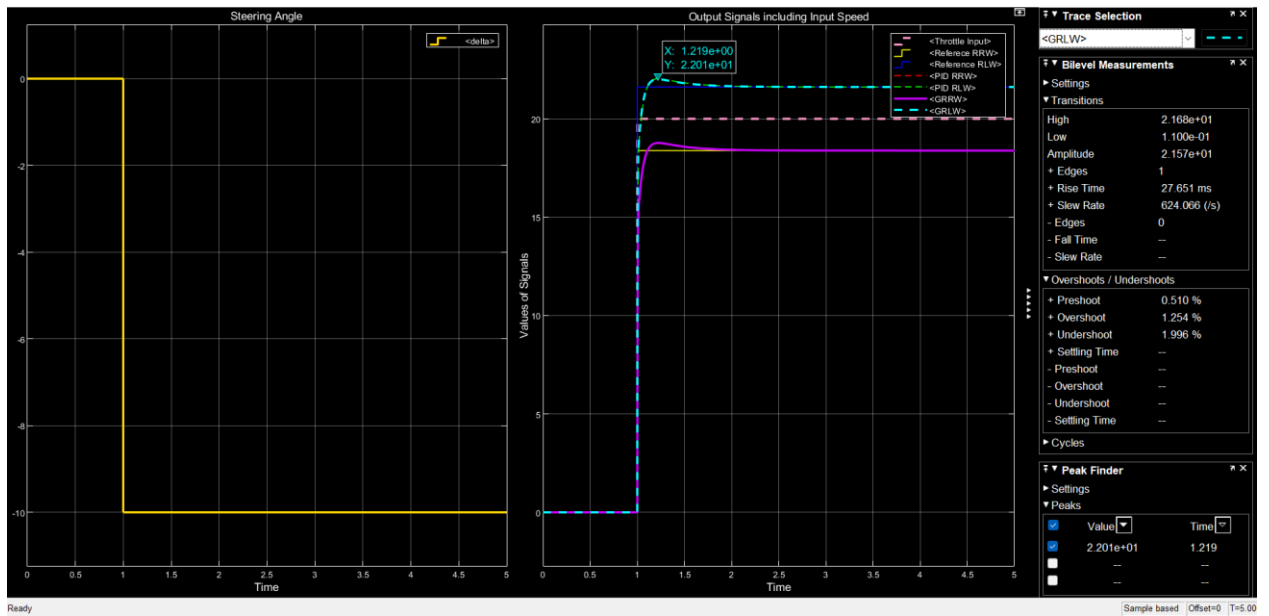


Figure 4.5 Throttle = 20 and Steering angle, $\delta = -10^\circ$ (cornering right)

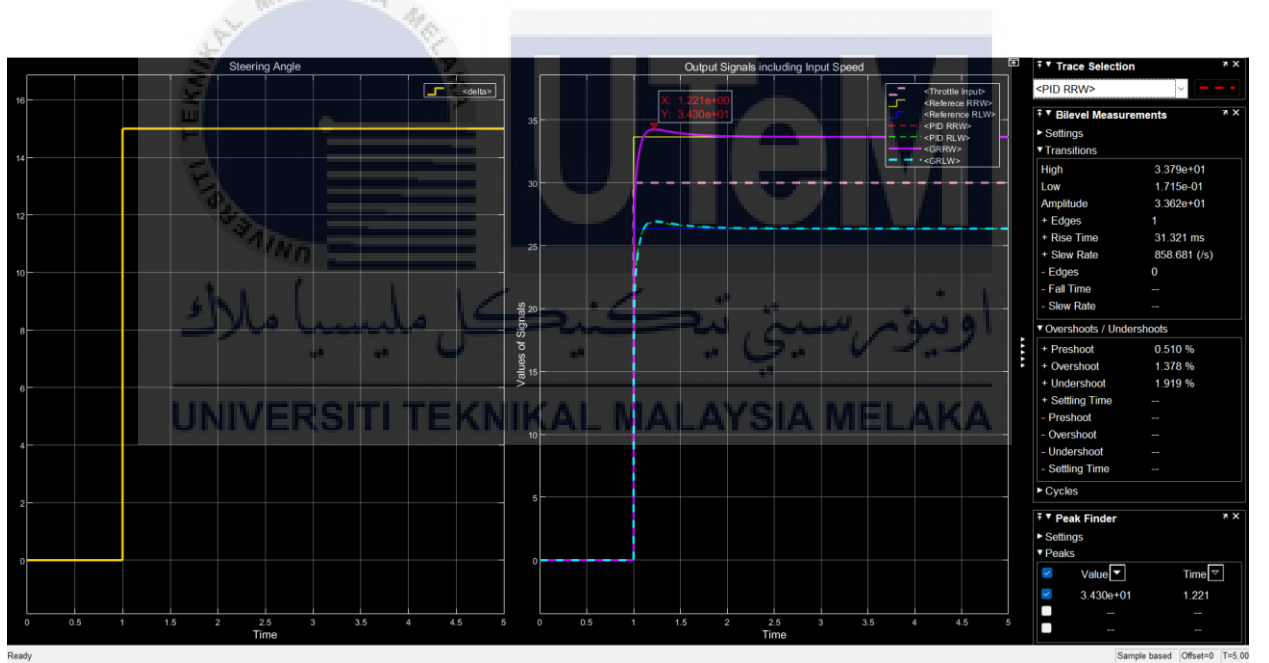


Figure 4.6 Throttle = 30 and Steering angle, $\delta = 15^\circ$ (cornering left)

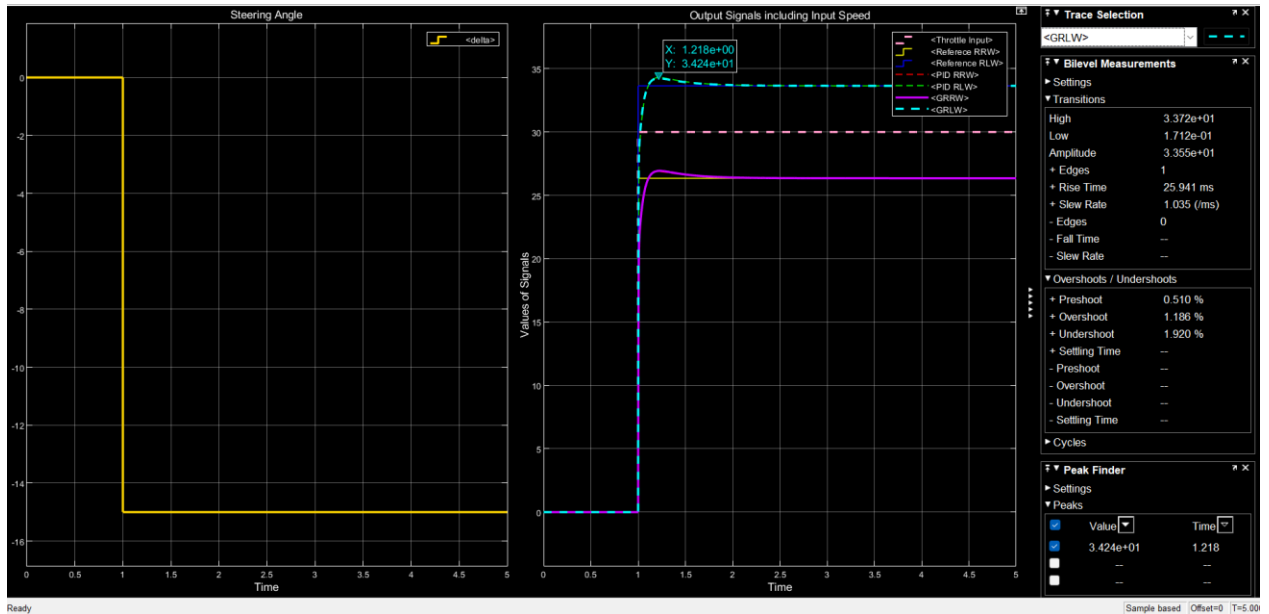


Figure 4.7 Throttle = 30 and Steering angle, $\delta = -15^\circ$ (cornering right)

Figure 4.1 to 4.7 demonstrates the resultant signal gained from the Simulation model where they show how the vehicular speed is different based on different directions, cornering angles and various throttle inputs.

4.2.1 Analysis of simulation result on different inputs

Table 4.1 Obtained Data from Simulation

INPUTS		GSRRW				GSRLW			
Th	δ	T_r (ms)	T_s (ms)	OS%	V_{RRW}	T_r (ms)	T_s (ms)	OS%	V_{RLW}
5	0°	31.321	2.574×10^3	1.378%	5.0	31.321	2.574×10^3	1.378%	5.0
10	-5°	33.311	2.671×10^3	1.432%	9.597	29.448	2.199×10^3	1.322%	10.40
	5°	29.448	2.209×10^3	1.322%	10.40	33.311	2.841×10^3	1.423%	9.597
20	-10°	31.783	2.222×10^3	2.332%	18.39	27.651	2.193×10^3	1.254%	21.62
	10°	27.651	2.127×10^3	1.254%	21.62	31.783	2.221×10^3	2.332%	18.39
30	-15°	33.995	2.502×10^3	2.401%	26.35	25.941	2.210×10^3	1.186%	33.65
	15°	25.941	2.278×10^3	1.186%	33.65	34.009	2.404×10^3	2.401%	26.36

Table 4.1 contains all the inputs and output values obtained from simulation. The effectiveness of the Gain Scheduling PID can be observed from the data obtained from simulations in different inputs. The vehicular speed for both wheels (V_{rr} and V_{rl}) are almost same as the reference model. The highest OS% is 2.401%. Since no overshoot exceeds 2.5% the system is accurately conditioned and reliable. When the vehicle is cornering to right, the RRW signal has higher rising time T_r , settling time T_s and OS% compared to the RLW signal. On the other hand, when cornering to left, RLW signal has higher rising time T_r , settling time T_s and OS% compared to the RRW signal.

These results prove the turning motion strategy in both wheels. Right wheel experiences more load and force during right turn causing to take more time to reach the desired result, while left wheel reach it faster due to less force and load on it. The occurrence is vice versa during left turn. But when the vehicle is moving in straight path there is no characteristic difference in both wheels.

4.2.2 Analysis of Gain Scheduler effectiveness

Table 4.2 Difference between PID and GSPID

INPUTS		PID with GS (GSPID)				PID without GS (PID)			
		RRW		RLW		RRW		RLW	
Th	δ	T_r (ms)	T_s (ms)	T_r (ms)	T_s (ms)	T_r (ms)	T_s (ms)	T_r (ms)	T_s (ms)
5	0°	31.321	2.574×10^3	31.321	2.574×10^3	31.321	2.574×10^3	31.321	2.574×10^3
10	-5°	33.311	2.671×10^3	29.448	2.199×10^3	31.321	2.747×10^3	31.321	2.241×10^3
	5°	29.448	2.209×10^3	33.311	2.841×10^3	31.321	2.223×10^3	31.321	2.996×10^3
20	-10°	31.783	2.222×10^3	27.651	2.193×10^3	31.321	2.358×10^3	31.321	2.313×10^3
	10°	27.651	2.127×10^3	31.783	2.221×10^3	31.321	2.300×10^3	31.321	2.358×10^3
30	-15°	33.995	2.502×10^3	25.941	2.210×10^3	31.321	2.455×10^3	31.321	2.420×10^3
	15°	25.941	2.278×10^3	34.009	2.404×10^3	31.321	2.433×10^3	31.321	2.519×10^3

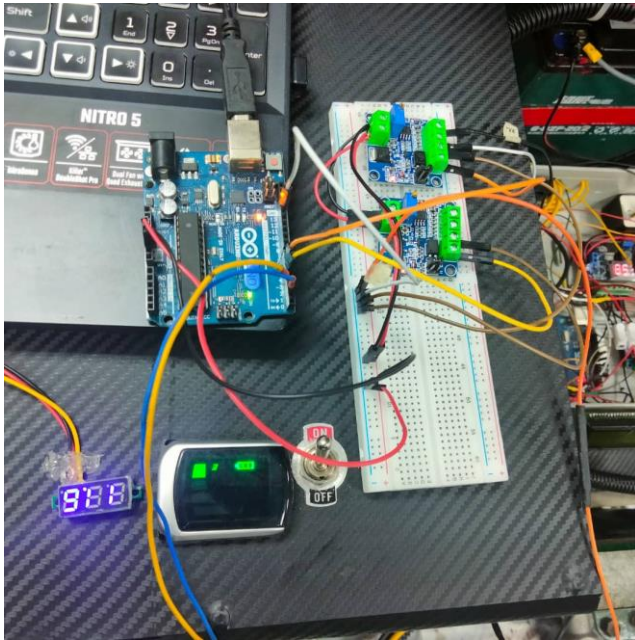
Table 4.2 contains the inputs and different output values when the PID system is with gain scheduling and without gain scheduling. When there is no Gain Scheduler with PID, in any input condition the rising times are all same. Although T_r values are all same, the settling times are different in each case, higher than the GSPID settling times values. In GSPID, the T_r and T_s both vary based on the different inputs. Only in few cases, GSPID rising time is slower than PID, but the signal reaches to the final value faster. These differences illustrate the effectiveness of Gain Scheduler along with PID.

The reason for using Gain Scheduler is to adjust the gain parameters (K_p , K_i and K_d) of PID controller on different operating conditions. It is commonly employed in the systems where the operating conditions change significantly, making a fixed controller less effective. Another reason for using GS is to vehicle dynamic or vehicle model. For example, in fixed linear TF, different operating conditions do not work. In EV, Gain Scheduler PID delivers more effective output in sudden change. The data analysis proved the working principle and reliability of Gain Scheduler.

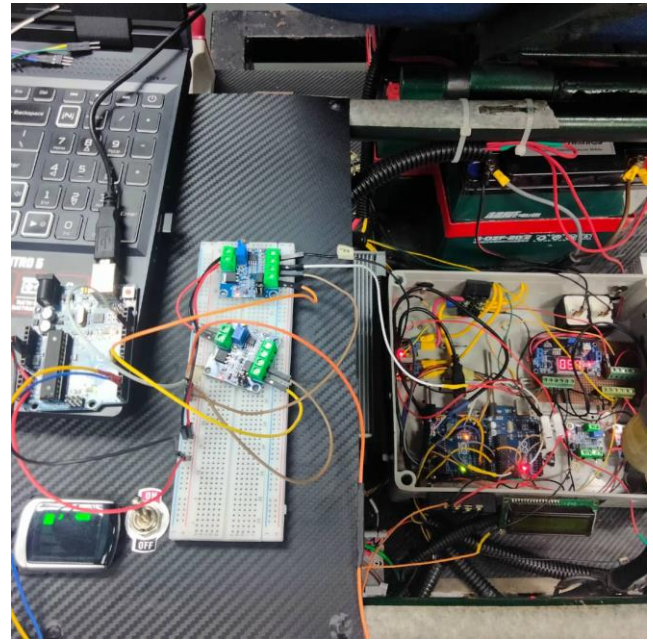


4.3 Hardware Implementation, Results and Analysis

The hardware implementation is based on two categories: electrical and mechanical. The Arduino UNO, PWM to voltage, motor driver, motor controller and other electrical component control the electric system, where throttle input, steering mechanism handle the mechanical part of the EV.

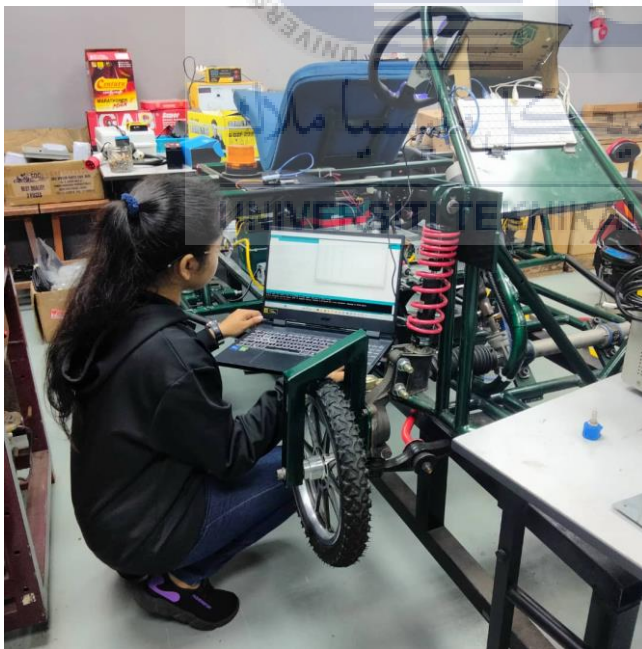


(a) Wiring Connection



(b) Wiring connection with EV

Figure 4.8 (a) Wiring Connection and (b) Wiring connection with EV



(a) Hardware setup



(b) Hardware implementation

Figure 4.9 Hardware setup and implementation for experimental diagram

4.3.1 Actual results from EV

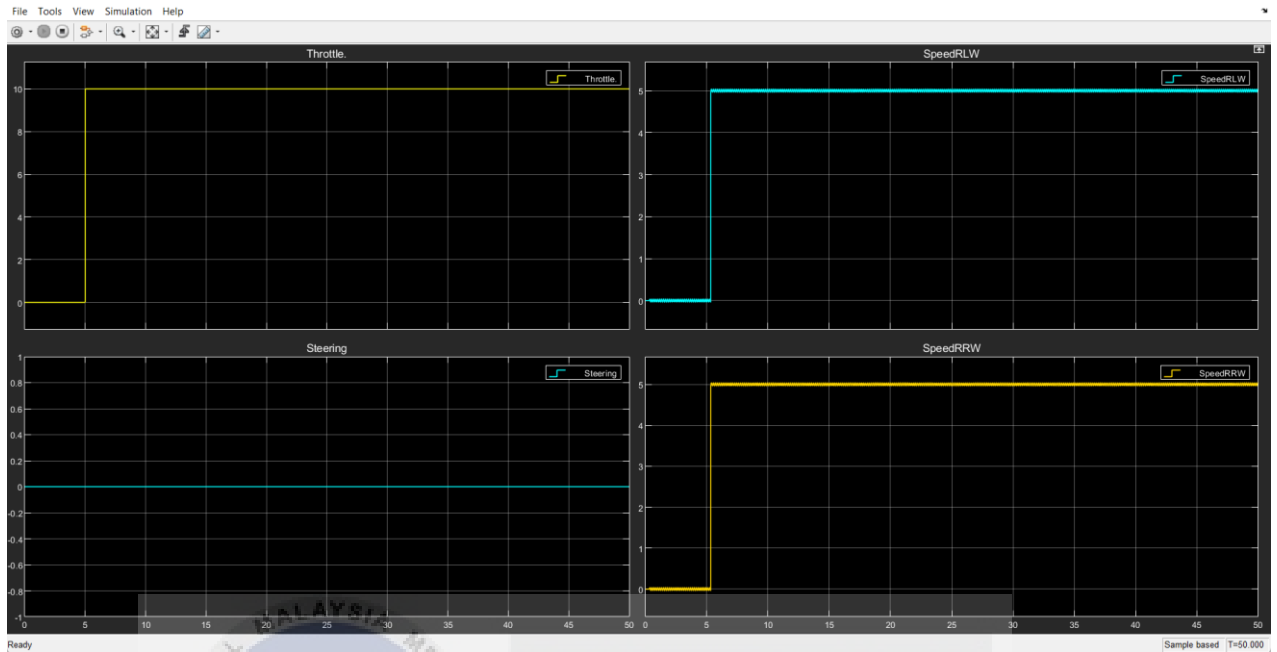


Figure 4.10 V_{RRW} and V_{RLW} when $\delta = 0^\circ$ and throttle = 5

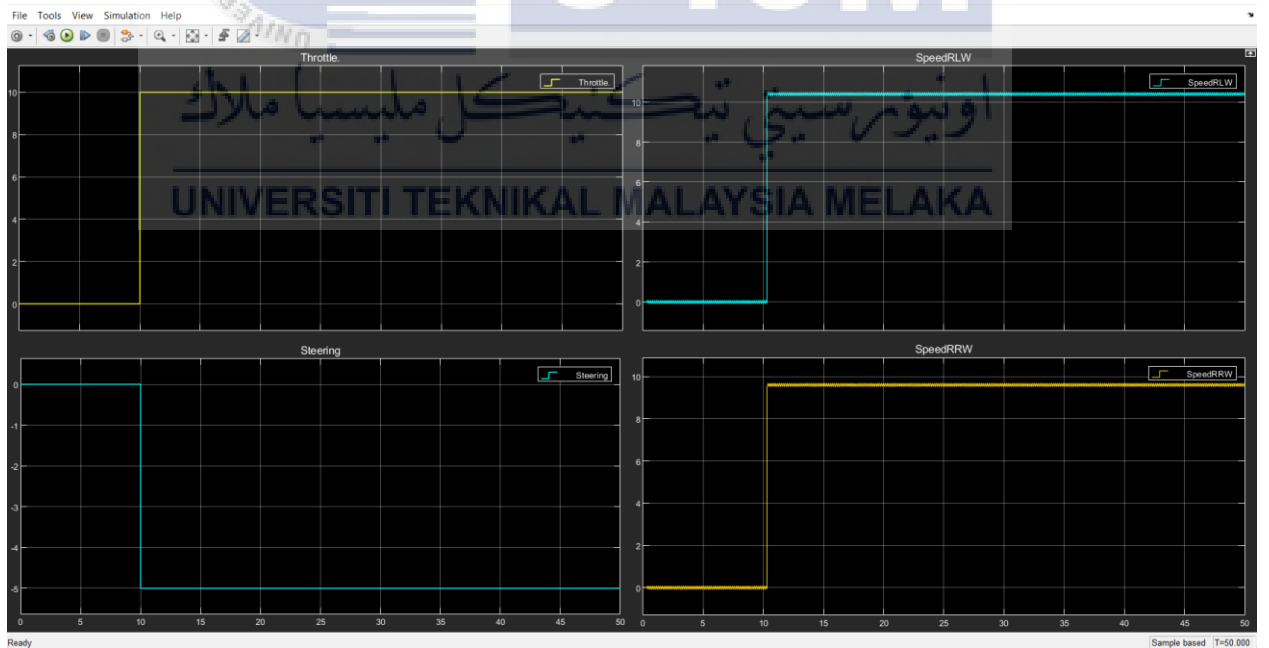


Figure 4.11 V_{RRW} and V_{RLW} when $\delta = -5^\circ$ and throttle = 10 (right turn)

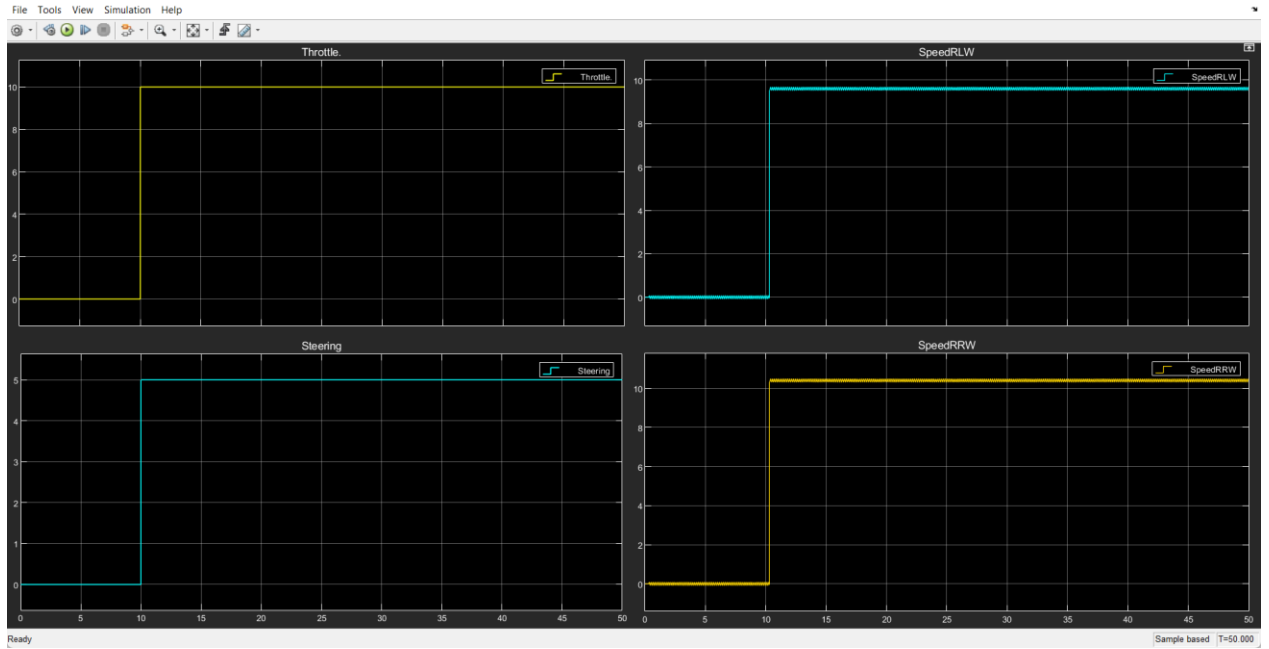


Figure 4.12 V_{RRW} and V_{RLW} when $\delta = 5^\circ$ and throttle = 10 (left turn)



Figure 4.13 V_{RRW} and V_{RLW} when $\delta = -10^\circ$ and throttle = 20 (right turn)

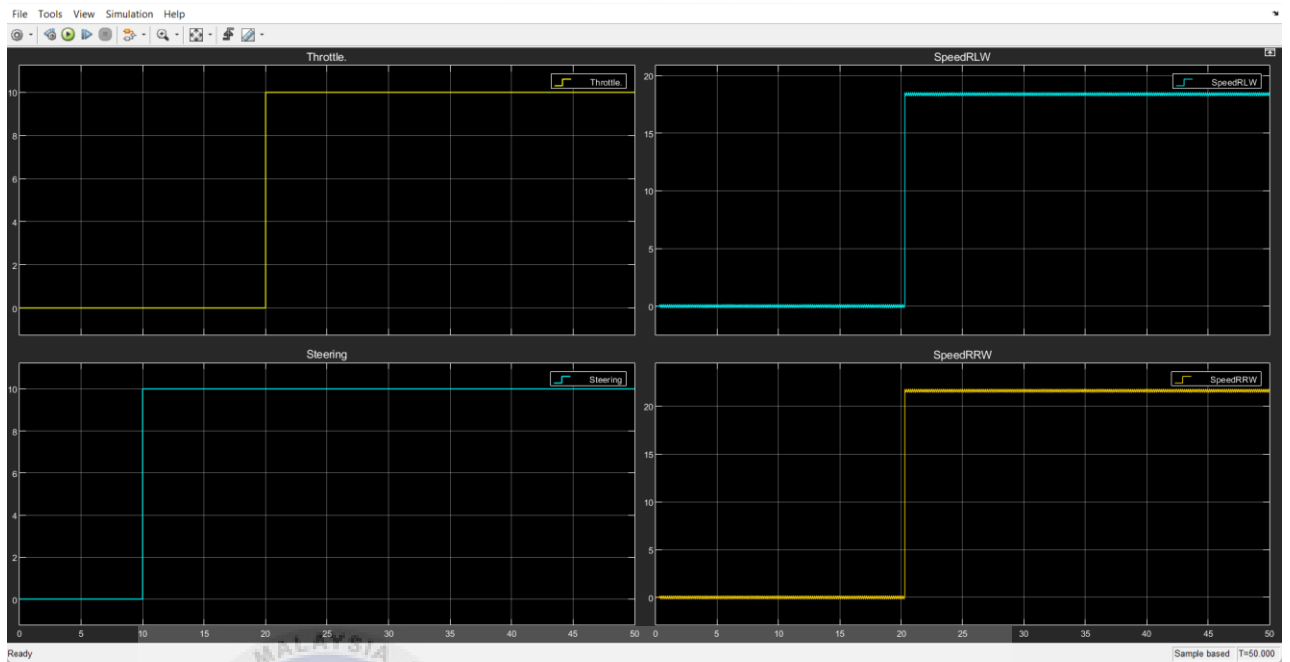


Figure 4.14 V_{RRW} and V_{RLW} when $\delta = 10^\circ$ and throttle = 20 (left turn)

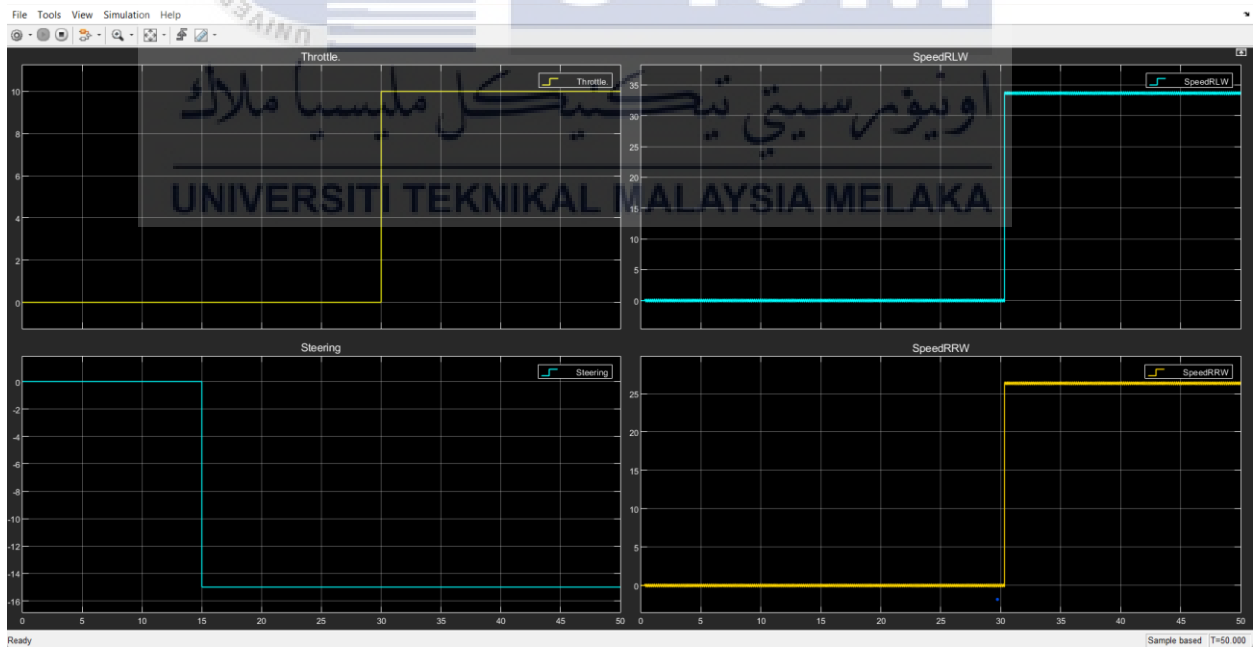


Figure 4.15 V_{RRW} and V_{RLW} when $\delta = -15^\circ$ and throttle = 30 (right turn)

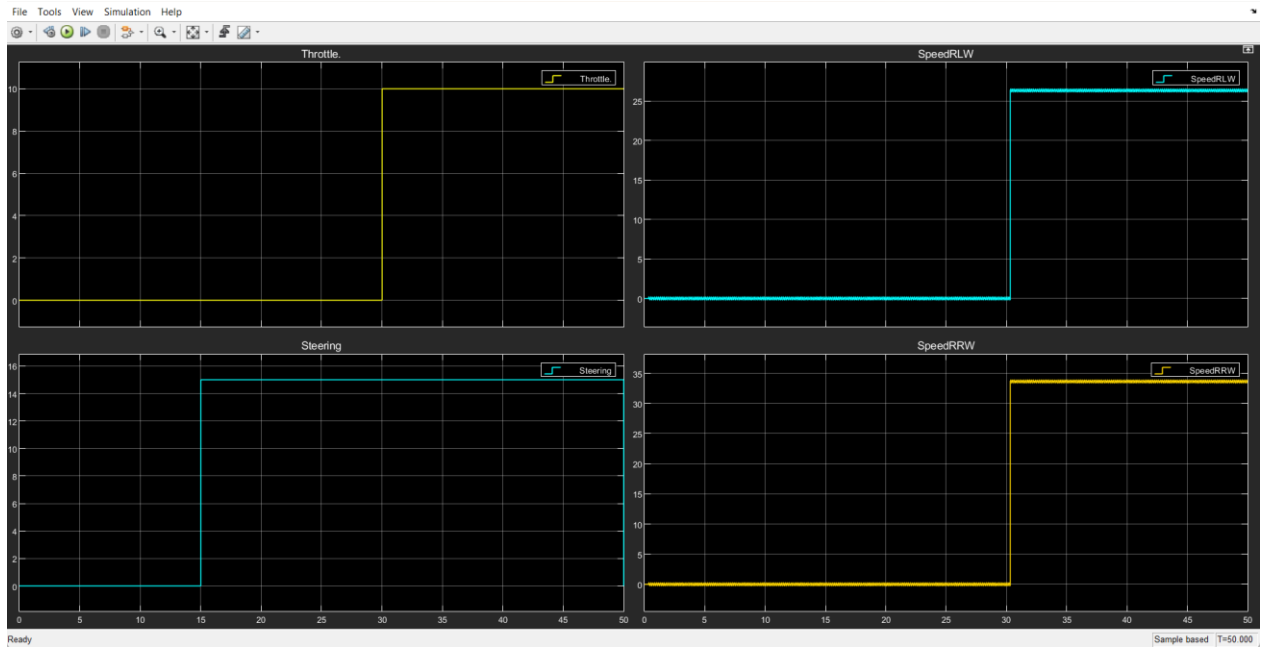


Figure 4.16 V_{RRW} and V_{RLW} when $\delta = 15^\circ$ and throttle = 30 (left turn)

Figure 4.8 shows the wiring connection of Arduino UNO with the EV and Figure 4.9 shows the setup and hardware implementation. Figure 4.10 illustrates the result graph obtained from actual performance when angle, δ is 0° and the throttle input is 5.

Figure 4.11 and Figure 4.12 demonstrate V_{RRW} and V_{RLW} when throttle = 10 but steering angle, $\delta = -5^\circ$ (in right direction) and $\delta = 5^\circ$ (in left direction). Figure 4.13 and Figure 4.14 show the output differences when throttle = 20, angle is $\delta = -10^\circ$ and $\delta = 10^\circ$. Figure 4.15 and Figure 4.16 depicts the velocity results of two wheels when throttle = 30, angle is $\delta = -15^\circ$ and $\delta = 15^\circ$.

4.3.2 Performance analysis

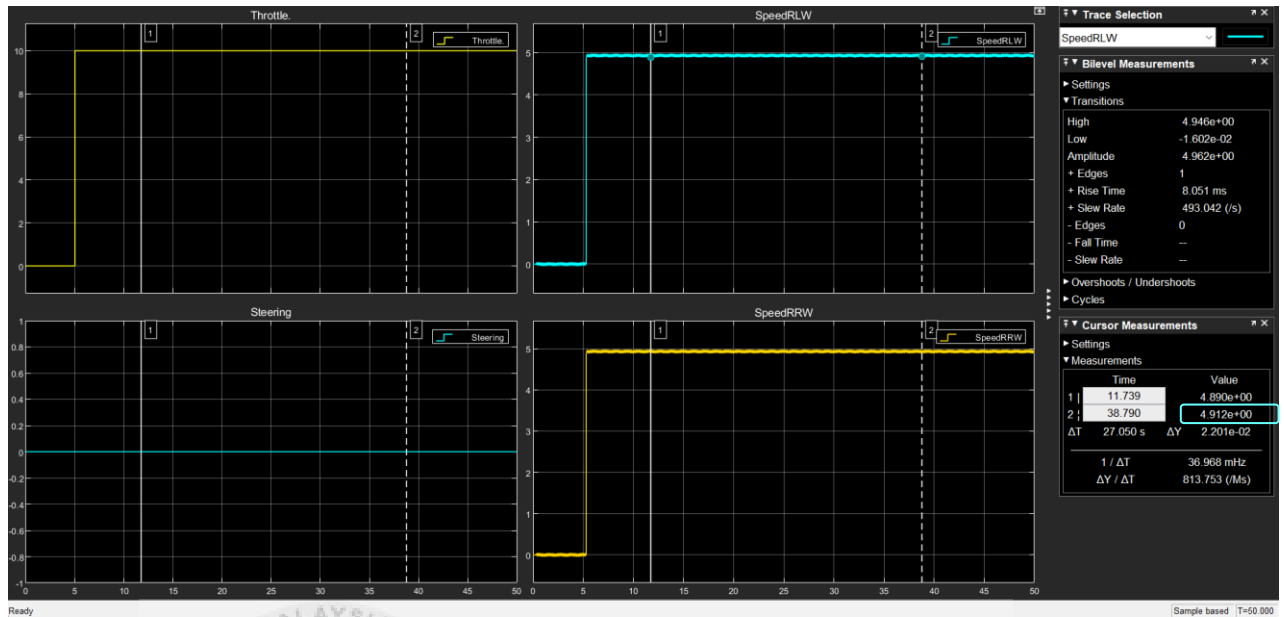


Figure 4.17 Final value from the actual results

Figure 4.17 shows the final vehicular speed value obtained from the graph. In this example, the input of throttle is 5 and the steering angle is 0° (vehicle moving in straight path), the speed result for both RRW and RLW is 4.912 km/h. All the actual data was obtained in the same way.

Table 4.3 Data analysis between simulation and actual results

INPUTS		RRW (V_{RRW} in km/h)			RLW (V_{RLW} in km/h)		
Th	δ	Simulation	Actual	%Error	Simulation	Actual	%Error
5	0°	5.0	4.91	1.8%	5.0	4.912	1.792%
10	-5°	9.597	9.34	2.678%	10.40	10.195	1.971%
	5°	10.40	10.191	2.009%	9.597	9.361	2.459%
20	-10°	18.39	17.85	2.936%	21.62	21.15	2.174%
	10°	21.62	21.142	2.211%	18.39	17.86	2.882%
30	-15°	26.35	25.46	3.378%	33.65	32.76	2.645%
	15°	33.65	32.73	2.734%	26.36	25.477	3.349%

Table 4.3 demonstrates the difference between simulation and actual results as well as the effectiveness of the system. When the vehicle moving in straight way, the speed is nearest to the simulated result and the error percentage is lowest in both rear wheels, 1.8% in RRW and 1.792% in RLW. As the input value increases, the % error also increases. This difference validates the characteristic of engine, to reach higher speed, system requires more power, energy, and force thus, more internal disturbance, noises interrupt the operation resulting higher percentage of error.

Vehicle turning motion characteristics are also noticeable from the data above. In right turning, the right wheel is delivering higher %error rather than left wheel and vice versa. It proves that under higher load, lateral and longitudinal force, the wheel motor requires more power to operate.

Additionally, RLW %error is slightly lower than RRW under same operation conditions. This indicates the motor and motor controller for RRW is having interruption, internal disturbances that need to be checked.

4.4 Coding implementation, Results and Analysis

```

VectorControl_PID_Gain_Scheduling | Arduino 1.8.19
File Edit Sketch Tools Help
VectorControl_PID_Gain_Scheduling
1 #include <PID_v1.h>
2
3 int potPin1 = A0; // pin connected to Steering potentiometer
4 int angle;
5 int potPin2 = A5; // pin connected to Throttle potentiometer
6 int throttle;
7 int PWM1;
8 int PWM2;
9
10 int Encoder1 = 3; // pin connected to Encoder
11 int Encoder2 = 2; // pin connected to Encoder
12 int row_num = 7, col_num = 11;
13
14 // Define PID parameters
15 double kp = 900.0; // Proportional gain
16 double ki = 2500.0; // Integral gain
17 double kd = 25.0; // Derivative gain
18
19 double Setpoint = 0; // Define PID Setpoint
20 double Input = 0; // Define PID Input
21 double OutputRRW = 0; // Define PID Output for RRW
22 double OutputRLW = 0; // Define PID Output for RLW
23
24 // Declare PID objects

```

```

COM5
Voltage1 value = 0.00 Volt
Angle value = -15 degree
Voltage2 value = 0.00 Volt
Throttle value = 0 (regulates Speed)
The speed from PWM1 RRW = 0.00 km/h
The speed from PWM2 RLW = 0.00 km/h
Voltage1 value = 0.00 Volt
Angle value = -15 degree
Voltage2 value = 0.78 Volt
Throttle value = 5 (regulates Speed)
The speed from PWM1 RRW = 4.39 km/h
The speed from PWM2 RLW = 5.61 km/h
Voltage1 value = 1.58 Volt
Angle value = -5 degree
Voltage2 value = 2.13 Volt
Throttle value = 20 (regulates Speed)
The speed from PWM1 RRW = 19.19 km/h
The speed from PWM2 RLW = 20.81 km/h
Autoscroll Show timestamp Newline 9600 baud Clear output

```

Sketch uses 7926 bytes (24%) of program storage space. Maximum is 32256 bytes.
Global variables use 1142 bytes (55%) of dynamic memory, leaving 906 bytes for local variables. Maximum is 2048 bytes.

Figure 4.18 Coding output from serial monitor

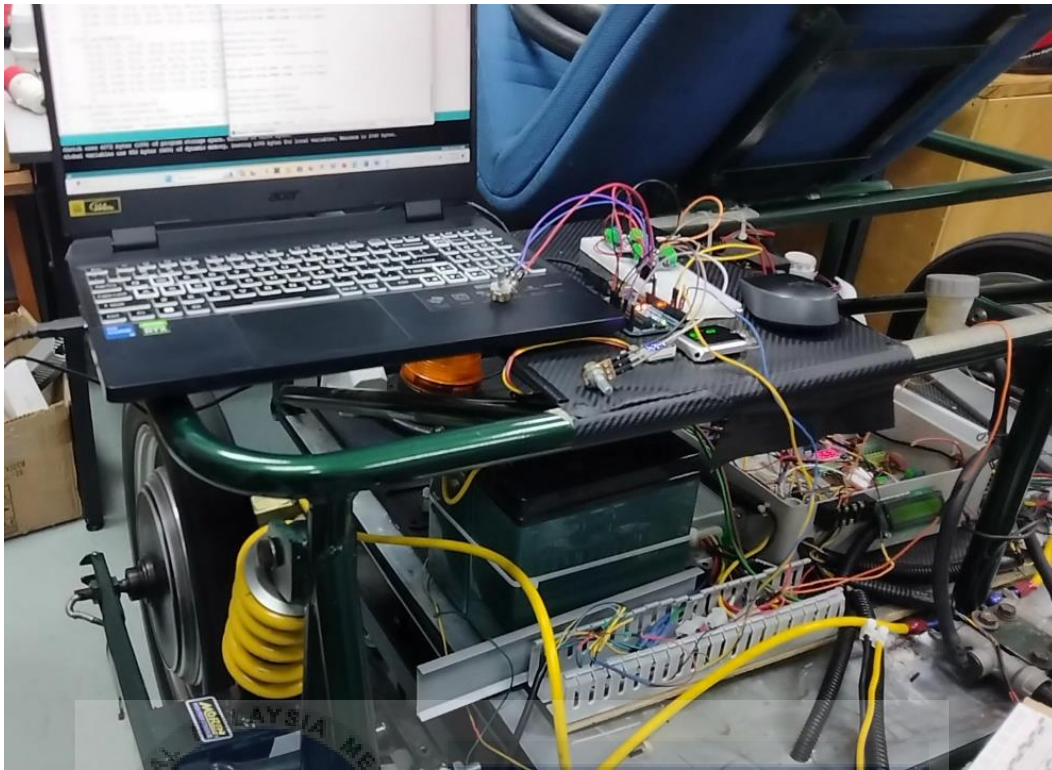


Figure 4.19 Wheel run from coding implementation

Figure 4.18 shows the coding simulation output from serial monitor and Figure 4.19 demonstrates wheel movement through coding implementation.

For the coding implementation, two potentiometers have been set for the steering and throttle input. Steering and throttle input connects with Arduino UNO analog pin A0 and A5 respectively.

Table 4.4 Data analysis between coding and actual results (run coding)

INPUTS		RRW (V_{RRW} in km/h)			RLW (V_{RLW} in km/h)		
Th	δ	Coding	Actual	%Error	Coding	Actual	%Error
5	0°	5.0	4.89	2.2%	5.0	4.90	2%
10	-5°	9.60	9.34	2.708%	10.40	10.15	2.404%
	5°	10.40	10.11	2.79%	9.60	9.36	2.5%
20	-10°	18.39	17.79	3.26%	21.62	21.93	3.19%
	10°	21.62	20.91	3.28%	18.39	17.83	3.054%
30	-15°	26.35	27.26	3.45%	33.65	34.77	3.328%
	15°	33.65	34.81	3.44%	26.35	27.22	3.302%

From the output from the coding implementation on vehicle traction system, it is noticeable that the %error is more than the result obtained from experimental diagram. When the throttle input and steering angle value are both high, the %error is also high. But from the coding implementation it is observed in highest inputs, the actual wheel speeds are higher than the real data. RRW has more disturbance therefore a higher %error. When the system stops RLW takes more time to stop. The internal disturbance on RRW makes the wheel stop before time. Sudden jerk observed if the input gets too or changes very quickly.

4.5 Conclusion

To conclude, when there is steering angle at the right direction The speed of the rear left wheel is always higher than the speed of the rear right wheel. The relative motion between two wheels and the turning radius are the factors that make these differences. Since the vehicle will take a right turn by following a curved way, the left wheel must travel longer distance rather than the right rear wheel thus, it will have higher speed. Besides the right wheel must carry more loads and will face more lateral forces due to the right turn. Therefore, its' speed and velocity get lower. The greater the cornering angle is, the greater the differences between both wheels' parameters are. The same thing happens to the right rear wheel when the vehicle turns to the left corner.

CHAPTER 5

CONCLUSION AND RECOMMENDATIONS

5.1 Conclusion

This thesis presents a method for obtaining desired torque at low speeds, improving the speed holding capability and the responsiveness to any sudden load changes of the electric vehicle. The work has addressed the traditional issues that occur when EVs drive in uncertain surfaces or areas. The vector control technique depicted great prospectives to solve these problems subsequently, successfully implemented and have been monitored. The system using Arduino UNO with PID gain scheduling has been performed and successfully executed by achieving improved stability, controllability, and safer drive of EV in various conditions. The actual data obtained from hardware implementation show a great potential and effective system characteristics where all the %error is less than 5%.

5.2 Future works

There are some recommendations and suggestions about the future works that can be implemented for more betterment.

- An addition of LCD display will be more useful, each input and output value can be seen accurately.
- To make the %error less than 0.5% try different PID tuning values, include filtering component to reduce internal noise and disturbance.
- Use filtering device to reduce the internal disturbance and noise.
- Driving the vehicle on different surface to check the reliability of vector control mechanism.

- Along with this project, additional work can be done by implementing model predictive control or advanced fuzzy logic control method to make the EVs' operation more stable and energy efficient.
- To improve the robust management of the traction system some auxiliary equipment can be applied such as GPS, accelerometer, gyroscope etc.



REFERENCES

- [1] IEEE Robotics and Automation Society and Institute of Electrical and Electronics Engineers, *2019 24th International Conference on Methods and Models in Automation and Robotics (MMAR)*.
- [2] Z. Zhao, H. Taghavifar, H. Du, Y. Qin, M. Dong, and L. Gu, "In-Wheel Motor Vibration Control for Distributed-Driven Electric Vehicles: A Review," *IEEE Transactions on Transportation Electrification*, vol. 7, no. 4. Institute of Electrical and Electronics Engineers Inc., pp. 2864–2880, Dec. 01, 2021. doi: 10.1109/TTE.2021.3074970.
- [3] H. Wang, T. Sun, X. Zhou, and Q. Fan, "Research on the Electric Vehicle Control System," *International Journal of u- and e-Service, Science and Technology*, vol. 8, no. 8, pp. 103–110, Aug. 2015, doi: 10.14257/ijunesst.2015.8.8.11.
- [4] S. K. Kommuri, M. Defoort, H. R. Karimi, and K. C. Veluvolu, "A Robust Observer-Based Sensor Fault-Tolerant Control for PMSM in Electric Vehicles," *IEEE Transactions on Industrial Electronics*, vol. 63, no. 12, pp. 7671–7681, Dec. 2016, doi: 10.1109/TIE.2016.2590993.
- [5] X. Wu, X. He, G. Yu, A. Harmandayan, and Y. Wang, "Energy-Optimal Speed Control for Electric Vehicles on Signalized Arterials," *IEEE Transactions on Intelligent Transportation Systems*, vol. 16, no. 5, pp. 2786–2796, Oct. 2015, doi: 10.1109/TITS.2015.2422778.
- [6] W. Enang and C. Bannister, "Modelling and control of hybrid electric vehicles (A comprehensive review)," *Renewable and Sustainable Energy Reviews*, vol. 74. Elsevier Ltd, pp. 1210–1239, 2017. doi: 10.1016/j.rser.2017.01.075.
- [7] M. Vajedi and N. L. Azad, "Ecological adaptive cruise controller for plug-in hybrid electric vehicles using nonlinear model predictive control," *IEEE Transactions on Intelligent Transportation Systems*, vol. 17, no. 1, pp. 113–122, Jan. 2016, doi: 10.1109/TITS.2015.2462843.
- [8] S. Ding, L. Liu, and W. X. Zheng, "Sliding Mode Direct Yaw-Moment Control Design for In-Wheel Electric Vehicles," *IEEE Transactions on Industrial Electronics*, vol. 64, no. 8, pp. 6752–6762, Aug. 2017, doi: 10.1109/TIE.2017.2682024.
- [9] J. Tian, J. Tong, and S. Luo, "Differential steering control of four-wheel independent-drive electric vehicles," *Energies (Basel)*, vol. 11, no. 11, Nov. 2018, doi: 10.3390/en11112892.
- [10] L. Jin, L. Gao, Y. Jiang, M. Chen, Y. Zheng, and K. Li, "Research on the control and coordination of four-wheel independent driving/steering electric vehicle," *Advances in Mechanical Engineering*, vol. 9, no. 4, pp. 1–13, Apr. 2017, doi: 10.1177/1687814017698877.
- [11] W. Xu, H. Chen, H. Zhao, and B. Ren, "Torque optimization control for electric vehicles with four in-wheel motors equipped with regenerative braking system," *Mechatronics*, vol. 57, pp. 95–108, Feb. 2019, doi: 10.1016/j.mechatronics.2018.11.006.
- [12] C. Qiu, G. Wang, M. Meng, and Y. Shen, "A novel control strategy of regenerative braking system for electric vehicles under safety critical driving situations," *Energy*, vol. 149, pp. 329–340, 2018, doi: <https://doi.org/10.1016/j.energy.2018.02.046>.

- [13] J. Xue and X. Jiao, "Speed cascade adaptive control for hybrid electric vehicle using electronic throttle control during car-following process," *ISA Trans*, vol. 110, pp. 328–343, Apr. 2021, doi: 10.1016/j.isatra.2020.10.058.
- [14] S. K. Tripathi, A. Shrivastava, K. C. Jana, A. Agrawal, and A. Rai, "Robust throttle control of Hybrid Electric Vehicle," in *IOP Conference Series: Materials Science and Engineering*, Institute of Physics Publishing, Sep. 2019. doi: 10.1088/1757-899X/594/1/012017.
- [15] T. D. Gillespie, *Fundamentals of Vehicle Dynamics*, Revised Edition. SAE Books, 2021. Accessed: Jun. 18, 2023. [Online]. Available: https://books.google.com.my/books?hl=en&lr=&id=LeybEAAQBAJ&oi=fnd&pg=PP1&dq=vehicle+dynamics&ots=WUJWubOvSF&sig=LS61cW8btkkeYsvtOjA7I28b57U&redir_esc=y#v=onepage&q=vehicle%20dynamics&f=false
- [16] R. V. Dukkupati, *VEHICLE DYNAMICS*. Narosa Publishing House, 2000. Accessed: Jun. 18, 2023. [Online]. Available: https://books.google.com.my/books?id=fgM19L9LZKkC&printsec=frontcover&source=gbs_atb#v=onepage&q&f=false
- [17] S. Lekshmi and L. P. Lal, "Mathematical modeling of Electric vehicles - A survey," *Control Eng Pract*, vol. 92, Nov. 2019, doi: 10.1016/j.conengprac.2019.104138.
- [18] N. Ibrahim, M. Abdelaziz, M. Ghoneima, and S. Hammad, "Implementation of vector control on electric vehicle traction system," *Bull Natl Res Cent*, vol. 44, no. 1, Dec. 2020, doi: 10.1186/s42269-019-0258-8.
- [19] B. Saeedi and M. Sadedel, "Implementation of Behavior-Based Navigation Algorithm on Four-Wheel Steering Mobile Robot," *Journal of Computational Applied Mechanics*, vol. 52, no. 4, pp. 619–641, Dec. 2021, doi: 10.22059/JCAMECH.2021.330072.648.
- [20] Y. Hori, Y. Toyoda, and Y. Tsuruoka, "Traction Control of Electric Vehicle: Basic Experimental Results Using the Test EV 'UOT Electric March.'"
- [21] S. De Pinto, C. Chatzikomis, A. Sorniotti, and G. Mantriota, "Comparison of Traction Controllers for Electric Vehicles with On-Board Drivetrains," *IEEE Transactions on Vehicular Technology*, vol. 66, no. 8. Institute of Electrical and Electronics Engineers Inc., pp. 6715–6727, Aug. 01, 2017. doi: 10.1109/TVT.2017.2664663.
- [22] D. Dogan and P. Boyraz, "Smart Traction Control Systems for Electric Vehicles Using Acoustic Road-Type Estimation," in *IEEE Transactions on Intelligent Vehicles*, Institute of Electrical and Electronics Engineers Inc., Sep. 2019, pp. 486–496. doi: 10.1109/TIV.2019.2919461.
- [23] D. Savitski *et al.*, "Wheel Slip Control for the Electric Vehicle with In-Wheel Motors: Variable Structure and Sliding Mode Methods," *IEEE Transactions on Industrial Electronics*, vol. 67, no. 10, pp. 8535–8544, Oct. 2020, doi: 10.1109/TIE.2019.2942537.
- [24] Institute of Electrical and Electronics Engineers, *2017 Innovations in Power and Advanced Computing Technologies (i-PACT) : 21-22 April 2017*.
- [25] Z. Yongqiang, Z. Xin, L. Jiashi, H. Haitao, M. Teng, and Z. Chunyu, "A research on evaluation and development of single-pedal function for electric vehicle based on PID," in *Journal of Physics: Conference Series*, Institute of Physics Publishing, Aug. 2020. doi: 10.1088/1742-6596/1605/1/012109.
- [26] M. Haseb and K. Sudhakaran Siddharth, "Design and fabrication of a Hybrid Go-Kart," in *Proceedings of 2021 2nd International Conference on Intelligent Engineering and Management, ICIEM 2021*, Institute of Electrical and Electronics Engineers Inc., Apr. 2021, pp. 155–159. doi: 10.1109/ICIEM51511.2021.9445273.

- [27] P. K. Agarwal, M. (Computer scientist) Gupta, I. D. of M. E. Motilal Nehru National Institute of Technology (Allahabad, Institute of Electrical and Electronics Engineers. Uttar Pradesh Section, IEEE Robotics and Automation Society, and Institute of Electrical and Electronics Engineers, *2017 International Conference on Advances in Mechanical, Industrial, Automation and Management Systems (AMIAMS) : proceedings : February 3-5, 2017*.
- [28] P. Wadagbalkar and C. Somani, "Formulation of a Standardized Procedure for Designing the Steering System of Small Vehicles Like Go-Karts." [Online]. Available: <http://www.ijert.org>
- [29] "A Review on Design and Assembly of Go-Kart Steering System", Accessed: Jun. 18, 2023. [Online]. Available: https://www.ijresm.com/Vol_1_2018/Vol1_Iss10_October18/IJRESM_V1_I10_134.pdf
- [30] G. De Filippis, B. Lenzo, A. Sorniotti, P. Gruber, and W. De Nijs, "Energy-Efficient Torque-Vectoring Control of Electric Vehicles with Multiple Drivetrains," *IEEE Trans Veh Technol*, vol. 67, no. 6, pp. 4702–4715, Jun. 2018, doi: 10.1109/TVT.2018.2808186.
- [31] M. Aktas, K. Awaili, M. Ehsani, and A. Arisoy, "Direct torque control versus indirect field-oriented control of induction motors for electric vehicle applications," *Engineering Science and Technology, an International Journal*, vol. 23, no. 5, pp. 1134–1143, Oct. 2020, doi: 10.1016/j.jestch.2020.04.002.
- [32] B. Gasbaoui and A. Nasri, "A Novel 4WD Electric Vehicle Control Strategy Based on Direct Torque Control Space Vector Modulation Technique," *Intelligent Control and Automation*, vol. 03, no. 03, pp. 236–242, 2012, doi: 10.4236/ica.2012.33027.
- [33] M. L. De Klerk and A. K. Saha, "Performance analysis of DTC-SVM in a complete traction motor control mechanism for a battery electric vehicle," *Heliyon*, vol. 8, no. 4, Apr. 2022, doi: 10.1016/j.heliyon.2022.e09265.
- [34] M. J. Akhtar and R. K. Behera, "Space Vector Modulation for Distributed Inverter-Fed Induction Motor Drive for Electric Vehicle Application," *IEEE J Emerg Sel Top Power Electron*, vol. 9, no. 1, pp. 379–389, Feb. 2021, doi: 10.1109/JESTPE.2020.2968942.
- [35] "Space Vector PWM Control Synthesis for a H-Bridge Drive in Electric Vehicles".
- [36] W. J. Rugh and J. ! S. Shamma, "Survey Paper Research on gain scheduling," 2000.
- [37] V. Veselý and A. Ilka, "Gain-scheduled PID controller design," *J Process Control*, vol. 23, no. 8, pp. 1141–1148, 2013, doi: 10.1016/j.jprocont.2013.07.002.
- [38] G. Qin, M. Liu, J. Zou, and X. Xin, "Vector Control Algorithm for Electric Vehicle AC Induction Motor Based on Improved Variable Gain PID Controller," *Math Probl Eng*, vol. 2015, 2015, doi: 10.1155/2015/875843.
- [39] P. Razmi, T. Rahimi, K. Sabahi, M. Gheisarnejad, and M. H. Khooban, "Adaptive fuzzy gain scheduling PID controller for frequency regulation in modern power system," *IET Renewable Power Generation*, 2022, doi: 10.1049/rpg2.12569.

APPENDICES

Appendix A Coding

```
#include <PID_v1.h>

int potPin1 = A0; // pin connected to Steering potentiometer
int angle;
int potPin2 = A5; // pin connected to Throttle potentiometer
int throttle;
int PWM1;
int PWM2;

int Encoder1 = 3; // pin connected to Encoder
int Encoder2 = 2; // pin connected to Encoder
int row_num = 7, col_num = 11;

// Define PID parameters
double kp = 900.0; // Proportional gain
double ki = 2500.0; // Integral gain
double kd = 25.0; // Derivative gain

double Setpoint = 0; // Define PID Setpoint
double Input = 0; // Define PID Input
double OutputRRW = 0; // Define PID Output for RRW
double OutputRLW = 0; // Define PID Output for RLW

// Declare PID objects
PID pidRRW(&Input, &OutputRRW, &Setpoint, kp, ki, kd, DIRECT);
PID pidRLW(&Input, &OutputRLW, &Setpoint, kp, ki, kd, DIRECT);

void setup() {
// Set Potentiometer as inputs
pinMode(A0, INPUT);
pinMode(A5, INPUT);

// Set PWM as output
pinMode(5, OUTPUT);
pinMode(6, OUTPUT);

// Set Encoder as input
pinMode(Encoder1, INPUT);
pinMode(Encoder2, INPUT);

Serial.begin(9600); // Set Baud rate of serial monitor/plotter to 9600 bits/s
}
```

```

void loop() {

//Gain Scheduler setup for RRW
float gainRRW[7][11] =
  {{0, 1.76, 4.39, 8.78, 13.18, 17.57, 21.96, 26.35, 30.74, 35.14, 43.92},
  {0, 1.84, 4.60, 9.19, 13.79, 18.38, 22.98, 27.57, 32.17, 36.76, 45.95},
  {0, 1.92, 4.80, 9.60, 14.39, 19.19, 23.99, 28.79, 33.59, 38.38, 47.98},
  {0, 2.00, 5.00, 10.00, 15.00, 20.00, 25.00, 30.00, 35.00, 40.00, 50.00},
  {0, 2.08, 5.20, 10.4, 15.61, 20.81, 26.01, 31.21, 36.41, 41.62, 52.02},
  {0, 2.16, 5.41, 10.81, 16.21, 21.62, 27.02, 32.43, 37.85, 43.24, 54.05},
  {0, 2.24, 5.61, 11.22, 16.82, 22.43, 28.04, 33.65, 39.26, 44.86, 56.08}
  };

//Gain Scheduler setup for RLW
float gainRLW[7][11] =
  {{0, 2.24, 5.61, 11.22, 16.82, 22.43, 28.04, 33.65, 39.26, 44.86, 56.08},
  {0, 2.16, 5.41, 10.81, 16.21, 21.62, 27.02, 32.43, 37.85, 43.24, 54.05},
  {0, 2.08, 5.20, 10.4, 15.61, 20.81, 26.01, 31.21, 36.41, 41.62, 52.02},
  {0, 2.00, 5.00, 10.00, 15.00, 20.00, 25.00, 30.00, 35.00, 40.00, 50.00},
  {0, 1.92, 4.80, 9.60, 14.39, 19.19, 23.99, 28.79, 33.59, 38.38, 47.98},
  {0, 1.84, 4.60, 9.19, 13.79, 18.38, 22.98, 27.57, 32.17, 36.76, 45.95},
  {0, 1.76, 4.39, 8.78, 13.18, 17.57, 21.96, 26.35, 30.74, 35.14, 43.92}
  };

// Read sensor value from A0
potPin1 = analogRead (A0);
//Convert analog into digital (max Volt=5V, 10 bits=1023)
float voltage1 = potPin1 * (5.0 /1023.0);

// Read sensor value from A5
potPin2 = analogRead (A5);
//Convert analog into digital (max Volt=5V, min Volt 0.6, 10 bits=1023)
float voltage2 = potPin2 * (5.0 /1023.0);

// Read throttle value from A5
PWM1 = analogRead(A5);
PWM2 = analogRead(A5);

// Read steering value from A0
PWM1 = analogRead(A0);
PWM2 = analogRead(A0);

// Set PWM values based on input readings
analogWrite(5,PWM1);
analogWrite(6,PWM2);

// Read sensor value from A5
Encoder1 = digitalRead(3);
Encoder2 = digitalRead(2);

```

```

//Below is for angle
if (potPin1 > 877) {
    angle = 15;
    row_num = 6;}
    else if (potPin1 > 731) {angle = 10, row_num = 5;}
    else if (potPin1 > 585) {angle = 5, row_num = 4;}
    else if (potPin1 > 438) {angle = 0, row_num = 3;}
    else if (potPin1 > 292) {angle = -5, row_num = 2;}
    else if (potPin1 > 146) {angle = -10, row_num = 1;}
else angle = -15, row_num = 0;

//Below is for velocity
if (potPin2 > 843) {
    throttle = 50;
    col_num = 10;}
    else if (potPin2 > 753) {throttle = 40, col_num = 9;}
    else if (potPin2 > 663) {throttle = 35, col_num = 8;}
    else if (potPin2 > 573) {throttle = 30, col_num = 7;}
    else if (potPin2 > 483) {throttle = 25, col_num = 6;}
    else if (potPin2 > 392) {throttle = 20, col_num = 5;}
    else if (potPin2 > 303) {throttle = 15, col_num = 4;}
    else if (potPin2 > 213) {throttle = 10, col_num = 3;}
    else if (potPin2 > 143) {throttle = 5; col_num = 2;}
    else if (potPin2 > 123) {throttle = 2; col_num = 1;}
else throttle = 0, col_num = 0;

// Interpolate gain values
float fraction_row = row_num - static_cast<int>(row_num); // Fractional part of the
row_num
float fraction_col = col_num - static_cast<int>(col_num); // Fractional part of the
col_num

// Linear interpolation function
auto interpolate = [](float v1, float v2, float fraction) {
    return v1 + fraction * (v2 - v1);
};

// Interpolate all the gain values
float gainRRW_interp = interpolate(
    interpolate(gainRRW[row_num][col_num], gainRRW[row_num + 1][col_num],
fraction_row),
    interpolate(gainRRW[row_num][col_num + 1], gainRRW[row_num + 1][col_num +
1], fraction_row),
    fraction_col
);

float gainRLW_interp = interpolate(
    interpolate(gainRLW[row_num][col_num], gainRLW[row_num + 1][col_num],
fraction_row),

```

```

        interpolate(gainRLW[row_num][col_num + 1], gainRLW[row_num + 1][col_num +
1], fraction_row),
        fraction_col
    );

// Calculate PID Gain Scheduling output for RLW
pidRLW.Compute();
OutputRRW = constrain(OutputRRW, 0, 255); // Ensure the output is within a valid range
OutputRRW = gainRRW_interp;

// Calculate PID Gain Scheduling output for RLW
pidRLW.Compute();
OutputRLW = constrain(OutputRLW, 0, 255); // Ensure the output is within a valid range
OutputRLW = gainRLW_interp;

// Print sensor values and calculated speeds
Serial.print("Voltage1 value = ");
Serial.print(voltage1);
Serial.println(" Volt");
Serial.print("Angle value = ");
Serial.print(angle);
Serial.println(" degree");

Serial.print("Voltage2 value = ");
Serial.print(voltage2);
Serial.println(" Volt");
Serial.print("Throttle value = ");
Serial.print(throttle);
Serial.println(" (regulates Speed)");
Serial.println(" ");

// Print PID Gain Scheduling outputs for both wheels
Serial.print("The speed from PWM1 RRW = ");
Serial.print(OutputRRW);
Serial.println(" km/h");
Serial.print("The speed from PWM2 RLW = ");
Serial.print(OutputRLW);
Serial.println(" km/h");
Serial.println(" ");

delay(4000);
}

```

Appendix B Gantt Chart for Final Year Project 1

Activity/ Task	W1	W2	W3	W4	W5	W6	W7	W8	W9	W10	W11	W12	W13	W14
Project briefing, title selection, synopsis														
Identify objectives, problem statements														
Research reviews														
Model and component selection														
Methodology, design simulation														
Final report, presentation preparation														



Appendix C Gantt Chart for Final Year Project 2

Activity/ Task	2023											2024		
	W1	W2	W3	W4	W5	W6	W7	W8	W9	W10	W11	W12	W13	W14
Understand EV part functions	█	█	█	█	█	█	█	█	█					
Build up simulation design			█	█	█	█	█							
Coding and algorithm set up						█	█	█			█			
Software-hardware synchronization							█	█	█	█				
Hardware setup and Implementation									█	█	█			
Data analysis and Optimization							█	█	█	█	█	█		
Testing and Troubleshooting												█	█	
Final report writing, presentation preparation												█	█	█

